University of Alberta

Structure and function analysis of the Merlin Sip1 complex

by

Albert Chun Cheung Leung

A thesis submitted to the Faculty of Graduate Studies and Research
in partial fulfillment of the requirements for the degree of

Master of Science

Medical Sciences - Medical Genetics

Fall 2011
Edmonton, Alberta

Abstract

Mutations in the NF2 gene lead to the disease Neurofibromatosis Type II which is characterized by the formation of multiple tumours in the central nervous system. The NF2 gene encodes the protein Merlin. Merlin interacts with a number of different proteins and these interactions may be important for Merlin tumour suppressor function. Amongst these proteins, EBP50 has been identified as a candidate scaffold protein.

In this thesis, I identified a potential novel binding site in *Drosophila* Merlin to the *Drosophila* EBP50 homolog, Sip1. I determined that this potential novel binding site is both necessary and sufficient for binding *in vitro*. In addition, a conserved potential novel phosphorylation site is also identified in this region and may be involved in the regulation of the Merlin Sip1 interaction. These results suggest that a regulatory protein complex may be involved in Merlin tumour suppressor activity.

Acknowledgments

First and foremost I would like to thank my committee members and especially my supervisor, Dr. Sarah Hughes, who always believed in me and pushed me to achieve more (once I had done the proper controls and experiments). My thesis committee members, Dr. Gary Eitzen and Dr. Fred Berry, were instrumental in the success of this project. In addition, I would like to acknowledge Dr. Paul Lapointe for being on my examining committee. To both my supervisor and all committee members, I am especially appreciative for the help in improving my thesis writing. I would also like to thank Dr. Andrew Simmonds for the use of his radiation bench (and general advice on life).

Although scientists often like to be solitary, research is a team effort and I would like to acknowledge all the individuals that contributed to this research. Angela Effa, an undergraduate student who is both talented and hardworking, carried out the main part of the phosphorylation project and some of her work is part of this thesis. David Primrose, our technician, for keeping everything in the lab organized and ordering the many supplies needed for experiments. Somehow, David and I went from not going to Tim Horton's in the morning to going only during roll-up-the-rim to going every morning. To all current and former members of the lab, it has been a pleasure working with you all.

Last but not least, special thanks go out to all my family and friends – most importantly, my parents for supporting my decisions and my friends for (still) being there.

Thank you again to everyone to who made my time here an enjoyable and wonderful experience (I would love to go through everyone individually but that would be a thesis in itself).

Table of Contents

List of Figures

Chapter Five

List of Tables

~	approximately
Δ	deletion
2D	two dimensional
AC	affinity chromatography
Akt/PKB	protein kinase B
CC	coiled-coiled
CNS	central nervous system
CPM	counts per minute
C-terminal	carboxy terminal
C-terminus	carboxy terminus
DDAB	dimethyl-dioctadecylammonium bromide
DNA	deoxyribonucleic acid
DTT	dithiothreitol
EBP50	ERM binding protein 50
EGFR	epidermal growth factor receptor
ERM	Ezrin-Radixin-Moesin
ERMAD	Ezrin-Radixin-Moesin association domain
F1	FERM F1 subdomain
F2	FERM F2 subdomain
F3	FERM F3 subdomain
FERM	Four-point-one Ezrin-Radixin-Moesin
GFP	green fluorescent protein
GST	Glutathione S-Transferase
HS	heat shock
HRS	hepatocyte growth factor regulated tyrosine kinase substrate
IPTG	isopropyl ß-D-1-thiogalactopyranoside
LB	Luria-Bertani
MARCM	mosaic analysis with a repressible cell marker
Mdm2	murine double minute 2
NF2	Neurofibromatosis Type 2
N-terminal	amino terminal
N-terminus	amino terminus
ORF	open reading frame
PAGE	polyacrylamide gel electrophoresis
PAK2	p21 activated kinase 2
PBS	phosphate buffered saline
PCR	polymerase chain reaction
PDZ	PSD95-Dlg1-zo1 domain
PIKE-L	phosphoinositide 3-kinase enhancer isoform 1
PKA	protein kinase A
RNA	ribonucleic acid

RNAi	RNA interference
RPM	rotations per minute
S2	*Drosophila* Schneider 2
S10	serine 10
S315	serine 315
S371	serine 371
S518	serine 518
Sip1	SRY interacting protein 1
T230	threonine 230
T374	threonine 374
T558	threonine 558
T564	threonine 564
T567	threonine 567
TnT	transcription and translation
SDS	sodium dodecyl sulfate
UAS	upstream activation sequence
v/v	volume per volume
w/v	weight per volume
YT	yeast tryptone

Chapter One:

General Introduction

1.1 Neurofibromatosis Type 2

Neurofibromatosis type 2 (NF2) is a hereditary disease in humans. It is characterized by the development of schwannomas, meningiomas, and ependymomas. In particular, a large majority of patients develop bilaterial schwannomas around the eighth cranial nerve (Evans et al., 1992a; Evans et al., 1992b). NF2 was initially reported to occur in ~1:33,000 to 1:40,000 individuals, but a recent study suggests that the occurrence may be higher at ~1:25,000 individuals (Evans et al., 2005). NF2 is inherited in an autosomal dominant pattern with nearly complete penetrance by the age of 60 but onset can be as early as the late teen years (Evans et al., 1992b; Evans et al., 2005). In 1993, the *NF2* gene was identified on chromosome 22q12 (Rouleau et al., 1993; Trofatter et al., 1993). One defective copy of the *NF2* gene is inherited from the parents and a second mutation is then acquired in the wildtype copy, consistent with Knudson's two hit hypothesis, before tumour formation and disease onset (Knudson, 1971; Rouleau et al., 1993; Stemmer-Rachamimov et al., 1998; Trofatter et al., 1993; Woods et al., 2003). Furthermore, the loss of the NF2 gene product, Merlin (Moesin-ezrin-radixin like protein), has been detected in sporadic schwannomas, meningiomas, and ependymomas (Gutmann et al., 1997).

Schwannomas and meningiomas are amongst the most common types accounting for ~25% of all brain tumours (Hanemann and Evans, 2006; Riemenschneider et al., 2006). Virtually all schwannomas, whether sporadic or inherited, have mutations in the *NF2* gene (Gutmann et al., 1997; Stemmer-Rachamimov et al., 1998; Stemmer-Rachamimov et al., 1997). In the majority of sporadic meningiomas, there is complete inactivation of the *NF2* gene (Gutmann et al., 1997; Ruttledge et al., 1994). In approximately half of sporadic ependymomas, mutations in the *NF2* gene can be found (Gutmann et al., 1997). Taken together, since mutations in the *NF2* gene can only be found in ~50-80% of schwannomas, meningiomas, and ependymomas, this suggests that additional factors may be involved in tumour formation. In fact, mathematical modelling using both "two-hit" and "three-hit" models fits the patient data for formation of vestibular schwannomas (Woods et al., 2003). The "two-hit" model was used to explain dominantly inherited cancers, where a mutation in one allele is inherited and present in all cells while a second mutation is acquired sporadically in the other allele over time and leads to disease (Knudson, 1996, 1971). Interestingly, it was suggested that when a tumour suppressor is ubiquitously expressed, only a benign lesion is formed after two hits and additional genetic events are necessary for disease progression (Knudson, 1996). The "three-hit" model was based

on this idea, that one mutation is inherited and two more mutations must be acquired before progression to disease occurs (Woods et al., 2003). This suggests that additional genes may be involved in development of NF2 and that the formation of NF2 tumours may also be a multistep process.

The *NF2* gene in humans consists of 17 exons and encodes the protein Merlin (Rouleau et al., 1993; Trofatter et al., 1993). Merlin has been classified as part of the moesin-ezrin-radixin (ERM) subfamily of proteins (Rouleau et al., 1993; Trofatter et al., 1993). The *NF2* gene is alternatively spliced to produce two major, isoforms of Merlin that produce unique C-termini: Isoform I which lacks exon 16 and Isoform II which lacks exon 17 (Hara et al., 1994). In addition, there have been multiple other alternatively spliced transcripts of Merlin that can be detected using northern blots but these are not widely expressed (Hara et al., 1994). Only Isoform I is known to have tumour suppressor function (Sherman et al., 1997).

1.2 Merlin

The protein Merlin is conserved and is found across multicellular eukaryotes (Golovnina et al., 2005). To understand the function and regulation of Merlin, studies have been primarily carried out in human cell lines, mice, and *Drosophila melanogaster* (*Drosophila*). Human Merlin shares 98% and 55% protein identity with

the mouse and *Drosophila* homolog respectively (Haase et al., 1994; McCartney and Fehon, 1996). In mice and *Drosophila*, Merlin expression is detectable in all tissues throughout all stages of development, with the highest levels in the brain and CNS (Gutmann et al., 1995; Huynh et al., 1996; McCartney and Fehon, 1996). Homozygous null Merlin mutations in mice result in embryonic lethality and pupal lethality in *Drosophila* (Fehon et al., 1997; McClatchey et al., 1997). Functionally, Merlin is conserved as human *NF2* can genetically rescue the lethal *Merlin* allele in *Drosophila* (LaJeunesse et al., 1998).

In humans, Merlin has been identified as a tumour suppressor as loss of Merlin protein leads to over proliferation and the development of NF2 (Evans et al., 1992a; Evans et al., 1992b; Rouleau et al., 1993; Trofatter et al., 1993). The role of Merlin in regulation of cell proliferation has been well established in studies using cultured cells. Cell proliferation can be inhibited in NIH 3T3 cells and primary cells derived from human schwannomas by over expression of wildtype Merlin (Lutchman and Rouleau, 1995; Schulze et al., 2002). As well, over expression of wildtype Merlin can reverse the Ras-induced malignant phenotype in NIH 3T3 cells (Tikoo et al., 1994). Merlin also controls G1/S cell cycle transition through negatively regulating Cyclin D1 and stabilizing p53 by degrading Mdm2, a p53 inhibitor (Kim et al.,

2004; Xiao et al., 2005). Merlin can also control cell growth through Rac and Ras signalling by inhibiting their activation (Kissil et al., 2002; Kissil et al., 2003; Morrison et al., 2007; Shaw et al., 2001; Xiao et al., 2002). In addition, Merlin has roles in polarity, apical membrane organization, and stabilization of adherens junctions which are important for maintaining cell-cell contact and control of cell proliferation (Gladden et al., 2010; James et al., 2001; Lallemand et al., 2003; McClatchey and Giovannini, 2005; Wiley et al., 2010; Xu and Gutmann, 1998). Although Merlin functions as a tumour suppressor and plays a role in plasma membrane organization, not all mechanisms of Merlin cell proliferation control have been elucidated.

1.2.1 Structure

Merlin has ~45% protein sequence identity to ERM proteins and is similar in secondary and tertiary protein structure (Bretscher et al., 2002; Nguyen et al., 2001). Merlin and ERM proteins have an N-terminal FERM (Four-point-one Ezrin Radixin Moesin) domain and a coiled-coiled domain. Merlin is thought to have an actin binding domain located within the FERM and coiled-coiled domains but this has yet to be determined conclusively (Huang et al., 1998; Scoles et al., 1998; Sivakumar et al., 2009; Xu and Gutmann, 1998). Merlin can also bind actin indirectly through interaction with beta II spectrin (Scoles et al., 1998). The N-terminal FERM domain folds into

a cloverleaf structure containing three sub-domains (F1, F2, F3) which can bind to the C-terminal tail through folding of the coiled-coiled, alpha helical region (Figure 1-1) (Gary and Bretscher, 1995; Pearson et al., 2000; Sherman et al., 1997). Merlin activity is regulated in part through the intramolecular interaction between the N-terminal head and C-terminal tail domains (Sherman et al., 1997). This interaction between the head and tail determines the activation state of Merlin, either as active or inactive (Figure 1-1). The tumour suppressor function of Merlin is active in a hypophosphorylated, closed form and inactive in a phosphorylated, open form (Kissil et al., 2002; Shaw et al., 1998; Sherman et al., 1997; Surace et al., 2004). This conformational change from closed to open is required for Merlin to interact with plasma membrane proteins and the actin cytoskeleton (James et al., 2001; Li et al., 2007; Xu and Gutmann, 1998).

1.2.2 Phosphorylation

Merlin has multiple phosphorylation sites that affects its function and localization; these include S10, T230, S315, and S518 (Kissil et al., 2002; Laulajainen et al., 2008; Okada et al., 2009; Rong et al., 2004a; Shaw et al., 2001; Surace et al., 2004; Tang et al., 2007; Xiao et al., 2002).

Figure 1-1: Diagram of the structure of ERM proteins and their open and closed conformation

The FERM domain folds up into a clover leaf shaped structure with three subdomains (F1, F2, and F3). The C-terminal tail and N-terminal FERM domain can interact resulting in a closed conformation. The N-terminal FERM domain is connected to the C-terminal tail through a coiled-coiled domain. The interaction between the C-terminal tail and N-terminal FERM domain is relieved by phosphorylation.

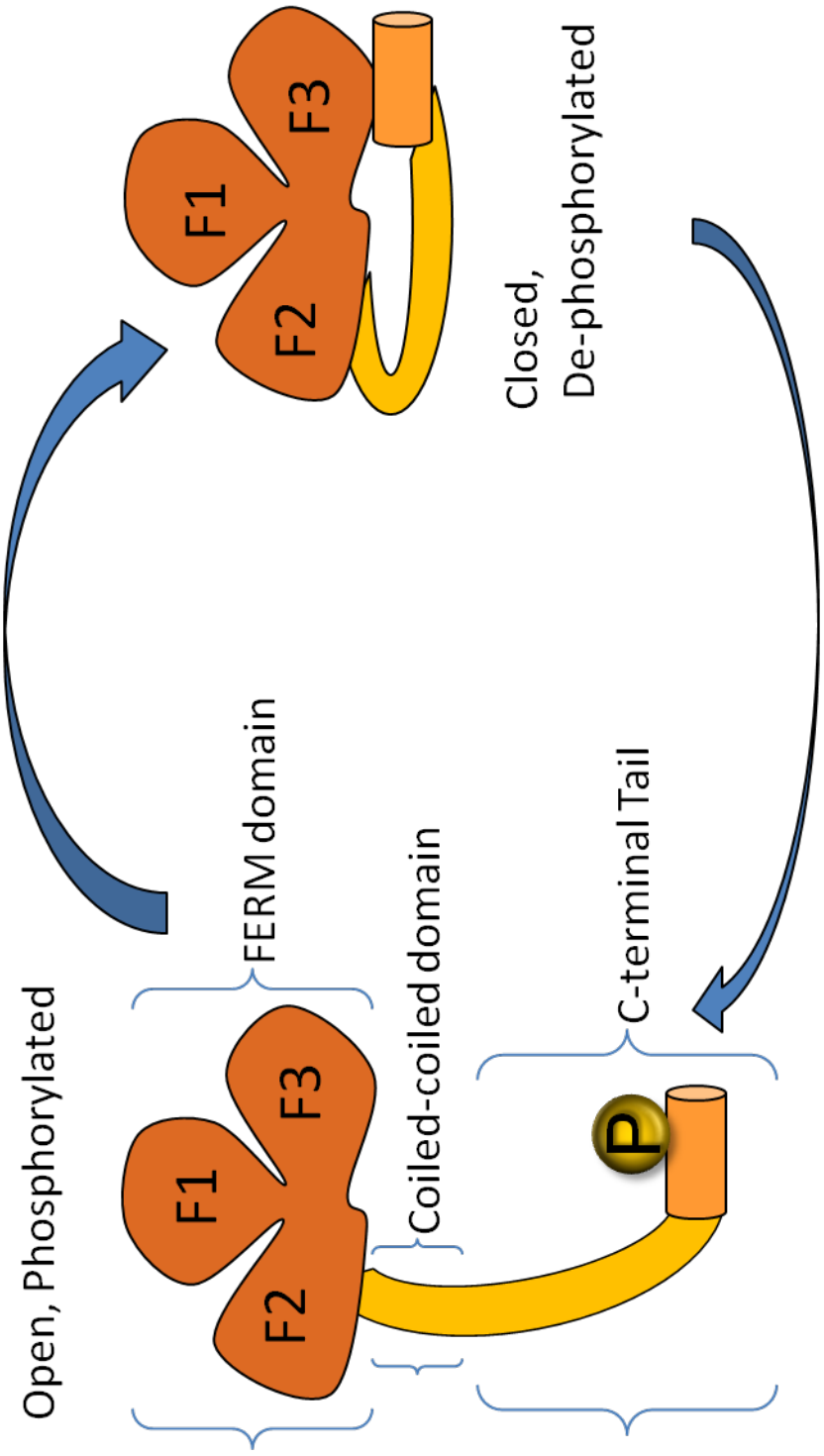
F1
F2
F3
Closed,
De-phosphorylated
FERM domain
Coiled-coiled domain
C-terminal Tail
P
F1
F2
F3
Open, Phosphorylated

Figure 1-1

Currently, there are three kinases identified that phosphorylate Merlin in mammalian cells: p21-activated kinase 2 (PAK2), protein kinase B (Akt/PKB), and protein kinase A (PKA) (Kissil et al., 2002; Laulajainen et al., 2008; Okada et al., 2009; Rong et al., 2004a; Shaw et al., 2001; Surace et al., 2004; Tang et al., 2007; Xiao et al., 2002).

Phosphorylation of S518 by PAK2 was first identified to affect Merlin localization and function (Kissil et al., 2002; Rong et al., 2004a). Phosphorylation of S518 leads to decreased binding of CD44 and HRS, and the interaction with CD44 and HRS are important for Merlin tumour suppressor function (Morrison et al., 2001; Sun et al., 2002). Interestingly, CD44 is involved in the activation of the Rho GTPase Rac1 (Murai et al., 2004). Previous research shows Merlin inhibition by Rac1 and Merlin interaction with CD44 functionally links Merlin to Rac-dependent signalling (Kissil et al., 2002; Shaw et al., 2001).

Akt/PKB phosphorylates Merlin on three sites, S10, T230 and S315 (Laulajainen et al., 2011; Tang et al., 2007). Phosphorylation of T230 and S315 are mutually regulated – blocking phosphorylation at one site prevents phosphorylation on the other (Tang et al., 2007). The phosphorylation of T230 and S315 leads to degradation by ubiquination of Merlin (Rong et al., 2004b; Tang et al., 2007).

PKA phosphorylates S10 and S518 in Merlin (Alfthan et al., 2004; Laulajainen et al., 2008). PKA phosphorylation of S10 affects the

actin cytoskeleton (Laulajainen et al., 2008). The S10 phosphomimic stabilizes F-actin filaments while a non-phosphorylatable S10 reduces the amount of cellular F-actin (Laulajainen et al., 2008). Phosphorylation of S10 after S518 also results in degradation of Merlin through the proteasome pathway (Laulajainen et al., 2011).

In *Drosophila*, a single sterile 20 family kinase, Slik affects the phosphorylation and activity of Merlin (Hughes and Fehon, 2006). Slik can interact with Merlin directly and increased Slik activity results in Merlin hyperphosphorylation (Hughes and Fehon, 2006). As well, loss of one copy of Slik enhances the activated Merlin phenotype which suggests Slik phosphorylates and inactivates Merlin (Hughes and Fehon, 2006).

In all cases, phosphorylation of Merlin leads to Merlin tumour suppressor inactivation (Hughes and Fehon, 2006; Kissil et al., 2002; Laulajainen et al., 2011). Additionally, phosphorylation of Merlin may lead to degradation and the ability of Merlin to bind to actin (Laulajainen et al., 2008; Tang et al., 2007).

1.2.3 Protein Interactions

Merlin interacts with many different proteins and potentially functions through larger protein complexes; however, the specific complexes involved in Merlin tumour suppression and their relation to NF2 pathogenesis has yet to be elucidated (Scoles, 2008). Merlin forms

protein complexes with CD44, adherens junctions, EGFR, and EBP50 (Bai et al., 2007; Curto et al., 2007; Gutmann et al., 2001; Lallemand et al., 2003; Morrison et al., 2001; Murthy et al., 1998; Nguyen et al., 2001; Wheeler et al., 2007). Merlin also interacts with ERM proteins (Gronholm et al., 1999). Some Merlin interacting proteins such as CD44 and EBP50 also interacts with ERMs suggesting a link between Merlin and ERM function (Reczek et al., 1997; Tsukita et al., 1994).

Merlin may be involved in both the control of cell proliferation and maintenance of epithelial integrity through interactions with protein complexes such as CD44, adherens junctions, EGFR and EBP50 (Bai et al., 2007; Curto et al., 2007; Gutmann et al., 2001; Lallemand et al., 2003; Morrison et al., 2001; Murthy et al., 1998; Nguyen et al., 2001; Wheeler et al., 2007). CD44 is a hyaluronan extracellular matrix transmembrane receptor and Merlin interaction with the cytoplasmic tail of CD44 has been implicated in cell contact inhibition (Bai et al., 2007; Morrison et al., 2001). When Merlin is tumour suppressor active, this interaction negatively regulates CD44 and prevents hyaluronan from binding to CD44 to promote cell growth (Bai et al., 2007; Morrison et al., 2001). However, when Merlin is phosphorylated and tumour suppressor inactive, it forms a complex with Ezrin, Moesin and CD44 suggesting that Merlin may be involved in both cell proliferation and adhesion (Morrison et al., 2001). Another

important component in cell-cell contact is the adherens junctions. The loss of Merlin in primary cells results in an inability to undergo contact dependent growth arrest and a loss of stable cadherin containing cell junctions (Lallemand et al., 2003). In fact, recent research has demonstrated that the loss of Merlin leads to immature, non-functional adherens junctions and a disorganization of the adherens junction proteins (Flaiz et al., 2008; Gladden et al., 2010). Merlin may also control cell proliferation through interaction with growth factor receptors either by direct binding or through adapter proteins containing PDZ domains like EBP50 (Curto et al., 2007; Curto and McClatchey, 2008; Lazar et al., 2004; Murthy et al., 1998). During cell contact dependent inhibition, Merlin stabilizes adherens junctions and negatively regulates EGFR with EBP50 by sequestering EGFR in a plasma membrane compartment where it cannot internalize or signal (Curto et al., 2007).

Interestingly, phosphatidyinositol 4,5-bisphosphate interacts with Merlin and targets Merlin to the plasma membrane and phosphatidylinositol 4,5-bisphosphate is required for Merlin tumour suppressor function (Mani et al., 2011). Phosphatidylinositol 4,5-bisphosphate also plays a role in ERM regulation suggesting a link between Merlin and ERMs (Fievet et al., 2004).

1.3 ERM Proteins

Ezrin, Radixin, and Moesin are paralogous proteins with partially redundant functions (Bretscher et al., 2002; Sato et al., 1992; Takeuchi et al., 1994). ERM proteins are important in maintaining epithelial integrity and function as protein linkers between the plasma membrane and the actin cytoskeleton (Bretscher et al., 2002; Sato et al., 1992; Speck et al., 2003). The first member of the family to be discovered was Ezrin and was initially found to be a component of microvilli and membrane ruffles at the cell surface (Bretscher, 1983; Gould et al., 1989; Pakkanen et al., 1987). Ezrin is also a substrate for tyrosine kinases and could be involved in receptor tyrosine kinase signalling (Gould et al., 1986). Expression of Ezrin has been found in a wide variety of epithelial cells and is necessary for the proper formation of the multicellular epithelium of the gut (Berryman et al., 1993; Saotome et al., 2004). Radixin was isolated from adherens junctions in liver cells and is associated with microvilli (Amieva et al., 1994; Funayama et al., 1991; Tsukita and Hieda, 1989). Moesin is enriched in actin rich plasma membrane structures and originally identified for its ability to bind to heparin at the plasma membrane (Amieva and Furthmayr, 1995; Franck et al., 1993; Lankes and Furthmayr, 1991). Expression of Moesin is primarily in endothelial cells (Berryman et al., 1993). In *Drosophila*, there is only one ERM

protein homolog, identified as Moesin due to the lack of a polyproline sequence found in Ezrin and Radixin (McCartney and Fehon, 1996; Sato et al., 1992). Moesin inhibits the small GTPase Rho in order to maintain epithelial integrity in *Drosophila* (Speck et al., 2003).

ERM proteins are regulated by the binding of phosphatidylinositol 4,5-bisphosphate to the FERM domain and the state of phosphorylation at the conserved C-terminal threonine residue: T567 for Ezrin, T564 for Radixin, and T558 for Moesin (Fievet et al., 2004; Hirao et al., 1996; Matsui et al., 1998; Nakamura et al., 1995; Yonemura et al., 2002). When the N-terminal FERM domain and C-terminal tail of ERM proteins interact, the protein adopts closed conformation (Figure 1-1) (Bretscher et al., 2002; Gary and Bretscher, 1995; Matsui et al., 1998; Nakamura et al., 1995). In a two-step mechanism, phosphatidylinositol 4,5-bisphosphate first binds to the FERM domain of ERMs affecting a conformational change and recruits ERMs to the plasma membrane (Fievet et al., 2004). This then allows subsequent phosphorylation of the conserved threonines residue to relieve this interaction and the protein adopts an open conformation (Fehon et al., 2010; Fievet et al., 2004; Gary and Bretscher, 1995; Hirao et al., 1996; Matsui et al., 1998; Nakamura et al., 1995; Yonemura et al., 2002). ERM proteins are inactive and unable to interact with membrane proteins and the actin cytoskeletion in their

unphosphorylated, closed form (Gary and Bretscher, 1995; Matsui et al., 1998). ERM proteins are active and can bind to membrane proteins and the actin cytoskeleton in their phosphorylated, open conformation (Gary and Bretscher, 1995; Matsui et al., 1998). Multiple kinases can phosphorylate the conserved threonine residue in ERM proteins; these include Rho kinase, protein kinase Cα, protein kinase Cθ, NF-κß-inducing kinase, Ste20 kinase MST4 and lymphocyte-oriented kinase (Hipfner et al., 2004; Matsui et al., 1998; Ng et al., 2001; Oshiro et al., 1998; Pietromonaco et al., 1998; Simons et al., 1998; Tran Quang et al., 2000). In *Drosophila*, Slik kinase affects the phosphorylation and activity of Moesin as well as Merlin and is the only known kinase to affect both Moesin and Merlin (Hipfner et al., 2004; Hughes and Fehon, 2006). The phosphorylation of both Merlin and Moesin by a single kinase provides a link between the control of proliferation by Merlin and the maintenance of epithelial integrity by Moesin and leads to the possibility that a protein complex is formed to regulate their function.

1.4 EBP50

Further support for the formation of a regulatory protein complex for Merlin and ERMs stems from the identification of EBP50, a scaffold protein (Reczek et al., 1997). EBP50 is able to interact with both Merlin and ERMs (Nguyen et al., 2001; Reczek and Bretscher,

1998). EBP50 is localized at the apical membrane of mammalian epithelial cells and is involved in linking the plasma membrane and cytoskeleton via ERM proteins (Fouassier et al., 2001; Morales et al., 2004). EBP50 also interacts with and regulates G protein coupled receptors (Wheeler et al., 2007). Merlin interacts with G proteins such as small GTPases. Since Merlin interacts with both G proteins and EBP50, this suggests that Merlin and EBP50 may be involved in the regulation of G protein signalling together (Morrison et al., 2007; Shaw et al., 2001; Wheeler et al., 2007). Recently, the *Drosophila* EBP50 homolog Sip1 has been identified in (Hughes et al., 2010). The loss of Sip1 results in the mislocalization of Slik kinase (Hughes et al., 2010). Additionally, Sip1 is necessary for the phosphorylation and activation of Moesin (Hughes et al., 2010). Since Slik also affects the activity of Merlin, this suggests that Sip1 may also be involved in the regulation of Merlin (Hughes and Fehon, 2006).

1.5 *Drosophila* as a Model

The study of Merlin and ERM proteins are more difficult in mammalian systems, such as mice, because of the multiple isoforms of Merlin and functional redundancy between Ezrin, Radixin, and Moesin (Hara et al., 1994; Takeuchi et al., 1994). In *Drosophila*, Merlin has only one isoform and there is only a single ERM protein, Moesin, in the genome (McCartney and Fehon, 1996). This eliminates the overlapping

functions that exist between the ERM proteins and reduces the complexity of studying Merlin's function. Furthermore, the evolutionary divergence of mammals and *Drosophila* allows for the identification of conserved regions that are important for Merlin function.

Some important insights into Merlin function have been discovered using *Drosophila*. A seven amino acid sequence known as the blue box domain is conserved between human and *Drosophila* Merlin in the FERM domain but not conserved with ERM proteins (LaJeunesse et al., 1998; McCartney and Fehon, 1996). The blue box domain when deleted or mutated to a series of seven alanines results in a dominant negative effect (LaJeunesse et al., 1998). Also, when the last 35 amino acids of *Drosophila* Merlin are deleted, the altered protein exhibits constitutively active tumour suppressor function and can genetically rescue a null Merlin mutation (LaJeunesse et al., 1998). It is interesting to note that regions important for Merlin function are often sequences that are not conserved in the ERM proteins. Finally, the ability of Slik kinase to affect the localization and activity of both Merlin and Moesin suggests that proliferation and epithelial integrity may be co-ordinately regulated.

1.6 Project Rationale

Merlin and ERM proteins bind to proteins associated with the plasma membrane and these interactions are critical for their functions (Bretscher et al., 2000; Morrison et al., 2001; Reczek et al., 1997; Scoles, 2008; Tsukita et al., 1994). One of these proteins, EBP50, binds to both Merlin and the ERM proteins (Bretscher et al., 2000; Nguyen et al., 2001; Reczek et al., 1997). EBP50 is a scaffold protein that is localized to the apical membrane of mammalian epithelial cells and is involved in linking the plasma membrane and cytoskeleton (Fouassier et al., 2001; Reczek et al., 1997). In response to cellular signals, scaffold proteins can recruit components of signalling pathways to specific subcellular locations (Wheeler et al., 2007). This interaction between Ezrin and EBP50 is masked by the C-terminal tail in the inactive, closed conformation (Finnerty et al., 2004). Sip1 is the homolog of EBP50 in flies and Sip1 is required for both the proper localization of Slik kinase and activation of Moesin to maintain epithelial integrity (Hughes et al., 2010). Slik also affects the localization and activity on both Merlin and Moesin homologs in *Drosophila* (Hughes and Fehon, 2006). Since Merlin is tumour suppressor active in a closed conformation and Moesin is active in an open conformation, phosphorylation of Merlin and Moesin by a single kinase suggests coordinate regulation of cell proliferation and

epithelial integrity. The regulation of both cell proliferation and epithelial integrity is required for proper tissue formation and both the control of cell proliferation and maintenance of epithelial integrity need to be tightly regulated (Huber et al., 2005; Thiery and Sleeman, 2006). Together, this suggests that a protein complex is required for the proper regulation and function of Merlin. My hypothesis is that Sip1 forms a complex with Merlin and regulates Merlin activity. Since not all NF2 tumours have mutations found in Merlin, the identification of a protein complex necessary for the regulation and function of Merlin may lead to additional targets for prognosis, diagnosis, and treatment.

Chapter Two:

Materials and Methods

2.1 Gateway® Cloning

The desired gene coding sequence was amplified by PCR with Phusion Polymerase (Finnzymes #F-530S) using a touchdown program (Table 2-1). Forward primers contain a CACC sequence at the 5' end for directional cloning into TOPO® pENTR/D entry vectors (Invitrogen #45-0218). Primers are in Appendix A. TOPO® reactions were set up using 1-2 μL of purified PCR product, 1 μL of salt solution included with the kit, 2 μL of sterile water, and 1 μL of TOPO® entry vector. The reactions were left at room temperature for 1 hour and then 3 μL of the reaction mixture was added to 50 μL of competent DH5α cells. The cells were incubated on ice for 10 minutes, plated on LB + kanamycin (50 μg/mL) plates and then incubated overnight at 37°C. Using the Gateway® LR clonase II kit (Invitrogen #11791-020), entry clones were recombined into various expression clones containing the desired promoters and epitope tags. These reactions were set up using 100-150 ng of entry clone, 100-150 ng of expression vector, sterile water to bring up final volume to 4 μL, and 1 μL of enzyme mix. Clonase reactions were left at room temperature for at least one hour before competent DH5α cells were transformed, plated on LB + ampicillin (100 μg/mL) plates and incubated overnight at 37°C. A list of clones created can be found in Appendix B. All entry and expression clones were confirmed through restriction enzyme digests and/or

sequencing. Restriction enzymes were chosen on the basis of at least one cut within the DNA insert and one cut within the vector. Sequencing was carried out at The Applied Genomics Center (TAGC). The M13 forward and reverse primers were used for sequencing of entry vectors to verify proper insertion and that the insert was in frame. For expression vectors, the actin forward primer (Actf) was used to sequence vectors containing the actin promoter and the heat shock forward primer (HSPf) was used to sequence vectors with the heat shock promoter or UAS promoter to verify proper 5' insertion of the desired sequence (Appendix A). The SV40 reverse primer (SVr) was used to sequence vectors with the actin, heat shock, or UAS promoters to verify proper 3' insertion (Appendix A). For pDest14 and pDest15 expression vectors, the T7 and T7 reverse primers were used to verify proper insertion. The Merlin FERM F3 primer was used to sequence nucleotide changes and deletions in the center of the ORF of Merlin for all DNA constructs. DNA was purified using 5 mL cultures grown at 37°C overnight for minipreps (Qiagen #27106). Maxipreps (Qiagen #12163) were done with 250 mL cultures grown overnight at 37°C. However, pDest14 (Invitrogen #11801016) expression constructs require at least a 500 mL culture grown overnight at 37°C for maxipreps.

Table 2-1: Touchdown PCR Program

Step	Process	Temp (°C)	Time (minutes)
1	Initial Denaturation	98	1:00
2	Denaturation	98	0:30
3	Annealing	65-50*	0:30
4	Extension	72	**
5	Repeat steps 2-4	-	x29
6	Hold	4	-

*Annealing temperature decreases 0.5°C/cycle

**Extension time for Phusion polymerase is 15 sec/kb and 1 min/kb for PfuTurbo

2.2 Site Directed Mutagenesis

To change the amino acids at specific positions of Merlin, nucleotides were mutated using site directed mutagenesis. A full length Merlin ORF in pEntr/D entry vector was used as the template. Forward primers were designed with the desired nucleotide changes in the middle and with complementary sequence on either side (Appendix A). Reverse primers were complementary to the forward primers. Standard PCR was done using PfuTurbo (Agilent #600250-52). The PCR program is described in Table 2-1. The template was then digested using DpnI for 1 hour at 37°C and then 5 μL of the reaction mixture was used to transform competent DH5α cells using the same method as above, plated on LB + kanamycin (50 μg/mL) plates and incubated at 37°C overnight. Minipreps (Qiagen #27106) were used to purify the DNA and sequencing to detect the mutation was done using the same method stated above.

2.3 Deletion Constructs

To remove specific amino acid sequences in Merlin, corresponding nucleotides in the ORF were deleted. A full length Merlin ORF in pEntr/D entry vector was used as the template. Primers flanking the desired region to be deleted were used with the same touchdown PCR program as above (Table 2-1, Appendix A). The linear PCR products were digested with DpnI at 37°C for an hour to remove

the methylated template then run out on a 0.8% w/v agarose gel and extracted with a gel extraction kit (Qiagen #28704). Purified linear PCR products (100-200 ng) were phosphorylated with 1 μL 10 U/μL T4 Kinase (Invitrogen #18004010) at 37°C for one hour. To self-ligate, 2 μL 1 U/μL T4 ligase (Invitrogen #15224017) was added and left overnight at room temperature. Half of the reaction mixture was used to transform DH5α cells and the cells were plated on LB + kanamycin (50 μg/mL) plates. DNA was purified using minipreps (Qiagen #27106) and sequenced to ensure the correct sequence was deleted.

2.4 GST Protein Expression and Purification

BL21 DE3 cells (Invitrogen) were transformed with pDest15 (Invitrogen #11802014) vectors containing the gene of interest and plated on LB + ampicillin (100 μg/mL) plates. Single colonies were grown in 5 mL YT media (8 g tryptone, 5 g yeast extract, 2.5 g NaCl per litre) for 8 hours at 37°C, then seeded into 500 mL YT media overnight (16-18 hrs) at 18°C. The cultures were induced with 250 μL of 1M IPTG (final concentration of 0.5 mM) for 4 hours at 18°C. Individual cultures were centrifuged at 4000x gravity for 10 minutes and resuspended in 45 mL of cold 1x PBS with EDTA free protease inhibitors (Roche #11873580001). The cultures were then transferred to 50 mL conical tubes and sonicated for 3-5 minutes on ice with the macro tip at power level 10 and 60% duty cycle. After sonication, 5 mL

of 20% v/v Triton-X 100 (final concentration of 2%) was added to each tube and rocked at room temperature for 30 minutes. Lysates were centrifuged at 12000x gravity for 10 minutes and transferred to a new 50 mL conical tube. Glutathione sepharose 4B beads (GE Healthcare #17-0756-01, 70% slurry in methanol) were washed with 1x PBS. The beads were made into 50% slurry by adding as much 1x PBS as there were beads after removing the wash (100 μL 1x PBS per 100 μL beads). The beads were then added to the lysate and incubated overnight at 4°C on a rocker. Depending on the protein, different amounts of beads were used. For example, GST-Sip1 was very soluble and expressed well so 800 μL-1000 μL of bead slurry was added per 50 mL tube of lysate while GST-Merlin was very insoluble or not expressed well and only 100-200 μL of bead slurry was added per 50 mL tube of lysate. Lysates were poured through disposable Bio-rad columns (#731-1550) and allowed to flowthrough by gravity and then washed with 200x bead volume of 1x PBS. Beads were transferred into 1.5 mL microfuge tubes, 1 μL of 10% w/v sodium azide was added per each mL of bead slurry and stored at 4°C. A 5 μL bead sample was run out on SDS-PAGE and stained with Biosafe coomasie (Biorad #7664-38-2) to check for protein expression. The amount of protein was also compared to BSA loading standards of 1 μg, 2 μg, 4 μg, and 8 μg.

2.5 Protein Labelling with ^{35}S Methionine

Proteins were made with quick coupled transcription and translation kits (Promega #L1170) with EasyTag ^{35}S Methionine (PerkinElmer #NEG709A500UC). The desired protein coding sequences were cloned into pDest14 (Invitrogen #11801016) vectors and 2 μg of DNA was used per 50 μL TnT reaction. The pDest14 vector has a T7 promoter and no epitope tags. TnT reactions were incubated at 30°C for 1-1.5 hours. Protein reactions were brought up to a total volume of 100 μL with AC buffer (10% v/v glycerol, 100 mM NaCl, 20 mM Tris pH 7.6, 0.5 mM EDTA, 0.1% v/v Tween-20) and spun through columns made with G-25 sephadex (Amersham Biosciences #17-0032-01). The G-25 sephadex allows large molecules to flowthrough and filters out unincorporated amino acids and other small components. The G-25 sephadex columns were made using 1mL tuberculin needles (Becton, Dickinson and Company #309623) without the needle attached. A small amount of glass wool was compressed at the bottom to act as a frit and a final volume of 1 mL of packed G-25 sephadex was in each column. A 50% G-25 sephadex slurry was allowed to drip through the column until the sephadex filled the column to the top. Then the columns were centrifuged at 2000 rpm using a centrifuge. Columns were washed 3 times with 100 μL of AC buffer before use.

2.6 GST Affinity Chromatography

The purified protein was measured using a scintillation counter and diluted with AC buffer (10% v/v glycerol, 100 mM NaCl, 20 mM Tris pH 7.6, 0.5 mM EDTA, 0.1% v/v Tween-20) to 10000 cpm so that the amount of protein used for each affinity chromatography was similar. For each affinity chromatography, 20-25 μL (50-100 μg of purified protein) of GST protein beads were used with 90 μL of diluted radiolabelled protein. GST only protein beads were used as negative controls. The total volume of each GST affinity chromatography experiment was brought up to 300 μL using AC buffer and placed on a rocker overnight at 4°C. Each tube was centrifuged at 900x gravity for 30 seconds and the flowthrough was transferred to a new 1.5 mL tube. 100 μL of 4x SDS sample buffer (200 mM Tris pH 6.8, 8% w/v SDS, 40% v/v glycerol, 20 mM DTT, 0.05% w/v bromophenol blue) was also added to the flowthrough. GST protein beads were washed 3 times with 400 μL AC buffer and centrifuged at 900x gravity for 30 seconds each time. Each tube was inverted several times per wash. Following the final wash, proteins were boiled in 300 μL of 1x PBS (154 mM NaCl, 14 mM Na_2HPO_4, 7 mM NaH_2PO_4) and 100 μL of 4x SDS sample buffer and used as the eluate. This ensured that both the eluate and flowthrough have the same total volume and the same volume of both the eluate and flowthrough (15 μL) is loaded for SDS-PAGE. For

proteins with sizes larger than 30 kD, 10% acrylamide gels were used. For proteins with sizes smaller than 30 kD, 18% acrylamide gels were used. Gels were run at 180 V for 1 hour. Gels were dried using a gel dryer at 80°C for one hour. X-ray film was then placed on the gels and exposed at room temperature for 20-48 hours.

2.7 Binding Assay

Using a constant volume of 25 μL of GST protein beads, a series of GST affinity chromatography experiments were set up with an increasing amount of radiolabelled protein. The total volume was then brought up to 300 μL using AC buffer (10% v/v glycerol, 100 mM NaCl, 20 mM Tris pH 7.6, 0.5 mM EDTA, 0.1% v/v Tween-20). 1 μL of the input protein in 5 mL of scintillation fluid was measured using the scintillation counter. The flowthrough was discarded and beads were washed 3 times with 400 μL of AC buffer. Eluate was made with 225 μL of 1x PBS (154 mM NaCl, 14 mM Na_2HPO_4, 7 mM NaH_2PO_4) and 75 μL of 4x SDS sample buffer (200 mM Tris pH 6.8, 8% w/v SDS, 40% v/v glycerol, 20 mM DTT, 0.05% w/v bromophenol blue) so the bound protein is evenly distributed in the eluate. 10 μL of eluate in 5 mL of scintillation fluid was measured using a scintillation counter. Due to lower radioactivity of the eluate, the measurements were more accurate with a higher volume.

2.8 Data Analysis of Binding Assays

The results from the binding assays were graphed on Microsoft Excel scatterplot graphs with the input cpm/μL on the horizontal axis and eluate cpm/μL on the vertical axis. Figure 2-1 is an example of the curves used and the data is summarized into bar graphs described below. Using Microsoft Excel, a logarithmic trendline was applied to the full length Merlin control data and an equation for the line was obtained for each set of binding assays. Using these equations, radioactive input protein values obtained experimentally with the different deletion constructs were used to calculate a corresponding full length Merlin control eluate value at that exact experimental protein input value. The experimental eluate values were divided by the calculated full length control eluate value to obtain a ratio. This ratio was converted to a percentage and displayed on a bar graph and represents the amount of binding relative to full length Merlin. The ratios for the same Merlin constructs compared to the full length Merlin for different sets of experiments yielded similar ratios and were averaged. Error bars were calculated using standard error. Loss of methionines was accounted for by dividing the counts obtained by the percentage of remaining methionines.

Figure 2-1: Example of titration curves used for binding assays

Using a constant amount of GST protein beads, a series of GST affinity chromatography experiments were set up with an increasing amount of radiolabelled protein. The input and eluate were measure using a scintillation counter and graphed using Microsoft Excel. By comparing the counts obtained from different deletion constructs to full length Merlin, the amount of binding to GST-Sip1 can be obtained. Different deletion constructs can then be compared to each other. GST only beads were used here to show that the binding was specific to GST-Sip1.

A) Titration curve using full length Merlin protein.

B) Titration curve using Merlin protein with the 100 amino acid deletion of the potential Sip1 binding domain

A)

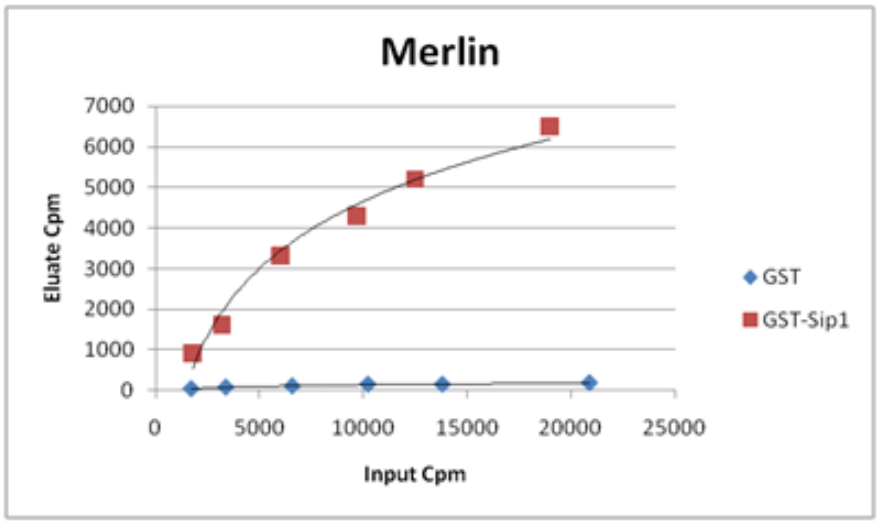
Merlin
7000
6000
5000
4000
3000
2000
1000
0
Eluate Cpm
0
5000
10000
15000
20000
25000
Input Cpm
GST
GST-Sip1

B)

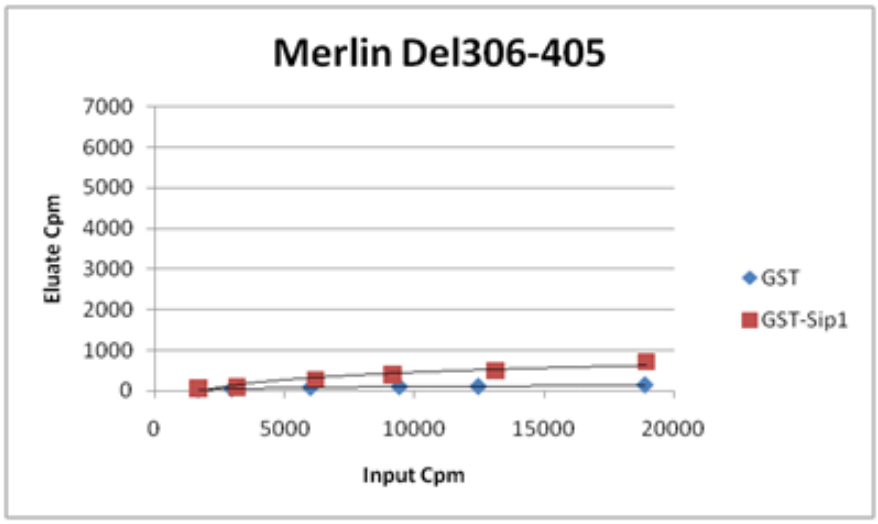
Merlin Del306-405
7000
6000
5000
4000
3000
2000
1000
0
Eluate Cpm
0
5000
10000
15000
20000
Input Cpm
GST
GST-Sip1

Figure 2-1

2.9 Cell Transfections

Drosophila Schneider 2 (S2) cells were grown in serum free insect media (SFX, Thermo Scientific #SH30278.01) + pen/strep (final concentration of 1% w/v, Invitrogen #15070-063) media at 25°C. Transfections for pulse chase experiments were carried out in 6 well plates. S2 cells were diluted to 10^6 cells/mL per well and each well had a total of 3 mL. The media was replaced with SFX media during cell transfections. A 2:1 solution of dimethyl-dioctadecylammonium bromide (DDAB, Sigma #382310), the transfection reagent, to SFX was mixed and incubated for 5 min. For 6 well plates, 180 μL (120 μL DDAB and 60 μL SFX) was used per well. The desired GFP tagged Merlin DNA construct under the control of a heat shock promoter was then added to this solution at a concentration of 2 μg/well and let sit for at least 20 minutes. The DNA mixture was added to each well of cells directly and swirled around. Transfections were incubated at 25 C for ~48 hours before use.

2.10 Pulse Chase Assay

DNA constructs with GFP tagged Merlin under a heat shock inducible promoter in S2 cells were transfected into S2 cells. Transfected S2 cells in 6 well plates were heat shocked at 37°C for 30 minutes and then returned to the 25°C incubator. Heat shock induces a pulse of protein expression and protein localization can be followed

over time using the GFP tag. 1 mL samples of cells were taken at 1 hour after heat shock, 3 hours after heat shock, and 6 hours after heat shock and centrifuged at 500x gravity for 30 seconds three times, each time rotating the tube 180°. The media was removed and replaced with 750 μL of 2% w/v paraformaldehyde and fixed for 15 minutes at room temperature. Cells were centrifuged again using the same method, the fix was removed and the cells were washed once with 1 mL sterile 1x PBS (154 mM NaCl, 14 mM Na_2HPO_4, 7 mM NaH_2PO_4). Cells were centrifuged once more the same way and resuspended in 20 μL of ProLong Gold fluorescent mounting media (Invitrogen #P36930). Finally, the cells were mounted onto microscope slides. Cells were analyzed under a fluorescent microscope (Carl Zeiss Axioskop) using oil immersion with a 100x magnification objective lens (Plan Neofluor, NA 1.3) and categorized according to the phenotypes reported in Hughes and Fehon, 2006.

2.11 Cell Immunostaining for Slik

1 mL of cells was taken and centrifuged using the above method. The media was removed and replaced with 750 μL of 2% w/v paraformaldehyde and fixed for 15 minutes at room temperature. The cells were centrifuged each time the solution needed to be changed or removed. 1 mL of 1x PBS (154 mM NaCl, 14 mM Na_2HPO_4, 7 mM NaH_2PO_4) was used to wash cells once then cells were incubated with

primary antibody (guinea pig anti-Slik, 1:10000) in 1x PBS + 1% v/v Normal Goat Serum + 0.1% w/v Saponin (PSN) at room temperature for 60-90 minutes. Cells were incubated with secondary antibody (goat Cy3 anti-guinea pig, 1:500) in PSN for 30-45 minutes. Cells were resuspended in 20uL of ProLong Gold fluorescent mounting media (Invitrogen #P36930) and mounted onto microscope slides (Fisher Scientific #12-552-5). Slides were analyzed using the same microscope and lens as the pulse chase assays.

2.12 Protein Sequence Alignment

Protein sequences were aligned using an interactive structure based sequences alignment program called STRAP (Gille and Frommel, 2001). This program can be downloaded for free at http://3d-alignment.eu/. Protein sequences were loaded into the program and aligned. The aligned sequences were then exported into a Microsoft Word document.

Chapter Three:

Interaction Analysis of Merlin, Moesin and Sip1

3.1 Introduction

Merlin interacts with many different proteins as discussed in Chapter 1. Due to Merlin being a part of different protein complexes, this suggests that formation of protein complexes may be required for Merlin tumour suppressor activity. ERM proteins interact with EBP50 via their FERM F3 subdomain and this interaction was inhibited when the ERM proteins were in a closed, hypophosphorylated conformation (Finnerty et al., 2004; Pearson et al., 2000). Although the FERM domain of human Merlin is sufficient for binding to EBP50, the specific amino acids required for the interaction between human Merlin and EBP50 have not yet been determined (Nguyen et al., 2001). To understand how interaction with EBP50 affects Merlin function, we first have to determine the interaction domains between Merlin and EBP50. To study this interaction, homologs of Merlin, ERMs (Moesin) and EBP50 (Sip1) in *Drosophila* will be used. This will allow us to determine how a complex between Merlin and Sip1 and Moesin and Sip1 is formed. These interactions will then offer us insight into how Merlin and Moesin are regulated.

3.2 Identifying the Moesin and Merlin Sip1 binding domains

To determine the specific amino acids required for interaction between Merlin and Sip1 and Moesin and Sip1, ^{35}S radiolabelled Merlin and Moesin proteins were incubated with GST tagged full

length Sip1 protein (GST-Sip1) coupled to glutathione sepharose beads in GST affinity chromatography experiments and visualized by autoradiography (Figure 3-1, 3-2, 3-3). Radiolabelled proteins are unmodified because they are made using *in vitro* transcription and translation reactions and no post translational modifications should occur. Consistent with research using human ERMs, the full length unmodified Moesin protein did not bind to GST-Sip1 because the unphosphorylated form of Moesin should be closed and unable to interact with other proteins (Figure 3-2) (Reczek and Bretscher, 1998). In contrast, the full length unmodified Merlin protein can bind to GST-Sip1 in the GST affinity chromatography assay (Figure 3-3).

To determine the interaction domains between Merlin or Moesin and Sip1, radiolabelled proteins of specific regions within Merlin or Moesin were used (Figure 3-1). The interaction domain of Moesin and Ezrin to EBP50 is at the C-terminal end of EBP50 (Finnerty et al., 2004; Nguyen et al., 2001; Reczek and Bretscher, 1998). Therefore, to determine the binding region of Sip1, a GST tagged Sip1 construct lacking the C-terminal 50 amino acids (GST-Sip1 1-246) and a GST tagged Sip1 construct containing only the C-terminal 50 amino acids were made (GST-Sip1 247-296; Figure 3-1).

The protein corresponding to the FERM domain of Moesin (Moesin FERM) binds to both GST-Sip1 and GST-Sip1 247-296 while

the protein corresponding to the C-terminal tail of Moesin (Moesin CC Tail) shows no binding to any of the GST-Sip1 constructs (Figure 3-2). The FERM F3 subdomain of Moesin (Moesin F3) binds to GST-Sip1 and GST-Sip1 247-296 (Figure 3-2). Binding between GST tagged full length Sip1 and the FERM F1 subdomain of Moesin (Moesin F1) can also be detected, which has not been previously shown (Figure 3-2). There is no detectable binding between the FERM F2 subdomain of Moesin (Moesin F2) and GST-Sip1 (Figure 3-2).

In contrast, the protein corresponding to the FERM domain of Merlin (Merlin FERM) and the protein corresponding to the C-terminal tail of Merlin (Merlin CC Tail) both bind to GST-Sip1 and GST-Sip1 247-296 (Figure 3-3). The FERM F3 subdomain of Merlin (Merlin F3) does not bind to any of the GST-Sip1 proteins but the proteins corresponding to FERM F1 (Merlin F1) and FERM F2 (Merlin F2) subdomain proteins of Merlin show binding to GST-Sip1 and GST-Sip1 247-296 (Figure 3-3). Interestingly, the protein of the 100 amino acids immediately following the FERM domain of Merlin (Merlin 306-405) clearly binds to both GST-Sip1 and the GST-Sip1 247-296 (Figure 3-3). Proteins corresponding to the remaining regions of the C-terminal tail of Merlin, amino acids 406-480

Figure 3-1: Schematic diagram of Sip1, Moesin, and Merlin protein constructs used in the mapping of specific interaction domains

GST tagged Sip1 protein constructs: GST tagged Sip1 proteins were expressed in *E. coli* and purified using glutathione sepharose beads. GST tagged full length Sip1 (GST-Sip1), GST tagged Sip1 construct lacking the C-terminal 50 amino acids (GST-Sip1 1-246) and a GST tagged Sip1 construct containing only the C-terminal 50 amino acids (GST-Sip1 247-296) were made.

^{35}S radiolabelled Merlin and Moesin proteins: Proteins were made using an *in vitro* rabbit reticulocyte system and radiolabelled with ^{35}S methionine. The amino acid positions of the amino acids included in each protein in relation to the full length protein are displayed.

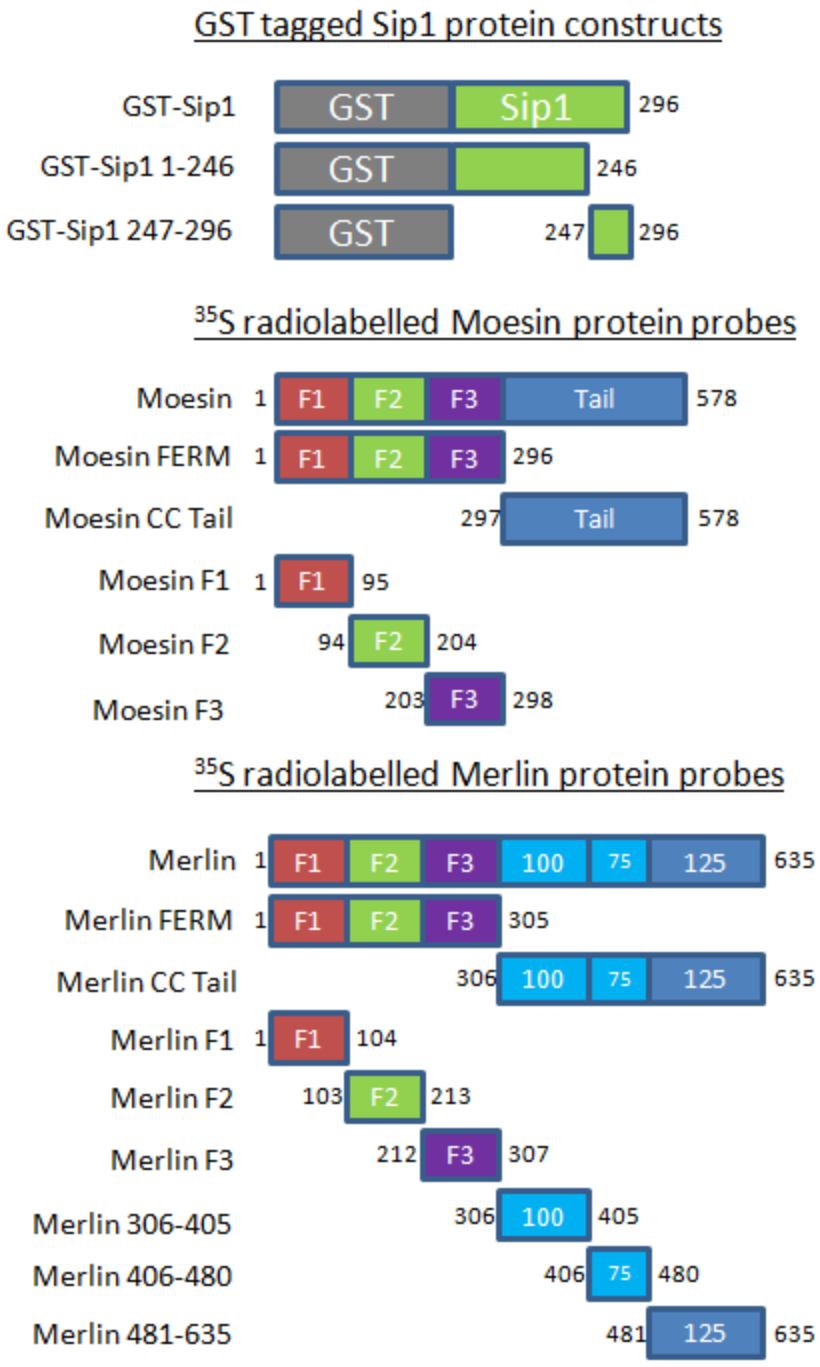
GST tagged Sip1 protein constructs
GST-Sip1
GST
Sip1
296
GST-Sip1 1-246
GST
246
GST-Sip1 247-296
GST
247
296
35S radiolabelled Moesin protein probes
Moesin
1
F1
F2
F3
Tail
578
Moesin FERM
1
F1
F2
F3
296
Moesin CC Tail
297
Tail
578
Moesin F1
1
F1
95
Moesin F2
94
F2
204
Moesin F3
203
F3
298
35S radiolabelled Merlin protein probes
Merlin
1
F1
F2
F3
100
75
125
635
Merlin FERM
1
F1
F2
F3
305
Merlin CC Tail
306
100
75
125
635
Merlin F1
1
F1
104
Merlin F2
103
F2
213
Merlin F3
212
F3
307
Merlin 306-405
306
100
405
Merlin 406-480
406
75
480
Merlin 481-635
481
125
635

Figure 3-1

Figure 3-2: FERM F3 subdomain of Moesin binds to GST-Sip1

Full length Moesin protein exhibits no binding to GST-Sip1. The Moesin FERM protein binds to both GST-Sip1 and GST-Sip1 247-296 while the Moesin CC Tail protein shows no binding with any of the GST-Sip1 constructs. The Moesin F3 protein binds to GST-Sip1 and GST-Sip1 247-296. Binding between GST-Sip1 and the Moesin F1 protein can also be detected. There is no detectable binding between the Moesin F2 protein and GST-Sip1. GST protein bound to glutathione sepharose beads are used as negative controls.

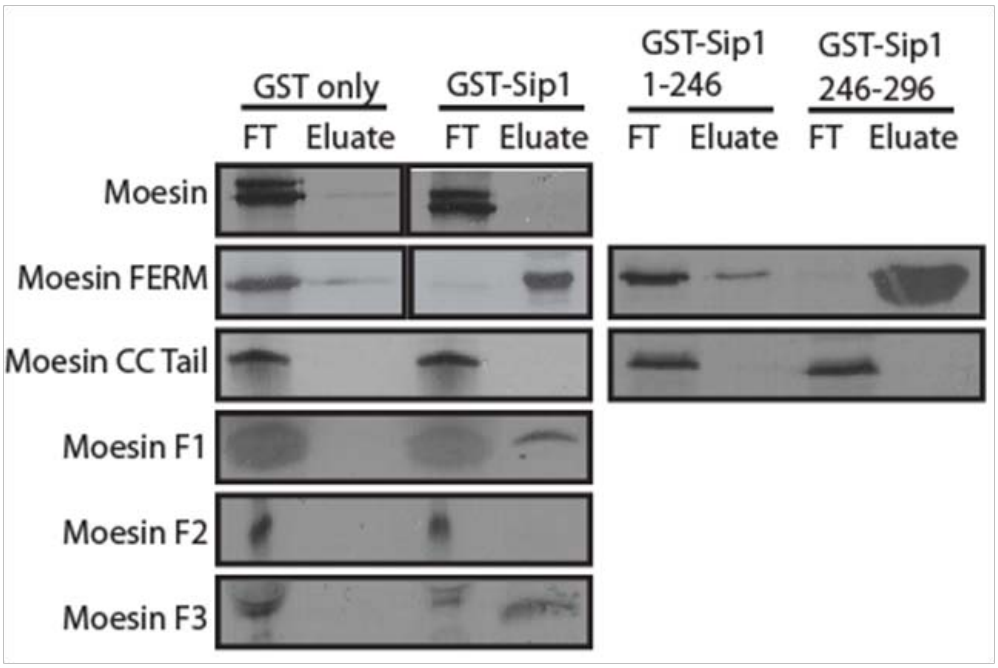
GST only
GST-Sip1
GST-Sip1 1-246
GST-Sip1 246-296
FT Eluate FT Eluate FT Eluate FT Eluate
Moesin
Moesin FERM
Moesin CC Tail
Moesin F1
Moesin F2
Moesin F3

Figure 3-2

Figure 3-3: Full length Merlin can interact with GST-Sip1

Full length Merlin protein can bind to both GST-Sip1 and GST-Sip1 247-296. The Merlin FERM protein and Merlin CC Tail protein are both sufficient for binding to GST-Sip1 and GST-Sip1 247-296. There is no binding between the Merlin F3 protein and GST-Sip1 or GST-Sip1 247-296, but the Merlin F1 and Merlin F2 proteins show some binding to GST-Sip1 and GST-Sip1 247-296. The Merlin 306-405 protein is clearly sufficient for binding to both GST-Sip1 and the GST-Sip1 247-296. The Merlin 406-480 and Merlin 481-635 proteins exhibit no binding to any of the GST-Sip1 proteins. The Merlin 306-355, Merlin 330-380, and Merlin 356-405 proteins are not sufficient for binding to any of the GST-Sip1 proteins. GST protein bound to glutathione sepharose beads are used as negative controls.

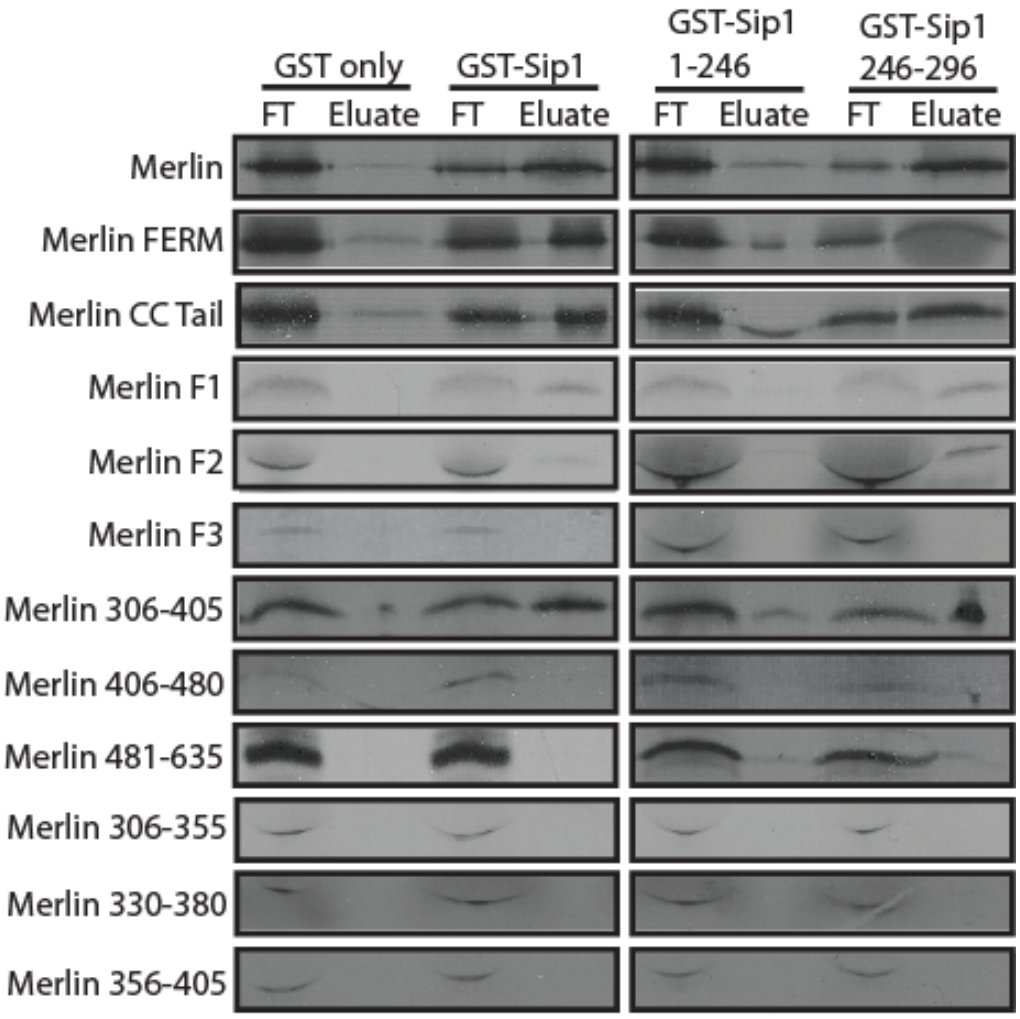
GST only
GST-Sip1
GST-Sip1 1-246
GST-Sip1 246-296
FT
Eluate
FT
Eluate
FT
Eluate
FT
Eluate
Merlin
Merlin FERM
Merlin CC Tail
Merlin F1
Merlin F2
Merlin F3
Merlin 306-405
Merlin 406-480
Merlin 481-635
Merlin 306-355
Merlin 330-380
Merlin 356-405

Figure 3-3

and amino acids 481-635 (Merlin 406-480, Merlin 481-635), show no binding to any of the GST-Sip1 proteins (Figure 3-3). Secondary structures necessary for protein interaction may be lost using proteins of only 50 amino acids. This may account for the proteins corresponding to amino acids 306-355, 330-380, and 356-405 of Merlin (Merlin 306-355, Merlin 330-380, Merlin 356-405) not binding to any of the GST-Sip1 proteins (Figure 3-3).

3.3 The coiled-coiled region of Merlin is necessary for Sip1 binding

GST affinity chromatography experiments using Merlin protein lacking the 100 amino acids immediately downstream of the FERM domain of Merlin (Merlin Δ306-405) results in a loss of binding to GST-Sip1 protein (Figure 3-4 B). Since the 100 amino acids (Merlin 306-405) are both necessary and sufficient for binding, this region was identified as a potential Sip1 binding domain (Figure 3-3, Figure 3-4B). However, deletion constructs in which 50 amino acid regions were removed within this potential Sip1 binding domain showed partial binding to GST-Sip1 protein in GST affinity chromatography experiments which made it difficult to ascertain which of the amino acids are most important for binding to Sip1 (Figure 3-4 B). To further analyze this binding region, a binding assay was used to quantify the amount of binding of different deletion constructs to GST-Sip1 protein. The

binding assay is performed using a series of GST affinity chromatography experiments with a constant amount of GST-Sip1 protein bound to glutathione sepharose beads incubated with increasing amounts of ^{35}S radiolabelled proteins corresponding to each of the deletion constructs. The input and eluate were measured using a scintillation counter. A control using full length Merlin protein was used for each binding assay and the eluate counts from proteins with different amino acid deletions were compared to the counts from full length Merlin to obtain a percentage of binding relative to the full length Merlin protein. The percentages obtained from the different deletion constructs could then be compared to determine which deletion construct results in the greatest loss of binding; thereby suggesting those amino acid regions as the most important for binding to Sip1 (Chapter 2.7-2.8, Figure 2-1).

Merlin deletion constructs encoding for proteins lacking the full 100 amino acids of the potential Sip1 binding domain (Δ306-405), the first 50 amino acids of the potential Sip1 binding domain (Δ306-355), the middle 50 amino acids of the potential Sip1 binding domain (Δ330-380), and the last 50 amino acids of the potential Sip1 binding domain (Δ356-406) were used to compare binding to GST-Sip1 protein (Figure 3-4 C). The Merlin Δ306-355 protein results in the greatest loss of binding to GST-Sip1 protein when compared to full length Merlin

protein (Merlin) (Figure 3-4 C). The loss of binding of the Merlin Δ306-355 protein to GST-Sip1 protein is similar to the loss of binding of the Merlin Δ306-405 protein to GST tagged full length Sip1 (Figure 3-4 C). The proteins of Merlin Δ330-380 and Merlin Δ356-405 both results in more binding to GST-Sip1 protein compared to proteins of Merlin Δ306-355 and Merlin Δ306-405 (Figure 3-4 C). The results obtained from the binding assays and the results in the GST affinity chromatography experiments indicate that the most important amino acids for Merlin Sip1 binding lies within amino acids 306-380 (Figure 3-4 B, C).

To further narrow down the most important amino acids for binding to Sip1, proteins of Merlin constructs with 15 amino acid overlapping deletions in amino acids 306-380 of the Sip1 binding region were used for binding assays (Figure 3-5 A). The Merlin deletion constructs lacking amino acids 356-370 (Δ356-370) and 366-380 (Δ366-380) serve as additional controls since the deletions past the first 50 amino acids of the potential Sip1 binding domain do not have as much of an effect on the binding to GST-Sip1 protein compared to deletions within the first 50 amino acids of the Sip1 binding region (Figure 3-4 C, Figure 3-5 A). Merlin proteins lacking the amino acids 316-330 (Δ316-330) and 326-340 (Δ326-340) results in the least binding to GST-Sip1 when compared to full length Merlin (Figure 3-5 B). As well, this

loss of binding is comparable to that observed with the radiolabelled Merlin Δ306-405 protein (Figure 3-5 B). The radiolabelled Merlin proteins lacking amino acids 306-320 (Δ306-320), 336-350 (Δ336-350), 346-360 (Δ346-360), 356-370 (Δ356-370), and 366-380 (Δ366-380) all results in more binding to GST-Sip1 protein when compared to the Merlin Δ316-330, Δ326-340 and Δ306-405 proteins (Figure 3-5 B). These results indicate that the most important amino acids for Sip1 binding in the potential Sip1 binding domain are within the amino acids 320-335 of Merlin.

To further validate the binding assay, Merlin proteins containing the first 405 (1-405), 480 (1-480) and 600 (1-600) amino acids were used (Figure 3-6 A). These constructs were chosen because they lack amino acids downstream of the potential Sip1 binding domain and deletion of amino acids outside of the potential Sip1 binding domain should have less effect on Merlin Sip1 binding. As expected, there was more binding to GST-Sip1 with Merlin 1-405, 1-480, and 1-600 proteins than Merlin proteins with deletions in the potential Sip1 binding domain (Figure 3-6 B). This suggests that the structure of Merlin is sensitive to deletions in the potential Sip1 binding domain. It also suggests that the amino

Figure 3-4: Amino acids 306-405 of Merlin is necessary for binding to GST-Sip1

A) Schematic diagram summarizing the amino acid deletions in the Merlin deletion constructs used for GST affinity chromatography experiments and binding assays.

B) GST affinity chromatography experiments using ^{35}S radiolabelled Merlin proteins with amino acid deletions in the potential Sip1 binding domain. GST protein bound to glutathione sepharose beads were used as negative controls. The Merlin Δ306-405, Δ306-355, and Δ330-380 proteins showed a loss of binding to GST-Sip1. The Merlin Δ356-405 protein still shows some binding when compared to the GST only control.

C) Binding assay with Merlin deletion constructs. Refer to Chapter 2.7-2.8 for experimental details. Error bars indicate standard deviation. The Merlin Δ306-405, Δ306-355, and Δ330-380 proteins show the greatest loss of binding to GST-Sip1as compared to full length Merlin and are consistent with the GST affinity chromatography experiments.

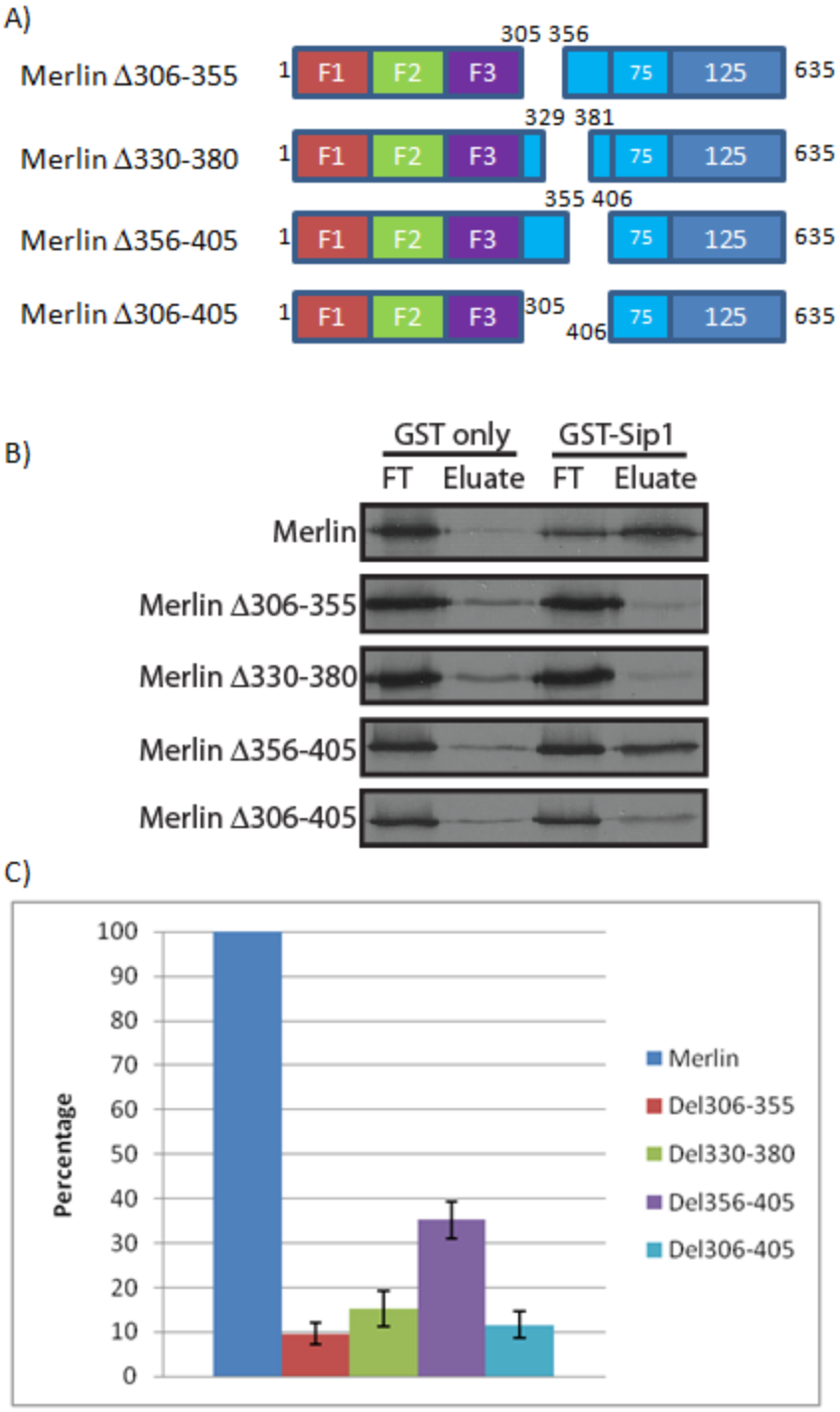
A)
Merlin Δ306-355
Merlin Δ330-380
Merlin Δ356-405
Merlin Δ306-405
1
F1
F2
F3
305 356
329 381
355 406
305
406
75
125
635
B)
GST only
GST-Sip1
FT
Eluate
FT
Eluate
Merlin
Merlin Δ306-355
Merlin Δ330-380
Merlin Δ356-405
Merlin Δ306-405
C)
Percentage
100
90
80
70
60
50
40
30
20
10
0
Merlin
Del306-355
Del330-380
Del356-405
Del306-405

Figure 3-4

Figure 3-5: Deletion of amino acids 316-330 and 326-340 of Merlin results in the least binding to GST-Sip1

A) Schematic diagram summarizing the 15 amino acid regions in the potential Sip1 binding domain that were removed in the deletion constructs for the binding assays below.

B) Binding assays using deletion constructs with 15 amino acid deletions. Refer to Chapter 2.7-2.8 for experimental details. The Merlin Δ316-330 and Δ326-340 proteins result in the greatest loss of binding to GST-Sip1 when compared to full length Merlin protein. As well, this loss of binding is comparable to the Merlin Δ306-405 protein. The Merlin Δ306-320, Δ336-350, Δ346-360, Δ356-370, and Δ366-380 proteins all result in more binding to GST-Sip1 when compared to the Merlin Δ316-330, Δ326-340 and Δ306-405 proteins. These results indicate that the most important amino acids for Sip1 binding in the potential Sip1 binding domain are within the amino acids 320-335 of Merlin.

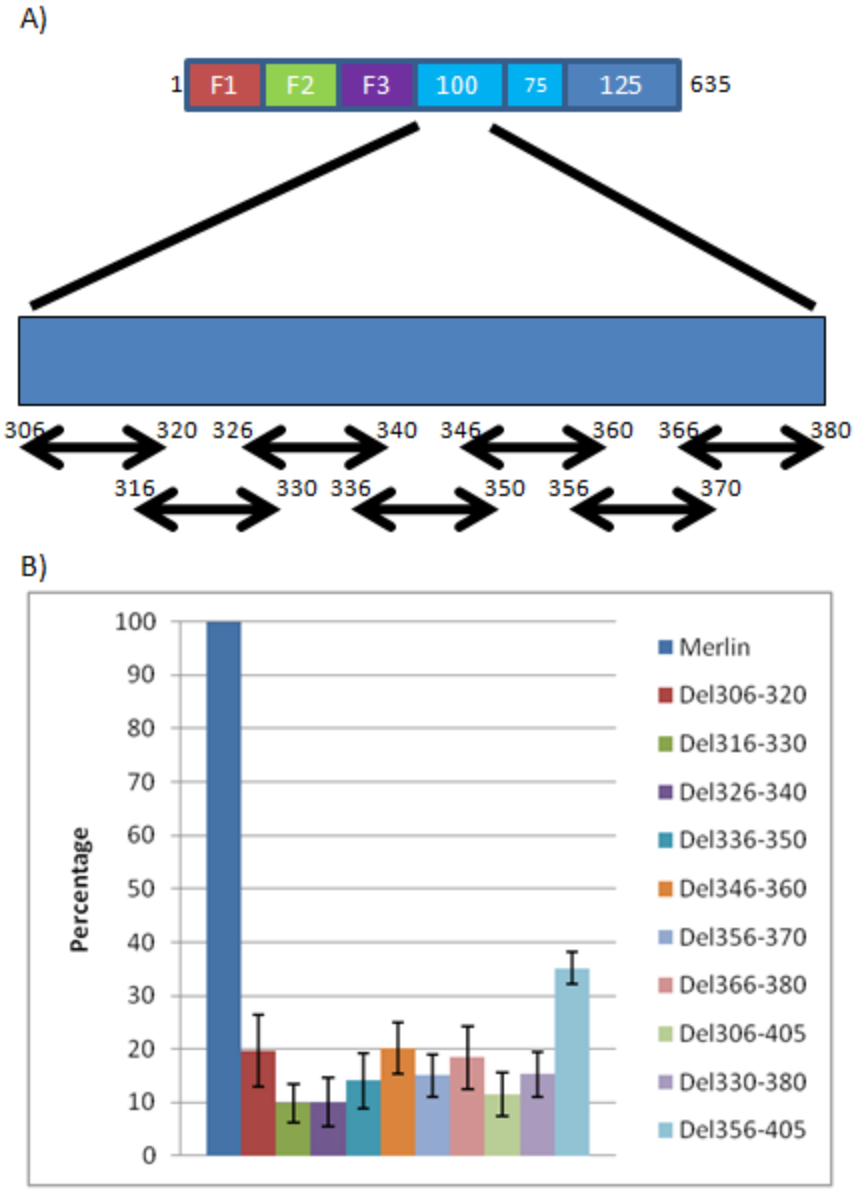
A)
1
F1
F2
F3
100
75
125
635
306
320
326
340
346
360
366
380
316
330
336
350
356
370
B)
Percentage
100
90
80
70
60
50
40
30
20
10
0
Merlin
Del306-320
Del316-330
Del326-340
Del336-350
Del346-360
Del356-370
Del366-380
Del306-405
Del330-380
Del356-405

Figure 3-5

Figure 3-6: Deletion of amino acids downstream of the potential Sip1 binding domain in Merlin affects binding to GST-Sip1 less

A) Schematic diagram of the Merlin deletion constructs used for the binding assay below.

B) A binding assay with Merlin 1-405, 1-480 and 1-600 proteins. Refer to Chapter 2.7-2.8 for experimental details. There was more binding to GST-Sip1 with Merlin 1-405, 1-480, and 1-600 proteins than Merlin proteins with deletions in the potential Sip1 binding domain.

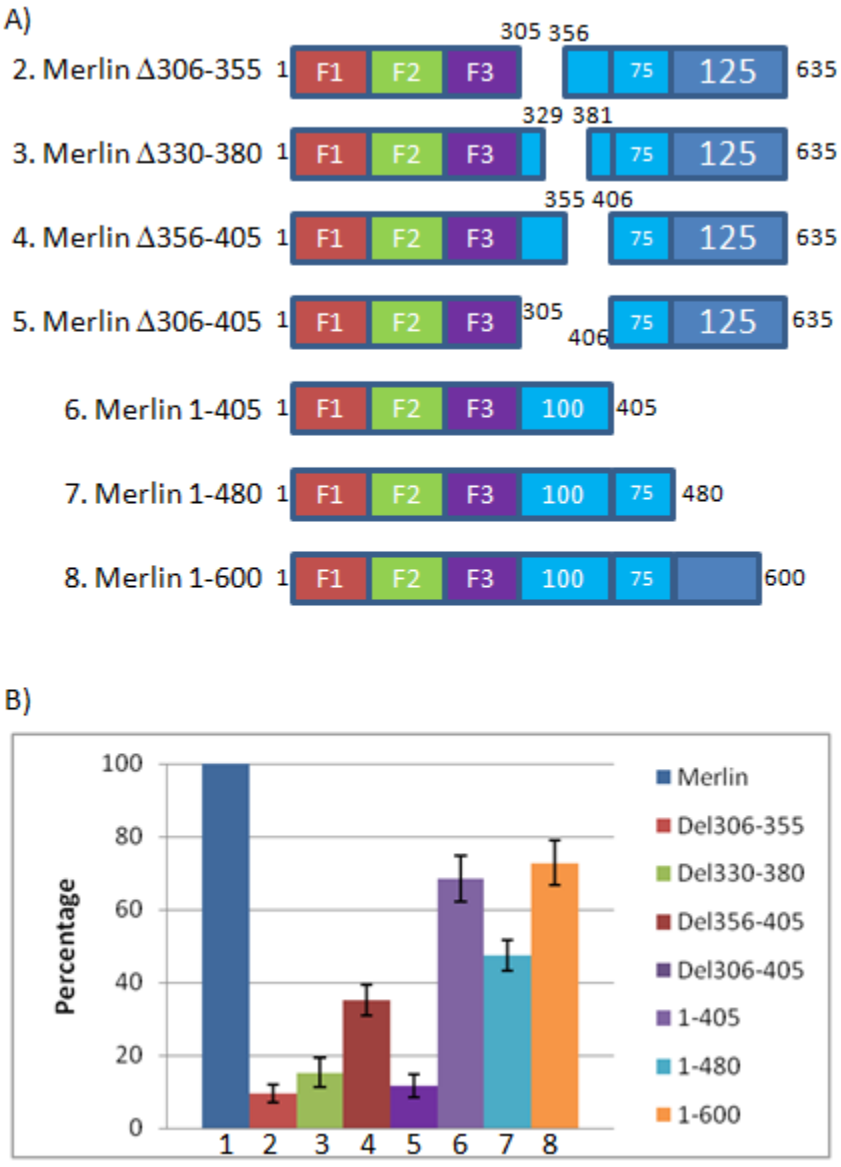
A)
2. Merlin Δ306-355
3. Merlin Δ330-380
4. Merlin Δ356-405
5. Merlin Δ306-405
6. Merlin 1-405
7. Merlin 1-480
8. Merlin 1-600
F1
F2
F3
75
125
100
305 356
329 381
355 406
635
600
405
480
B)
Percentage
Merlin
Del306-355
Del330-380
Del356-405
Del306-405
1-405
1-480
1-600

Figure 3-6

acids in the potential Sip1 binding domain are important for Merlin Sip1 binding. This binding assay is limited in that it can only suggest the regions which are most important for Merlin Sip1 interaction and does not determine which regions are not important.

3.4 Conserved arginine residues in amino acid region 320-335 of Merlin are necessary for interaction with Sip1

Protein alignments of Merlin across different species and human and *Drosophila* Moesin, revealed two conserved arginine residues (R325 and R335) between amino acids 320 and 335 in the potential Sip1 binding domain of Merlin (Figure 3-7). These arginines are not conserved in either human or *Drosophila* Moesin (Figure 3-7). To determine whether or not these two arginine residues play a role in Merlin Sip1 binding, the two arginine residues were replaced by Moesin residues at that position based on the protein alignment (Figure 3-7). Three different Merlin mutant constructs were created: one with an arginine to alanine substitution at amino acid position 325 (R325A), one with an arginine to leucine substitution at amino acid position 335 (R335L), and one with both substitutions (R325A R335L). Using GST affinity chromatography experiments, Merlin R325A and Merlin R335L proteins showed reduced binding to GST-Sip1 with Merlin R325A R335L protein showing even less binding to GST-Sip1 than either of the single substitutions alone (Figure 3-8 A). Binding assays for Merlin R325A, R335L, and R325A R335L proteins to

Figure 3-7: Sequence alignments of the potential Sip1 binding domain of Merlin protein from different species compared to Moesin protein from human and *Drosophila*

Sequence alignment of the potential Sip1 binding domain of: human Merlin (hMerlin), *Drosophila* Merlin (dMerlin), mouse Merlin (mMerlin), rat Merlin (rMerlin), *Xenopus* Merlin (xMerlin), and zebrafish Merlin (zMerlin) compared to human Moesin (hMoesin), *Drosophila* Moesin (dMoesin). Within amino acids 320-335 in dMerlin, there are two arginine residues (R325 and R335) that are conserved across different species of Merlin proteins but are not conserved in either human or *Drosophila* Moesin. The two conserved arginines are outlined in boxes. The same colour indicates amino acids with similar properties (Arginine and lysine are both positively charged and are blue or methionine and cysteine both contain sulphur and are yellow).

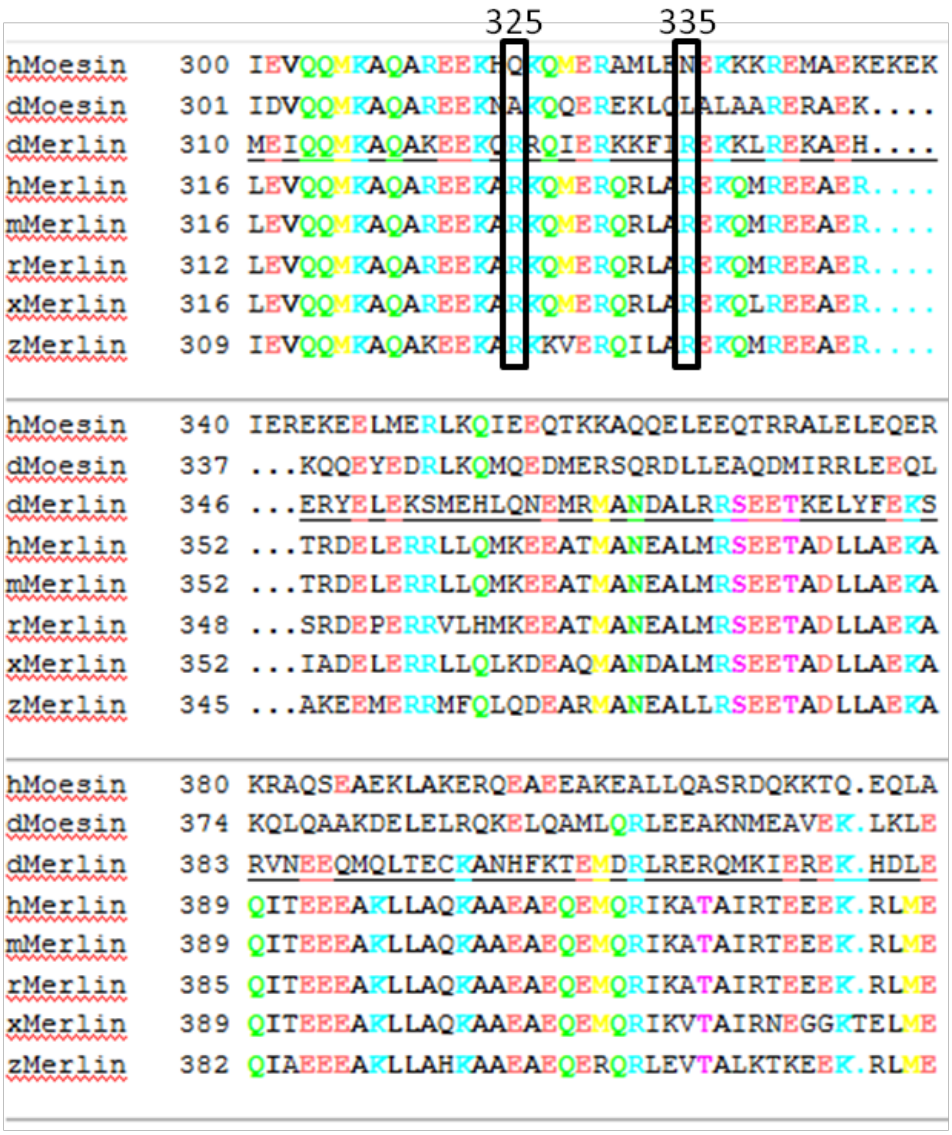
325
335
hMoesin 300 IEVQQMKAQAREEKHQKQMERAMLENEKKKREMAEKEKEK
dMoesin 301 IDVQQMKAQAREERNAKQQEREKLQLALAARERAEK....
dMerlin 310 MEIQQMKAQAKEEKQRRQIERKKFIREKKLREKAEH....
hMerlin 316 LEVQQMKAQAREEKARKQMERQRLAREKQMREEAER....
mMerlin 316 LEVQQMKAQAREEKARKQMERQRLAREKQMREEAER....
rMerlin 312 LEVQQMKAQAREEKARKQMERQRLAREKQMREEAER....
xMerlin 316 LEVQQMKAQAREEKARKQMERQRLAREKQLREEAER....
zMerlin 309 IEVQQMKAQAKEEKARKKVERQILAREKQMREEAER....
hMoesin 340 IEREKEELMERLKQIEEQTKKAQQELEEQTRRALELEQER
dMoesin 337 ...KQQEYEDRLKQMQEDMERSQRDLLEAQDMIRRLEEQL
dMerlin 346 ...ERYELEKSMEHLQNEMRMANDALRRSEETKELYFERS
hMerlin 352 ...TRDELERRLLQMKEEATMANEALMRSEETADLLAEKA
mMerlin 352 ...TRDELERRLLQMKEEATMANEALMRSEETADLLAEKA
rMerlin 348 ...SRDEPERRVLHMKEEATMANEALMRSEETADLLAEKA
xMerlin 352 ...IADELERRLLQLKDEAQMANDALMRSEETADLLAEKA
zMerlin 345 ...AKEEMERRMFQLQDEARMANEALLRSEETADLLAEKA
hMoesin 380 KRAQSEAEKLAKERQEAEEAKEALLQASRDQKKTQ.EQLA
dMoesin 374 KQLQAAKDELELRQKELQAMLQRLEEAKNMEAVEK.LKLE
dMerlin 383 RVNEEQMQLTECKANHFKTEMDRLRERQMKIERER.HDLE
hMerlin 389 QITEEEAKLLAQKAAEAEQEMQRIKATAIRTEEEK.RLME
mMerlin 389 QITEEEAKLLAQKAAEAEQEMQRIKATAIRTEEEK.RLME
rMerlin 385 QITEEEAKLLAQKAAEAEQEMQRIKATAIRTEEEK.RLME
xMerlin 389 QITEEEAKLLAQKAAEAEQEMQRIKVTAIRNEGGKTELME
zMerlin 382 QIAEEEAKLLAHKAAEAEQERQRLEVTALKTKEEK.RLME

Figure 3-7

Figure 3-8: Amino acid substitution of conserved arginines at amino acid position 325 and 335 of Merlin results in a loss of binding to GST-Sip1

A) GST affinity chromatography experiments with radiolabelled Merlin R325A and Merlin R335L proteins showed reduced of binding to GST-Sip1 with radiolabelled Merlin R325A R335L protein showing an even greater reduction in binding to GST-Sip1 than each of the single substitutions alone.

B) Binding assays for radiolabelled Merlin R325A, R335L, and R325A R335L proteins to GST-Sip1. Refer to Chapter 2.7-2.8 for experimental details. Both radiolabelled Merlin R325A and Merlin R335L proteins showed a large reduction in binding to GST-Sip1. Consistent with the GST affinity chromatography results, the radiolabelled Merlin R325A R335L protein showed less binding to GST-Sip1 than the proteins with single substitutions.

A)

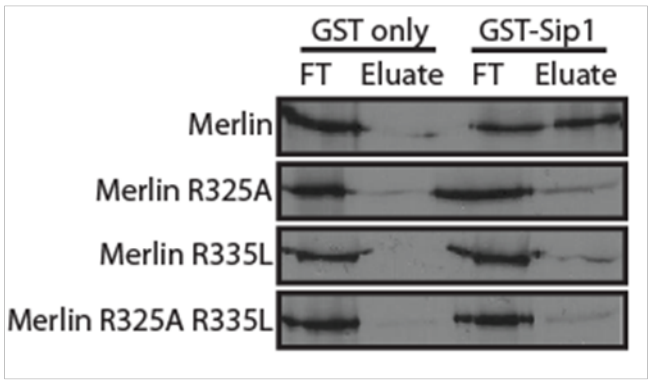
GST only
GST-Sip1
FT
Eluate
FT
Eluate
Merlin
Merlin R325A
Merlin R335L
Merlin R325A R335L

B)

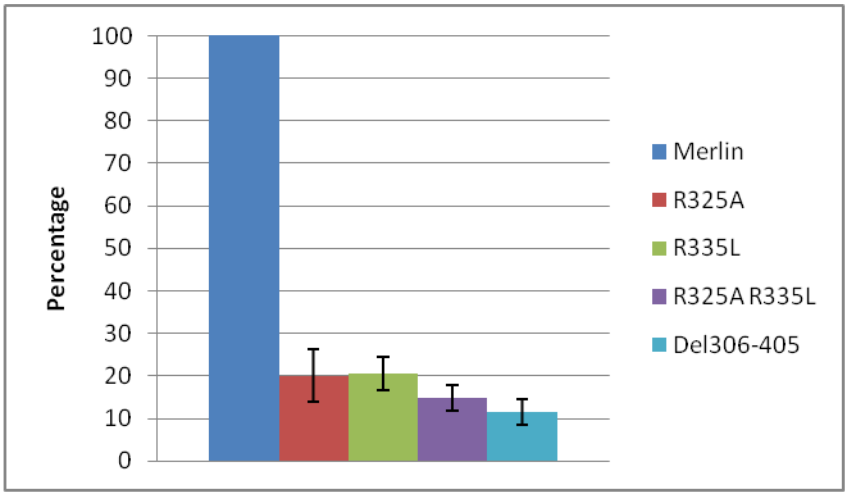
Percentage
100
90
80
70
60
50
40
30
20
10
0
Merlin
R325A
R335L
R325A R335L
Del306-405

Figure 3-8

GST-Sip1 were also carried out. Both Merlin R325A and Merlin R335L proteins showed a large reduction in binding to GST tagged full length Sip1 (Figure 3-8 B). Consistent with the GST affinity chromatography results, the Merlin R325A R335L protein showed less binding to GST-Sip1 than the proteins with single substitutions (Figure 3-8 A, B). Since both the arginine at amino acid position 325 and 335 are conserved in the Merlin protein across different species but not found in either human or *Drosophila* Moesin and the loss of these arginines results in an almost complete loss of binding to GST-Sip1, this suggests that these arginines are critical for the interaction between Merlin and Sip1.

3.5 Merlin directly interacts with a kinase and a phosphatase that may be part of the Sip1 complex

Previous research shows Sip1 is required for the proper localization of Slik kinase and the phosphorylation and activation of Moesin (Hughes and Fehon, 2006; Hughes et al., 2010). Additionally, Slik affects the phosphorylation and tumour suppressor activity of Merlin (Hughes and Fehon, 2006). In addition, Slik can interact with Merlin and Moesin directly using GST affinity chromatography experiments (Hughes and Fehon, 2006). The phosphatase Flapwing is also able to affect the phosphorylation and activity of both Merlin and Moesin by affecting Merlin and Moesin localization resulting in

changes in cell proliferation and cell adhesion in the wings of *Drosophila* (Yang et al., Unpublished). Therefore, it is likely that Flapwing can also directly interact with Merlin, Moesin, and Sip1 to form a complex to regulate their activity. Using Flapwing proteins, binding to GST tagged full length Merlin (GST-Merlin), GST tagged full length Moesin (GST-Moesin) and GST tagged full length Sip1 (GST-Sip1) protein can be detected (Figure 3-9 A, B). As well, preliminary results show that Slik and Flapwing proteins can bind to both the GST tagged FERM domain (GST-MerF) and GST tagged C-terminal tail (GST-MerC) of Merlin (Figure 3-9 A, B). The ability of Slik and Flapwing to interact with both GST-Merlin constructs may suggest that they act on a site close to the region where the FERM domain and C-terminal tail of Merlin connect. It is also possible that they can affect phosphorylation at multiple sites on Merlin. Based on previous research where Sip1 is necessary for proper Slik localization and Moesin phosphorylation and recent Flapwing interaction data (Hughes et al., 2010; Yang et al., Unpublished), it supports the idea that a complex is necessary for the regulation of Merlin and Moesin function.

Figure 3-9: Slik and Flapwing can interact directly with GST-Merlin, GST-Moesin, and GST-Sip1

A) Schematic diagrams summarizing the GST tagged protein constructs used for the GST affinity chromatography experiments below.

B) GST affinity chromatography experiments using ^{35}S radiolabelled Flapwing and Slik proteins. The Flapwing protein binds to GST-Sip1, GST-Moesin and GST-Merlin. Flapwing and Slik proteins can bind to both the FERM domain of Merlin (GST-MerF) and the C-terminal tail of Merlin (GST-MerC).

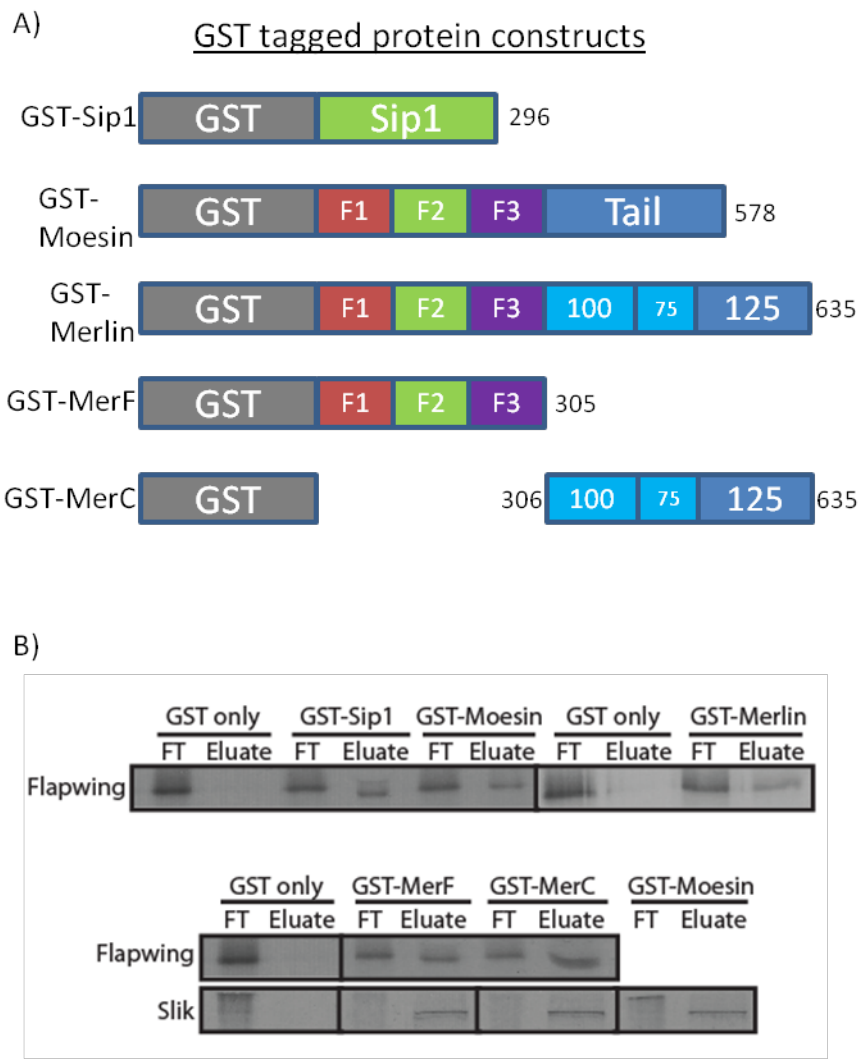
A)
GST tagged protein constructs
GST-Sip1
GST
Sip1
296
GST-Moesin
GST
F1
F2
F3
Tail
578
GST-Merlin
GST
F1
F2
F3
100
75
125
635
GST-MerF
GST
F1
F2
F3
305
GST-MerC
GST
306
100
75
125
635
B)
GST only
GST-Sip1
GST-Moesin
GST only
GST-Merlin
FT Eluate FT Eluate FT Eluate FT Eluate FT Eluate
Flapwing
GST only
GST-MerF
GST-MerC
GST-Moesin
FT Eluate FT Eluate FT Eluate FT Eluate
Flapwing
Slik

Figure 3-9

3.6 Summary

In this chapter, a novel Merlin Sip1 binding domain downstream of the FERM domain of Merlin in amino acids 306-405 was identified. The substitution of two conserved arginines at amino acid positions 325 and 335 to an alanine and a leucine results in a loss of Merlin binding to Sip1. Together with Slik and Flapwing interaction data, this supports the hypothesis of a Merlin Sip1 regulatory complex.

Chapter Four:

Merlin and Sip1 interactions may be regulated by phosphorylation

Merlin S371A/D and Merlin T374A/D DNA constructs were created and Merlin S371A/D and Merlin T374A/D pulse chase experiments were performed by Angela Effa.

4.1 Introduction

Merlin has multiple known phosphorylation sites that affect its function and localization as discussed in Chapter 1 (Hughes and Fehon, 2006; Kissil et al., 2002; Laulajainen et al., 2008; Okada et al., 2009; Rong et al., 2004a; Shaw et al., 2001; Surace et al., 2004; Tang et al., 2007; Xiao et al., 2002). We have identified a potential novel phosphorylation site that is present in the novel Sip1 binding domain of Merlin, suggesting that the interaction between Merlin and Sip1 may be regulated by phosphorylation.

4.2 Identification of a potential novel phosphorylation site

Using two different phosphorylation prediction programs, Netphos 2.0 and GPS 2.1, the serine at amino acid position 371 of Merlin (S371) was predicted to have a >90% chance of phosphorylation and the sequence is recognizable by known kinases such as sterile family kinases. Protein alignments of Merlin across different species compared to human and *Drosophila* Moesin reveal that this sequence is conserved amongst the Merlin proteins and absent in the human and *Drosophila* Moesin (Figure 4-1). However, within this conserved sequence, there is a threonine at amino acid position 374 which may also be phosphorylated since threonines are phosphorylated by similar kinases.

Figure 4-1: Sequence alignments of the potential Sip1 binding domain of Merlin protein from different species compared to Moesin protein from human and *Drosophila*

Sequence alignment of the potential Sip1 binding domain of: human Merlin (hMerlin), *Drosophila* Merlin (dMerlin), mouse Merlin (mMerlin), rat Merlin (rMerlin), *Xenopus* Merlin (xMerlin), and zebrafish Merlin (zMerlin) compared to human Moesin (hMoesin), *Drosophila* Moesin (dMoesin). The serine at position 371 in dMerlin is conserved across different species of Merlin proteins but is not conserved in either human or *Drosophila* Moesin. The potential phosphorylation site is outlined in a box. The same colour indicates amino acids with similar properties (Arginine and lysine are both positively charged and are blue or methionine and cysteine both contain sulphur and are yellow).

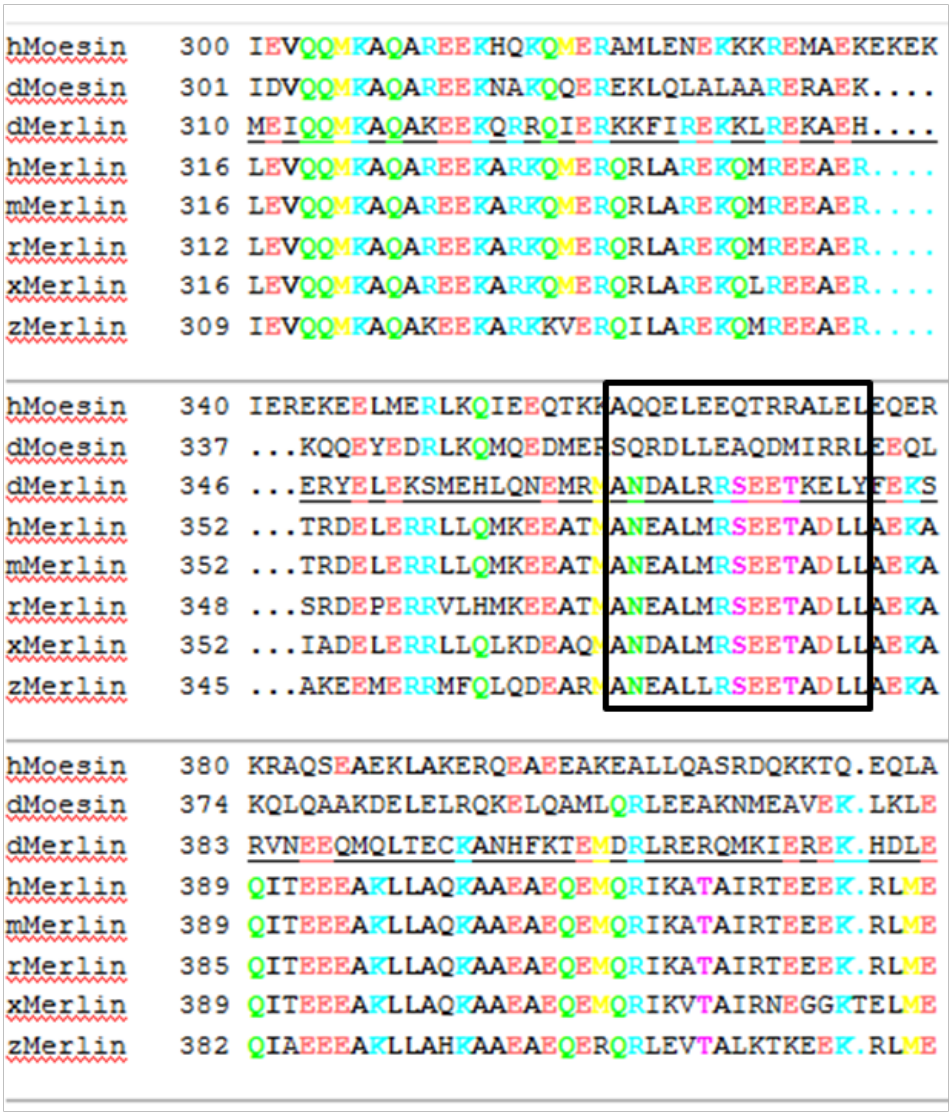
hMoesin 300 IEVQQMKAQAREEKHQKQMERAMLENEKKKREMAEKEKEK
dMoesin 301 IDVQQMKAQAREEKNAKQQEREKLQLALAAREKAEK....
dMerlin 310 MEIQQMKAQAKEEKQRRQIERKKFIREKKLREKAEH....
hMerlin 316 LEVQQMKAQAREEKARKQMERQRLAREKQMREEAER....
mMerlin 316 LEVQQMKAQAREEKARKQMERQRLAREKQMREEAER....
rMerlin 312 LEVQQMKAQAREEKARKQMERQRLAREKQMREEAER....
xMerlin 316 LEVQQMKAQAREEKARKQMERQRLAREKQLREEAER....
zMerlin 309 IEVQQMKAQAKEEKARKKVERQILAREKQMREEAER....
hMoesin 340 IEREKEELMERLKQIEEQTKKAQQELEEQTRRALELEQER
dMoesin 337 ...KQQEYEDRLKQMQEDMERSQRDLLEAQDMIRRLEEQL
dMerlin 346 ...ERYELEKSMEHLQNEMRNANDALRRSEETKELYFEKS
hMerlin 352 ...TRDELERRLLQMKEEATNANEALMRSEETADLLAEKA
mMerlin 352 ...TRDELERRLLQMKEEATNANEALMRSEETADLLAEKA
rMerlin 348 ...SRDEPERRVLHMKEEATNANEALMRSEETADLLAEKA
xMerlin 352 ...IADELERRLLQLKDEAQNANDALMRSEETADLLAEKA
zMerlin 345 ...AKEEMERRMFQLQDEARNANEALLRSEETADLLAEKA
hMoesin 380 KRAQSEAEKLAKERQEAEEAKEALLQASRDQKKTQ.EQLA
dMoesin 374 KQLQAAKDELELRQKELQAMLQRLEEAKNMEAVEK.LKLE
dMerlin 383 RVNEEQMQLTECKANHFKTEMDRLRERQMKIERER.HDLE
hMerlin 389 QITEEEAKLLAQKAAEAEQEMQRIKATAIRTEEEK.RLME
mMerlin 389 QITEEEAKLLAQKAAEAEQEMQRIKATAIRTEEEK.RLME
rMerlin 385 QITEEEAKLLAQKAAEAEQEMQRIKATAIRTEEEK.RLME
xMerlin 389 QITEEEAKLLAQKAAEAEQEMQRIKVTAIRNEGGKTELME
zMerlin 382 QIAEEEAKLLAHKAAEAEQERQRLEVTALKTKEEK.RLME

Figure 4-1

4.3 Amino acid changes at S371 affect Merlin binding to Sip1

To determine the effect on binding to Sip1, S371 was changed to either an alanine (S371A) or an aspartate (S371D). The S371A substitution results in a non-phosphorylatable site and the S371D substitution is a phosphomimic. The GST affinity chromatography experiments using amino acid substitutions and deletions at this site all result in a loss of binding to GST-Sip1 (Figure 4-2 A). Using the same binding assays described in Chapter 2.7-2.8 to quantify differences in binding to GST-Sip1, proteins with the S371A or S371D results in a reduction in binding to GST-Sip1 (Figure 4-2 B). Merlin protein with the deletion of amino acids 371-374 (Merlin Δ371-374) also results in a similar loss of binding to GST-Sip1 (Figure 4-2 B). Interestingly, a protein with multiple substitutions at amino acids 371-374 from SEET to AQQA (Merlin AQQA) results in more binding and this could be due to these amino acids maintaining a structure closer to wildtype (Figure 4-2 B). Since substitutions at the potential phosphorylation site affect binding to Sip1, this suggests that Merlin's interaction with Sip1 may be regulated by phosphorylation at this site. However, since loss of binding to Sip1 results from a variety of substitutions and deletions at this site, it is also possible that these substitutions are merely disrupting Merlin structure.

Figure 4-2: Amino acid changes at S371 affect Merlin binding to Sip1

A) GST affinity chromatography experiments with ^{35}S radiolabelled Merlin proteins and GST-Sip1. Compared to the full length Merlin protein and the GST alone, the mutant constructs all show some loss in binding.

B) Binding assays with the radiolabelled proteins used in GST affinity chromatography experiments compared to full length Merlin show a large reduction in binding to GST-Sip1 with each of the substitutions. Refer to Chapter 2.7-2.8 for experimental details. The Merlin S371D protein results in the greatest loss of binding to GST-Sip1.

A)

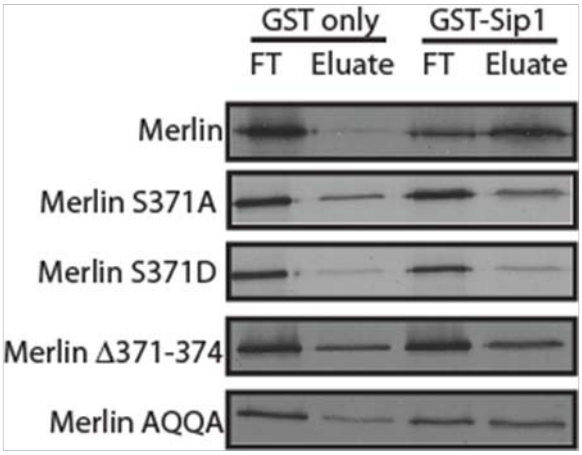
GST only
GST-Sip1
FT
Eluate
FT
Eluate
Merlin
Merlin S371A
Merlin S371D
Merlin Δ371-374
Merlin AQQA

B)

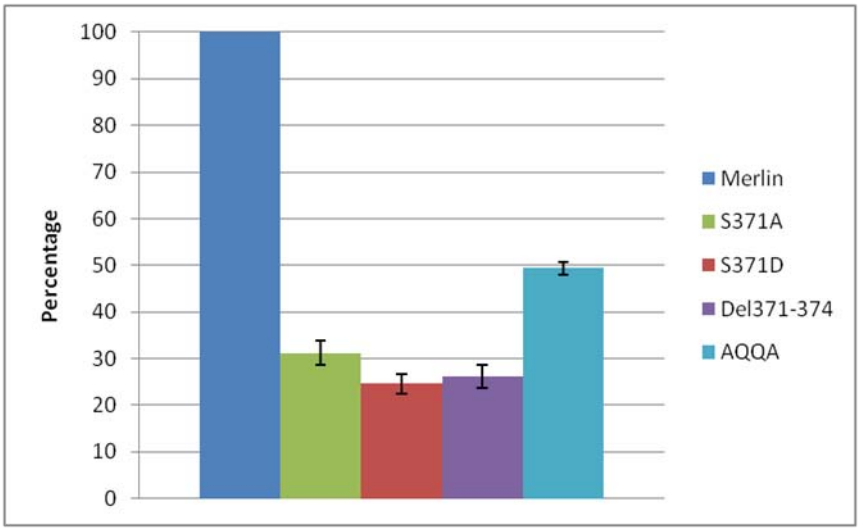
Percentage
100
90
80
70
60
50
40
30
20
10
0
Merlin
S371A
S371D
Del371-374
AQQA

Figure 4-2

4.4 Amino acid substitutions at S371 affect Merlin localization in S2 cells

To determine the effects of the amino acid substitutions at the potential phosphorylation site on the subcellular localization of Merlin *in vivo*, pulse chase assays using GFP tagged Merlin constructs under a heat shock inducible promoter in S2 cells were used. After a pulse of expression by heat shock, GFP tagged wildtype Merlin (HS-Merlin) is localized initially at the plasma membrane and then localizes to cytoplasmic vesicles over time. Cells are fixed at three time points and scored; the four phenotypes are (A) completely plasma membranous, (B) mostly plasma membranous, (C) mostly cytoplasmic vesicles, and (D) large cytoplasmic vesicles. It has been previously established that the localization of Merlin is correlated with its function and substitutions at a potential phosphorylation site, T616, to an alanine (T616A) or aspartate (T616D) resulted in a change in Merlin subcellular localization over time (Hughes and Fehon, 2006; LaJeunesse et al., 1998). The Merlin T616A substitution resulted in more localization to cytoplasmic vesicles over time and the Merlin T616D substitution resulted in more localization at the plasma membrane (Hughes and Fehon, 2006). It is important to note that pulse chase assays cannot determine the activity of the protein. Pulse chase assays with HS-Merlin^{S371A} results in subcellular localization

Figure 4-3: Pulse chase assays using HS-Merlin and HS-Merlin^{S371A} show no difference in Merlin subcellular localization

Cells are fixed at three time points (1h, 3h, 6h) and scored; the four phenotypes are: (A) completely plasma membranous, (B) mostly plasma membranous, (C) mostly cytoplasmic vesicles, and (D) large cytoplasmic vesicles. Images of the cell phenotypes are shown at the bottom of the figure. This experiment was done three times and one hundred cells were counted for each and the percentage of cells at each phenotype was graphed. Error bars are standard error. This experiment was performed by Angela Effa.

A) Subcellular localization of HS-Merlin at each time point. After a pulse of expression, HS-Merlin is initially localized at the plasma membrane and moves off to cytoplasmic vesicles over time.

B) Subcellular localization of HS-Merlin^{S371A} at each time point. The subcellular localization over time of HS-Merlin^{S371A} is similar to HS-Merlin.

A)

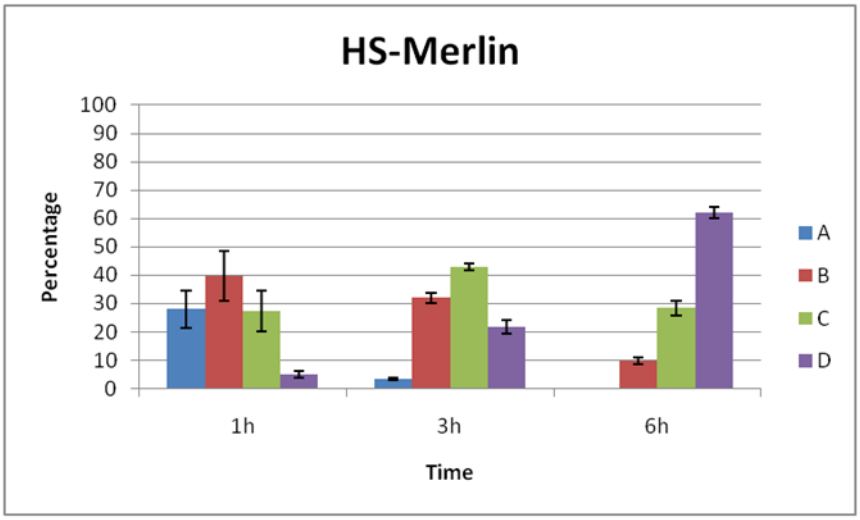
HS-Merlin
100
90
80
70
60
50
40
30
20
10
0
Percentage
1h
3h
6h
Time
A
B
C
D

B)

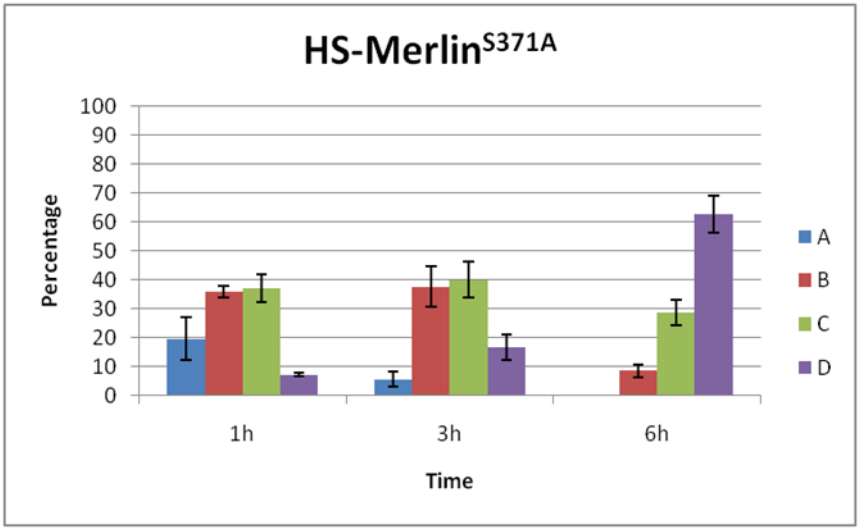
HS-Merlin S371A
100
90
80
70
60
50
40
30
20
10
0
Percentage
1h
3h
6h
Time
A
B
C
D

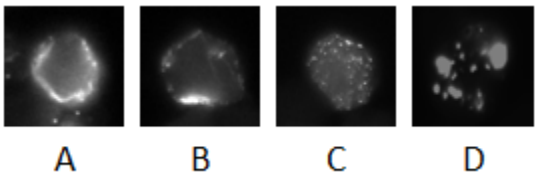
A
B
C
D

Figure 4-3

Figure 4-4: Pulse chase assays using HS-Merlin and HS-Merlin^{S371D} show a difference in Merlin subcellular localization

Cells are fixed at three time points (1h, 3h, 6h) and scored; the four phenotypes are: (A) completely plasma membranous, (B) mostly plasma membranous, (C) mostly cytoplasmic vesicles, and (D) large cytoplasmic vesicles. Images of the cell phenotypes are shown at the bottom of the figure. This experiment was done three times and one hundred cells were counted for each and the percentage of cells at each phenotype was graphed. Error bars are standard error. This experiment was performed by Angela Effa.

A) Subcellular localization of HS-Merlin at each time point. After a pulse of expression, HS-Merlin is initially localized at the plasma membrane and moves off to cytoplasmic vesicles over time.

B) Subcellular localization of HS-Merlin^{S371D} at each time point. HS-Merlin^{S371D} is localized more on the plasma membrane over time when compared to HS-Merlin.

A)

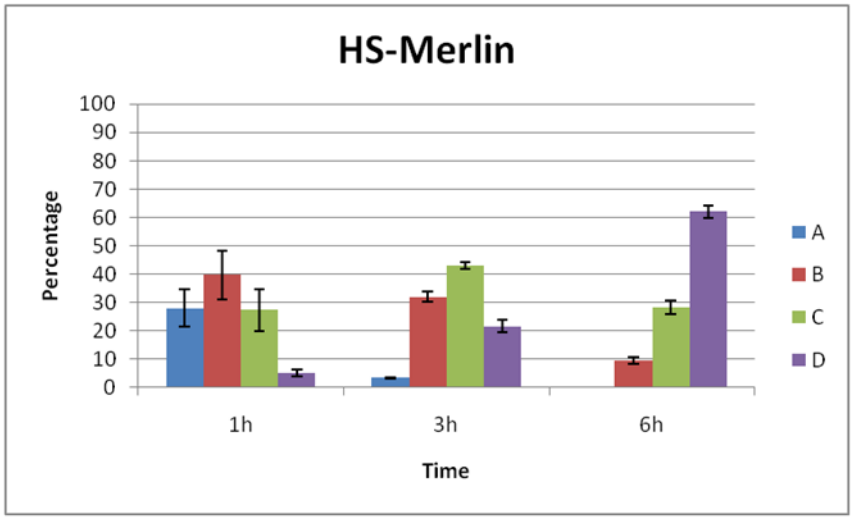
HS-Merlin
100
90
80
70
60
50
40
30
20
10
0
Percentage
1h
3h
6h
Time
A
B
C
D

B)

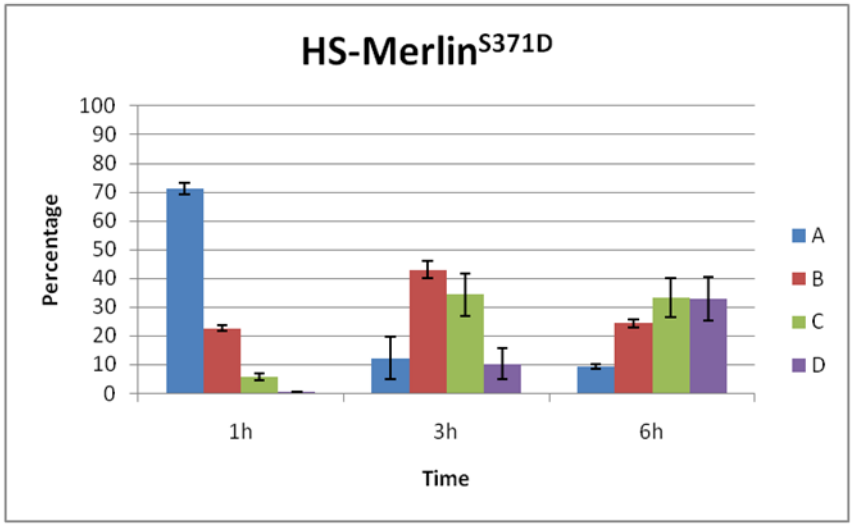
HS-Merlin S371D
100
90
80
70
60
50
40
30
20
10
0
Percentage
1h
3h
6h
Time
A
B
C
D

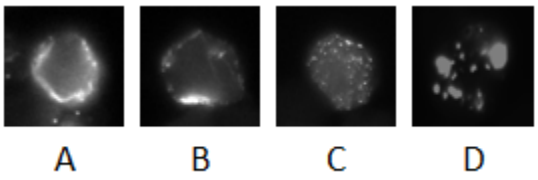
A
B
C
D

Figure 4-4

that is similar to HS-Merlin (Figure 4-3: B vs A). However, HS-Merlin^{S371D} was localized more at the plasma membrane compared to HS-Merlin (Figure 4-4: B vs A). This suggests that S371 is a potential novel phosphorylation site based on previous research with T616 (Hughes and Fehon, 2006).

4.5 Amino acid substitutions at a threonine near S371 has no effect on Merlin localization in S2 cells

As threonines can also be phosphorylated, a nearby threonine at amino acid position 374 of Merlin (T374) was mutated to an alanine (T374A) and aspartate (T374D) to determine its effects on Merlin subcellular localization. Using GFP tagged Merlin T374A (HS-Merlin^{T374A}) and T374D (HS-Merlin^{T374D}) constructs, pulse chase assays show no alterations in the pattern of Merlin subcellular localization over time when compared to HS-Merlin suggesting that T374 is not a potential phosphorylation site (Figure 4-5 B versus A and 4-6 B versus A). Multiple substitutions changing the amino acids SEET to AQQA (HS-Merlin AQQA) also causes no additional effects in Merlin subcellular localization when compared to the pulse chase assays of HS-Merlin^{S371A}, HS-Merlin^{T374A}, and HS-Merlin (Figure 4-7 B versus A, Figure 4-8).

By summarizing the total number of cells at each phenotype for each pulse chase assay, all of the different substitutions can be compared to each other in one graph. The percentage of each

Figure 4-5: Pulse chase assays using HS-Merlin and HS-Merlin^{T374A} show no difference in Merlin subcellular localization

Cells are fixed at three time points (1h, 3h, 6h) and scored; the four phenotypes are: (A) completely plasma membranous, (B) mostly plasma membranous, (C) mostly cytoplasmic vesicles, and (D) large cytoplasmic vesicles. Images of the cell phenotypes are shown at the bottom of the figure. This experiment was done three times and one hundred cells were counted for each and the percentage of cells at each phenotype was graphed. Error bars are standard error. This experiment was performed by Angela Effa.

A) Subcellular localization of HS-Merlin at each time point. After a pulse of expression, HS-Merlin is initially localized at the plasma membrane and moves off to cytoplasmic vesicles over time.

B) Subcellular localization of HS-Merlin^{T374A} at each time point. The subcellular localization of HS-Merlin^{T374A} over time is similar to HS-Merlin.

A)

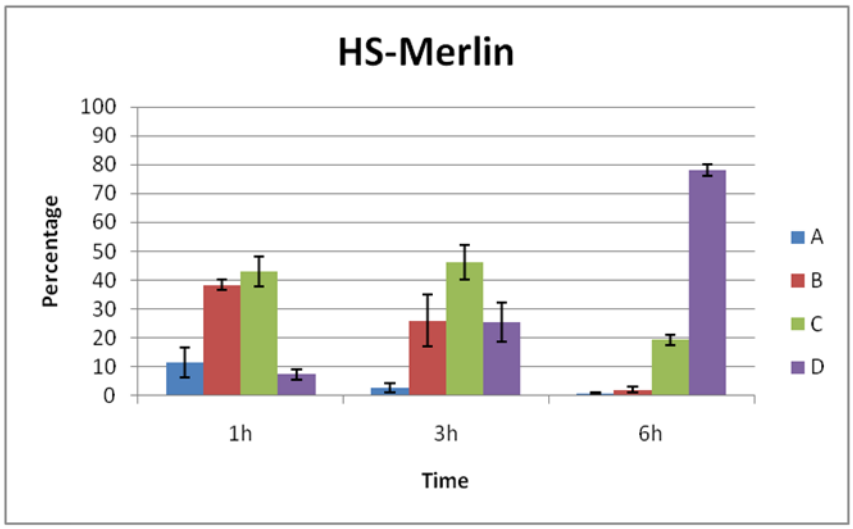
HS-Merlin
Percentage
100
90
80
70
60
50
40
30
20
10
0
1h
3h
6h
Time
A
B
C
D

B)

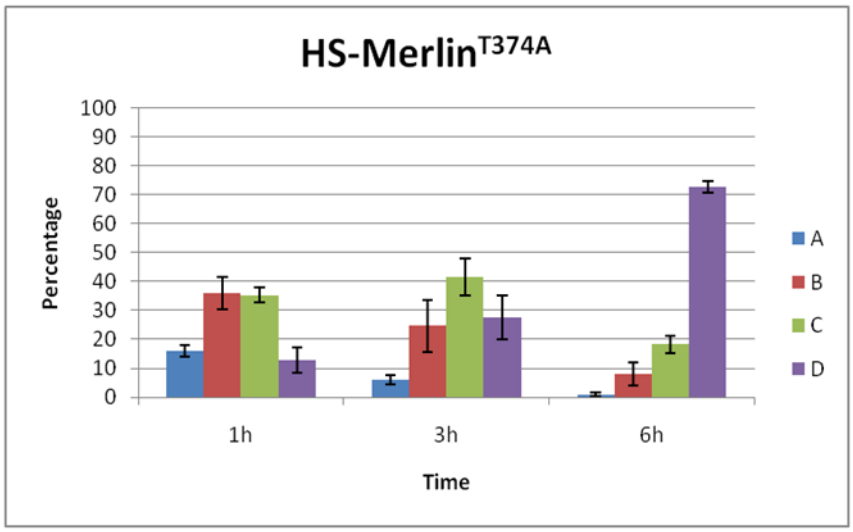
HS-Merlin^{T374A}
Percentage
100
90
80
70
60
50
40
30
20
10
0
1h
3h
6h
Time
A
B
C
D

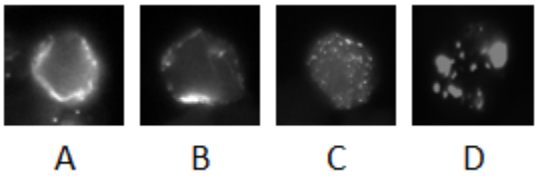
A
B
C
D

Figure 4-5

Figure 4-6: Pulse chase assays using HS-Merlin and HS-Merlin^{T374D} show no difference in Merlin subcellular localization

Cells are fixed at three time points (1h, 3h, 6h) and scored; the four phenotypes are: (A) completely plasma membranous, (B) mostly plasma membranous, (C) mostly cytoplasmic vesicles, and (D) large cytoplasmic vesicles. Images of the cell phenotypes are shown at the bottom of the figure. This experiment was done three times and one hundred cells were counted for each and the percentage of cells at each phenotype was graphed. Error bars are standard error. This experiment was performed by Angela Effa.

A) Subcellular localization of HS-Merlin at each time point. After a pulse of expression, HS-Merlin is initially localized at the plasma membrane and moves off to cytoplasmic vesicles over time.

B) Subcellular localization of HS-Merlin^{T374D} at each time point. The subcellular localization of HS-Merlin^{T374D} over time is similar to HS-Merlin.

A)

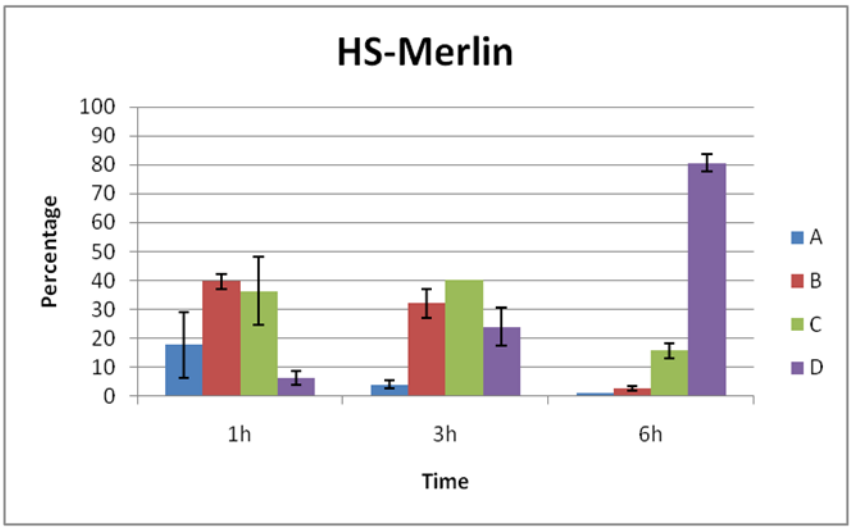
HS-Merlin
Percentage
100
90
80
70
60
50
40
30
20
10
0
1h
3h
6h
Time
A
B
C
D

B)

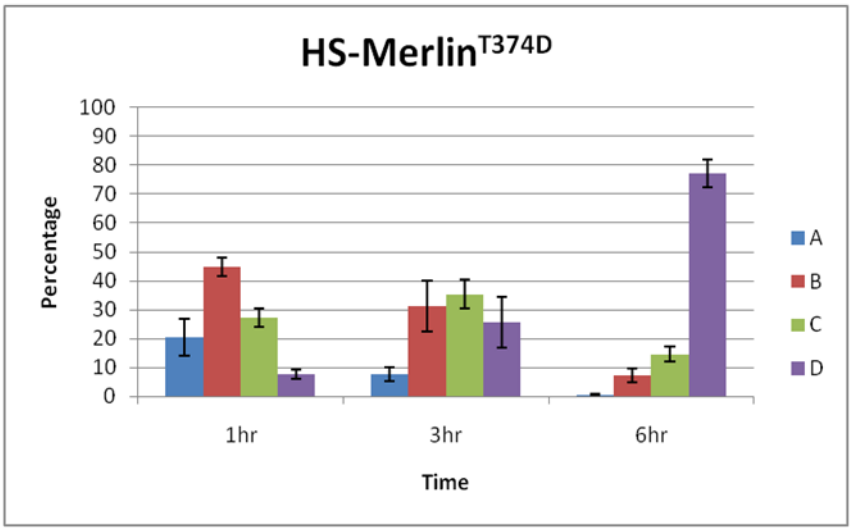
HS-Merlin T374D
Percentage
100
90
80
70
60
50
40
30
20
10
0
1hr
3hr
6hr
Time
A
B
C
D

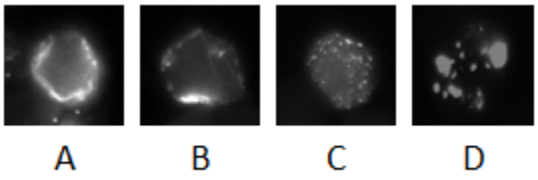
A
B
C
D

Figure 4-6

Figure 4-7: Pulse chase assays using HS-Merlin and HS-Merlin AQQA show no difference in Merlin subcellular localization

Cells are fixed at three time points (1h, 3h, 6h) and scored; the four phenotypes are: (A) completely plasma membranous, (B) mostly plasma membranous, (C) mostly cytoplasmic vesicles, and (D) large cytoplasmic vesicles. Images of the cell phenotypes are shown at the bottom of the figure. This experiment was done four times and one hundred cells were counted for each and the percentage of cells at each phenotype was graphed. Error bars are standard error.

A) Subcellular localization of HS-Merlin at each time point. After a pulse of expression, HS-Merlin is initially localized at the plasma membrane and moves off to cytoplasmic vesicles over time.

B) Subcellular localization of HS-Merlin AQQA at each time point. The subcellular localization of HS-Merlin AQQA over time is similar to HS-Merlin.

A)

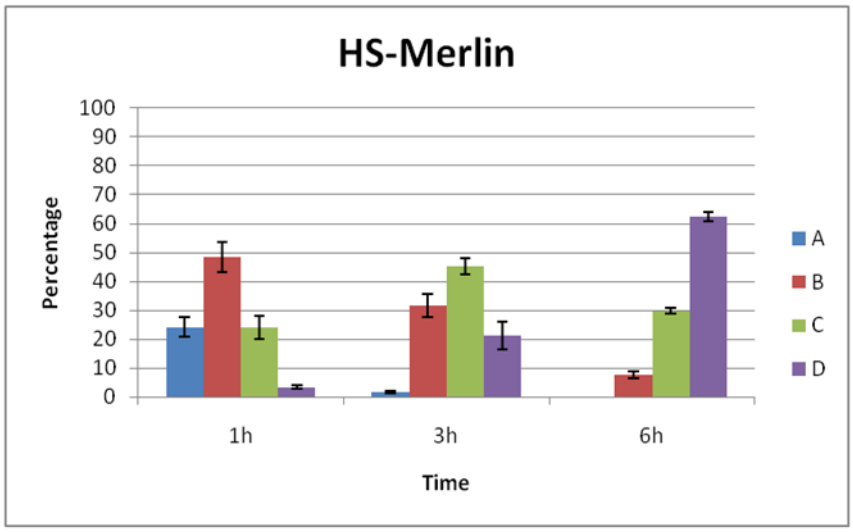
HS-Merlin
Percentage
100
90
80
70
60
50
40
30
20
10
0
1h
3h
6h
Time
A
B
C
D

B)

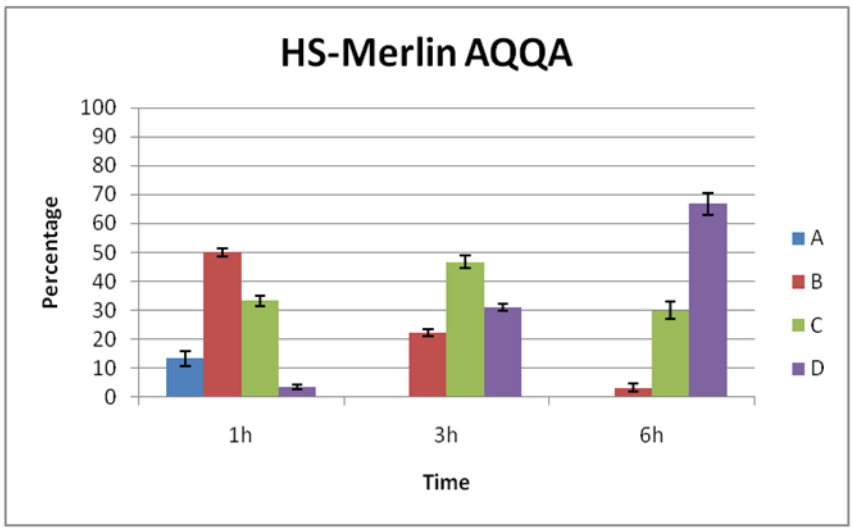
HS-Merlin AQQA
Percentage
100
90
80
70
60
50
40
30
20
10
0
1h
3h
6h
Time
A
B
C
D

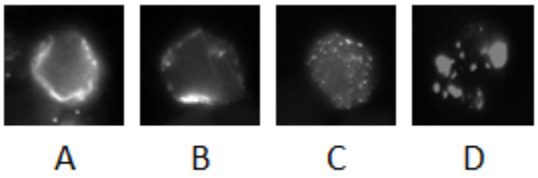
A
B
C
D

Figure 4-7

Figure 4-8: Summary of pulse chase analysis shows an alteration in the localization of HS-Merlin^{S371D} over time when compared to HS-Merlin and HS-Merlin^{T374D}

Each stacked bar represents the percentage of all cells at a specific phenotype over all time points: (A) is completely plasma membranous, (B) is mostly plasma membranous, (C) is mostly small cytoplasmic vesicles, and (D) is large internal cytoplasmic vesicles. Images of the cell phenotypes are shown at the bottom of the figure. HS-Merlin^{S371A}, HS-Merlin^{S371D}, HS-Merlin^{T374A}, and HS-Merlin^{T374D} pulse chase assays were performed by Angela Effa.

HS-Merlin^{S371A}, HS-Merlin^{T374A}, HS-Merlin^{T374D}, and HS-Merlin AQQA appear to have no effect on subcellular localization over time. However, HS-Merlin^{S371D} shows an obvious change compared to HS-Merlin and HS-Merlin^{T374D}. This suggests that S371 is a potential phosphorylation site.

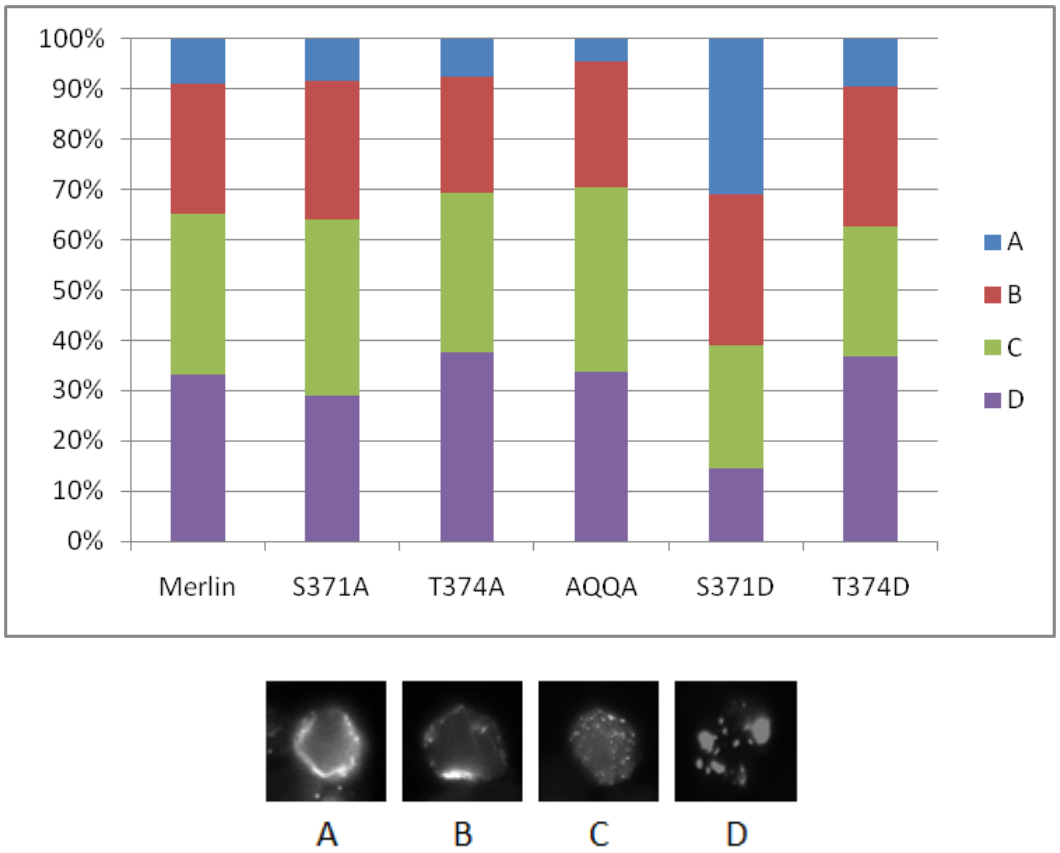
100%
90%
80%
70%
60%
50%
40%
30%
20%
10%
0%
Merlin
S371A
T374A
AQQA
S371D
T374D
A
B
C
D
A
B
C
D

Figure 4-8

phenotype is graphed. HS-Merlin, HS-Merlin^{S371A}, HS-Merlin^{T374A}, HS-Merlin AQQA, and HS-Merlin^{T374D} have very similar amounts of cells at each phenotype (Figure 4-8). On the other hand, HS-Merlin^{S371D} has a clear increase in the number of cells with Merlin localized at the plasma membrane over time compared to HS-Merlin and HS-Merlin^{T374D} (Figure 4-8). Together this data suggests that only S371 is potentially phosphorylated at this site.

4.6 Merlin S371A and S371D subcellular localization in S2 cells does not change with coexpression of Slik kinase

Slik affects the phosphorylation state of Merlin (Hughes and Fehon, 2006). Using pulse chase assays, coexpression of Slik under an UAS promoter (UAS-Slik) with HS-Merlin showed increased Merlin localization at the plasma membrane over time (Figure 4-9) (Hughes and Fehon, 2006). Thus, to determine whether or not Slik may be regulating phosphorylation at this site, UAS-Slik was coexpressed with HS-Merlin^{S371A} or HS-Merlin^{S371D} in S2 cells for pulse chase assays. If coexpression of Slik does not alter HS-Merlin^{S371A} and HS-Merlin^{S371D} subcellular localization, this would suggest the possibility of Slik regulating phosphorylation at this site. Expression of Slik was detected using antibody staining. Coexpression of UAS-Slik with HS-Merlin^{S371A} or HS-Merlin^{S371D} when compared to HS-Merlin^{S371A} or HS-Merlin^{S371D} alone shows no obvious change in the subcellular localization over time (Figure 4-10 and Figure 4-11).

Similar to Figure 4-8, the total percentage of cells at each phenotype can be summed up for Merlin and Slik coexpression experiments to compare all pulse chase experiments on one graph. When you compare Slik coexpression with HS-Merlin to HS-Merlin expression only, there are increased numbers of cells with Merlin localized at the plasma membrane over time (Figure 4-12). Whereas Slik coexpression with either HS-Merlin^{S371A} or HS-Merlin^{S371D} shows no obvious increase in plasma membrane localization when compared to HS-Merlin^{S371A} or HS-Merlin^{S371D} alone (Figure 4-12). These results do not exclude the possibility of Slik regulation at this potential phosphorylation site. However, since this site may regulate interaction with Sip1 and phosphorylation and activation of Moesin by Slik is dependent on Sip1, the absence of an effect could be due to the inability or reduced ability of Merlin to interact with Sip1 (Hughes et al., 2010).

Figure 4-9: Pulse chase assays with coexpression of UAS-Slik and HS-Merlin show an alteration in HS-Merlin subcellular localization

Cells are fixed at three time points (1h, 3h, 6h) and scored; the four phenotypes are: (A) completely plasma membranous, (B) mostly plasma membranous, (C) mostly cytoplasmic vesicles, and (D) large cytoplasmic vesicles. Images of the cell phenotypes are shown at the bottom of the figure. This experiment was done three times and one hundred cells were counted for each and the percentage of cells at each phenotype was graphed. Error bars are standard error.

A) Subcellular localization of HS-Merlin at each time point. After a pulse of expression, HS-Merlin is initially localized at the plasma membrane and moves off to cytoplasmic vesicles over time.

B) Coexpression of UAS-Slik and HS-Merlin results in more HS-Merlin localization at the plasma membrane. A Gal4 construct under the ubiquitin promoter (Ubi-Gal4) was co-transfected with UAS-Slik to induce expression.

A)

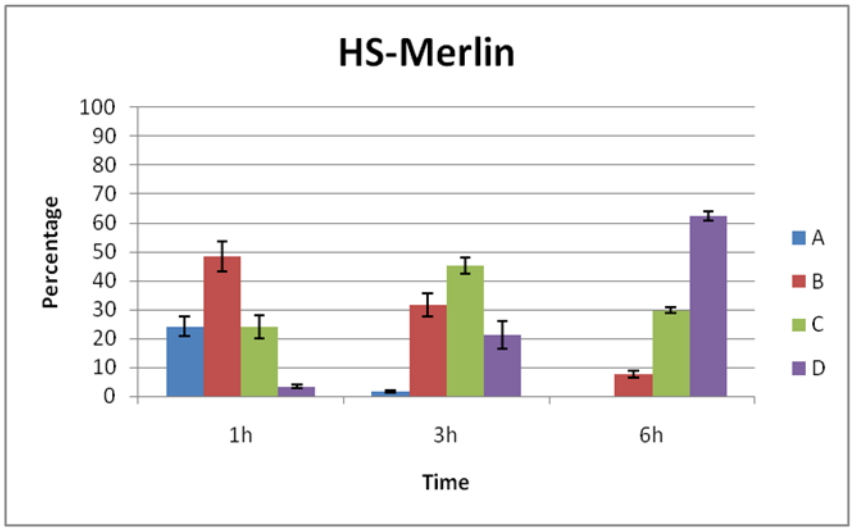
HS-Merlin
Percentage
100
90
80
70
60
50
40
30
20
10
0
1h
3h
6h
Time
A
B
C
D

B)

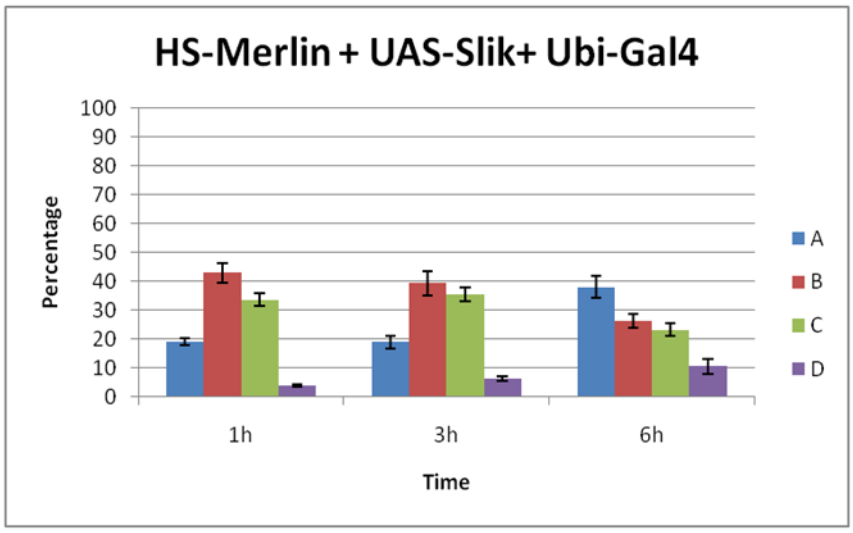
HS-Merlin + UAS-Slik+ Ubi-Gal4
Percentage
100
90
80
70
60
50
40
30
20
10
0
1h
3h
6h
Time
A
B
C
D

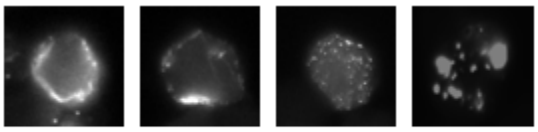
A
B
C
D

Figure 4-9

Figure 4-10: Pulse chase assays with coexpression of UAS-Slik and HS-Merlin^{S371A} show no alteration in HS-Merlin^{S371A} subcellular localization

Cells are fixed at three time points (1h, 3h, 6h) and scored; the four phenotypes are: (A) completely plasma membranous, (B) mostly plasma membranous, (C) mostly cytoplasmic vesicles, and (D) large cytoplasmic vesicles. Images of the cell phenotypes are shown at the bottom of the figure. This experiment was done three times and one hundred cells were counted for each and the percentage of cells at each phenotype was graphed. Error bars are standard error.

A) Subcellular localization of HS-Merlin^{S371A} at each time point. Pulse chase assay with HS-Merlin^{S371A} was performed by Angela Effa.

B) Coexpression of UAS-Slik and HS-Merlin^{S371A} results in no change to HS-Merlin^{S371A} localization. A Gal4 construct under the ubiquitin promoter (Ubi-Gal4) was co-transfected with UAS-Slik to induce expression.

A)

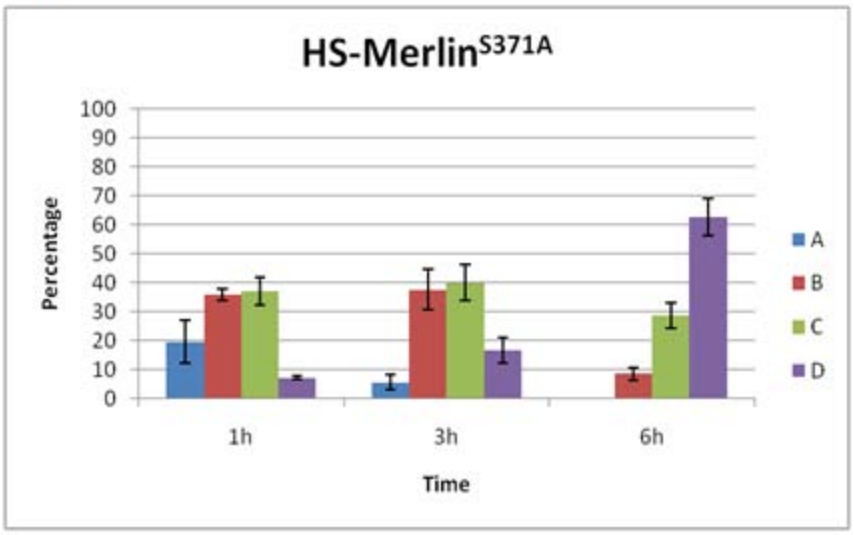

B)

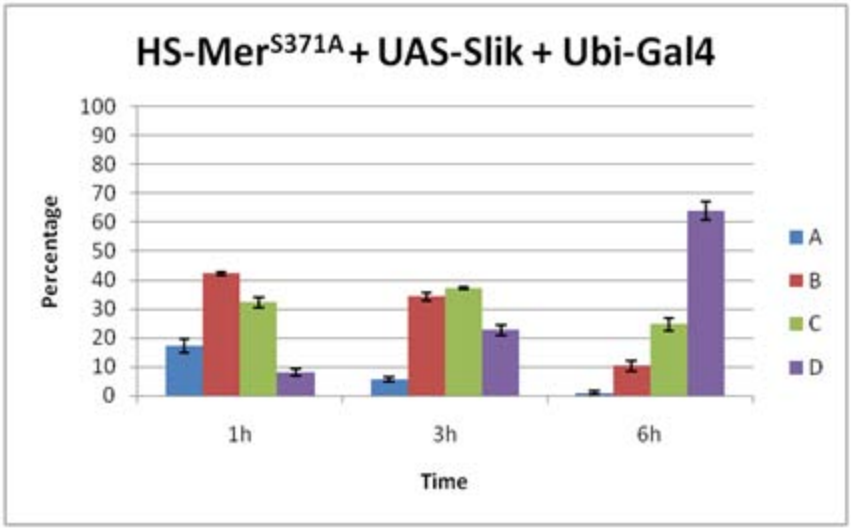

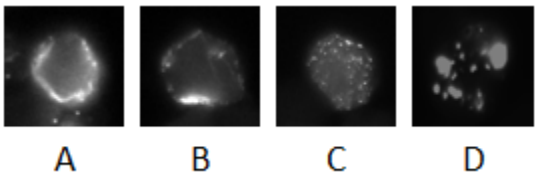

Figure 4-10

Figure 4-11: Pulse chase assays with coexpression of UAS-Slik and HS-Merlin^{S371D} show no alteration in HS-Merlin^{S371D} subcellular localization

Cells are fixed at three time points (1h, 3h, 6h) and scored; the four phenotypes are: (A) completely plasma membranous, (B) mostly plasma membranous, (C) mostly cytoplasmic vesicles, and (D) large cytoplasmic vesicles. Images of the cell phenotypes are shown at the bottom of the figure. This experiment was done three times and one hundred cells were counted for each and the percentage of cells at each phenotype was graphed. Error bars are standard error.

A) Subcellular localization of HS-Merlin^{S371D} at each time point. Pulse chase assay with HS-Merlin^{S371D} was performed by Angela Effa.

B) Coexpression of UAS-Slik and HS-Merlin^{S371D} results in no change to HS-Merlin^{S371D} localization. A Gal4 construct under the ubiquitin promoter (Ubi-Gal4) was co-transfected with UAS-Slik to induce expression.

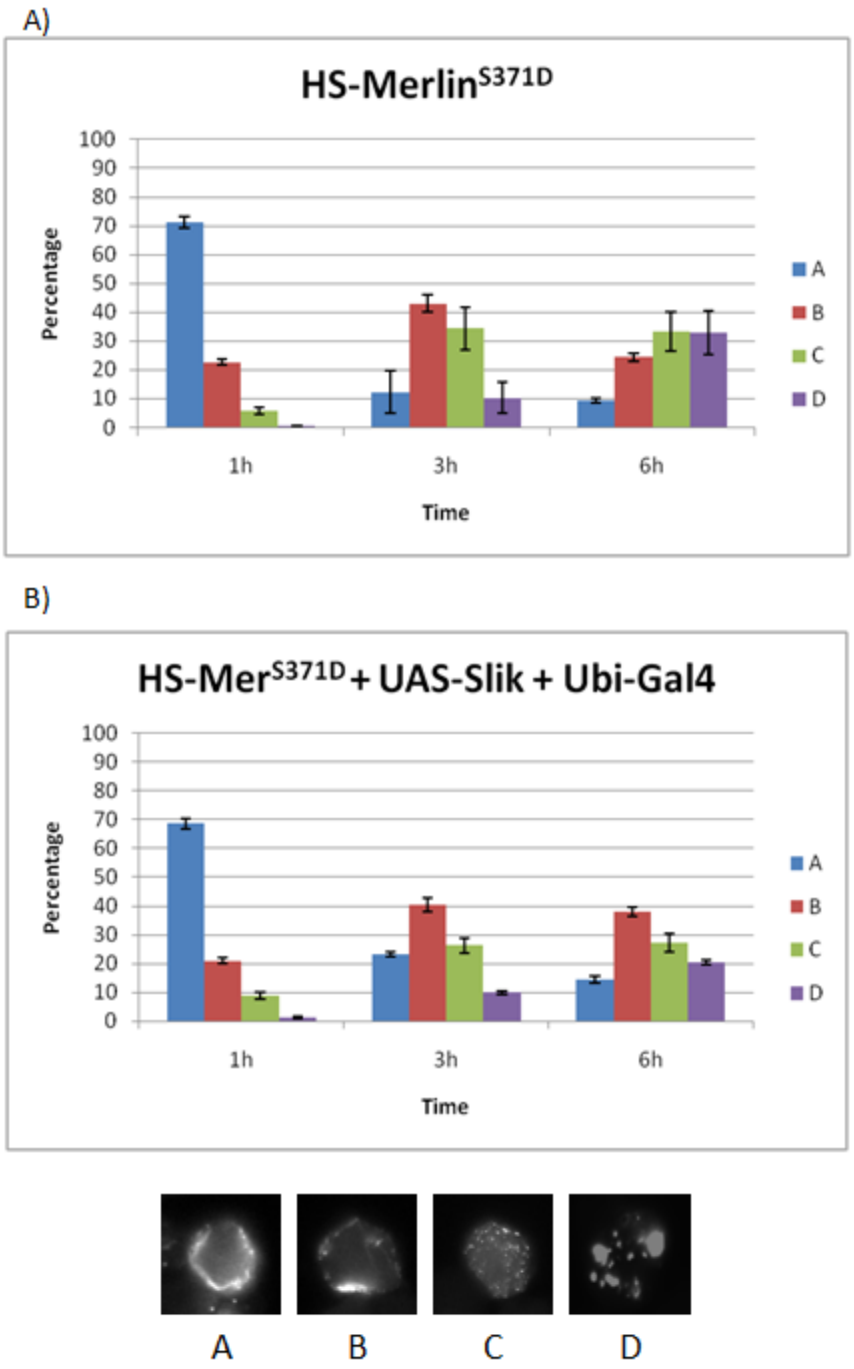
A)
HS-Merlin^{S371D}
Percentage
100
90
80
70
60
50
40
30
20
10
0
1h
3h
6h
Time
A
B
C
D
B)
HS-Mer^{S371D} + UAS-Slik + Ubi-Gal4
Percentage
100
90
80
70
60
50
40
30
20
10
0
1h
3h
6h
Time
A
B
C
D
A
B
C
D

Figure 4-11

Figure 4-12: Summary of pulse chase analysis with Slik coexpression and HS-Merlin^{S371A} or HS-Merlin^{S371D} shows no alteration in subcellular localization over time

Each stacked bar represents the percentage of all cells at a specific phenotype over all time points: (A) is completely plasma membranous, (B) is mostly plasma membranous, (C) is mostly small cytoplasmic vesicles, and (D) is large internal cytoplasmic vesicles. Images of the cell phenotypes are shown at the bottom of the figure. Pulse chase experiments with HS-Merlin^{S371A} and HS-Merlin^{S371D} alone were performed by Angela Effa.

The coexpression of Slik kinase with HS-Merlin^{S371A} and HS-Merlin^{S371D} does not alter the localization of HS-Merlin^{S371A} and HS-Merlin^{S371D} over time when compared to HS-Merlin^{S371A} or HS-Merlin^{S371D} alone.

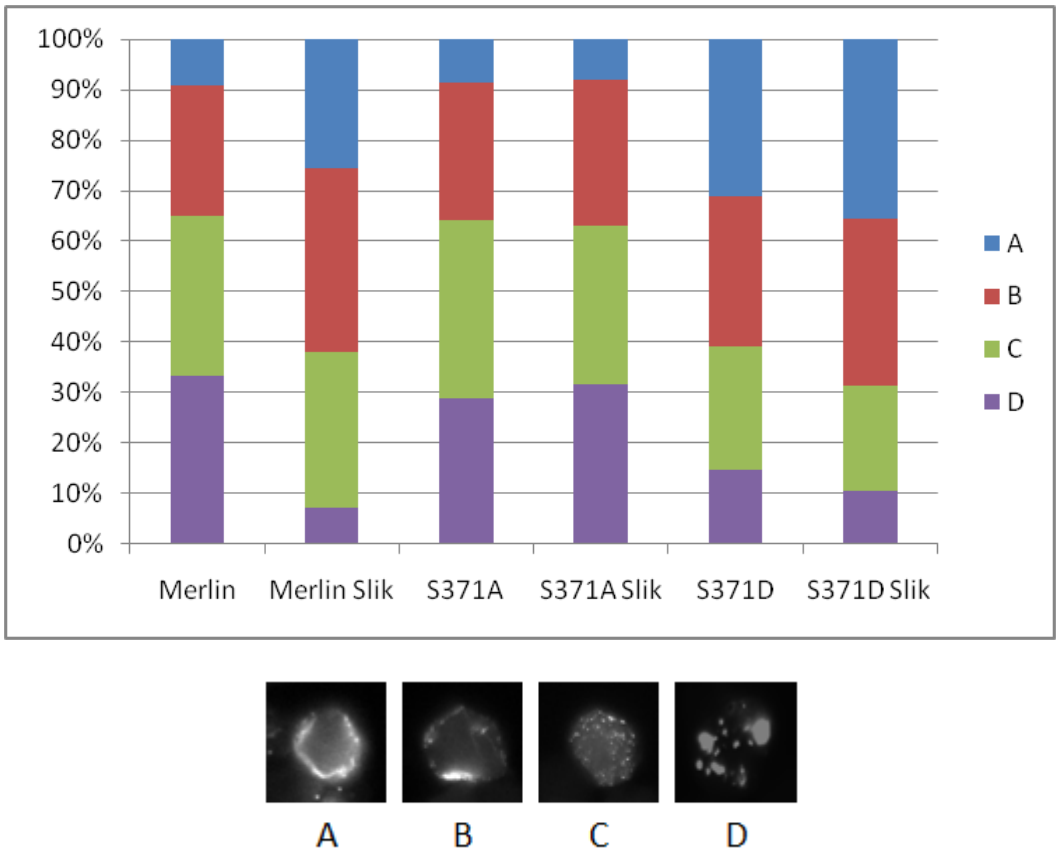
100%
90%
80%
70%
60%
50%
40%
30%
20%
10%
0%
Merlin
Merlin Slik
S371A
S371A Slik
S371D
S371D Slik
A
B
C
D
A
B
C
D

Figure 4-12

4.7 Summary

In this chapter, a potential novel phosphorylation site, S371, was identified in the coiled-coiled region. Substitution of this amino acid to an aspartate, which may mimic phosphorylation, results in an inability of Merlin to traffic off the membrane. As well, coexpression of Slik kinase with Merlin S371D does not change subcellular localization when compared to Merlin S371D alone. This suggests that Slik may regulate phosphorylation at this site. Amino acid substitutions and deletions in this potential novel phosphorylation site also affect Merlin binding to Sip1 in GST affinity chromatography experiments. Since only Merlin S371D affects subcellular localization but both Merlin S371A and S371D results in loss of binding to Sip1, they may represent distinct disruptions in the protein structure.

Chapter Five:

Discussion

5.1 Merlin forms a complex with Sip1

ERM proteins interact with EBP50 via their FERM F3 subdomain (Finnerty et al., 2004; Nguyen et al., 2001; Reczek and Bretscher, 1998) and my results analyzing the interaction between Moesin and Sip1 are consistent with this data. The entire FERM domain of Moesin and the FERM F3 subdomain of Moesin can bind to Sip1 (Figure 3-2).

Previously, it has been shown that the entire FERM domain of human Merlin interacts with the C-terminal end of EBP50 (Nguyen et al., 2001). I show that both the entire FERM domain and entire C-terminal tail of *Drosophila* Merlin binds to either full length Sip1 or the C-terminal 50 amino acids of Sip1 (Figure 3-3). In contrast to Moesin, although the entire FERM domain of Merlin binds to Sip1, the FERM F3 subdomain of Merlin alone does not bind to Sip1 (Figure 3-3). Instead, a 100 amino acid region (Merlin 306-405) immediately downstream of the FERM domain does (Figure 3-3). Additionally, the deletion of the 100 amino acid region results in a loss of binding to Sip1 (Figure 3-4). Within the 100 amino acid region of Merlin, the substitution of two conserved arginines at positions 325 and 335 to the corresponding residues found in Moesin results in a similar loss of binding to Sip1 (Figure 3-8). Thus, this 100 amino acid region has been identified as a potential Sip1 binding region. Direct binding of both

Merlin and Moesin to Sip1 provides a basis for formation of a regulatory complex.

Slik kinase interacts directly with Merlin and Moesin (Figure 3-9) (Hughes and Fehon, 2006). Flapwing phosphatase also interacts directly with Merlin, Moesin, and Sip1 (Figure 3-9) (Yang et al., Unpublished). The identification of a kinase and phosphatase that can interact directly with Merlin and Sip1 further supports the formation of a regulatory complex. Since both Merlin and Moesin bind to the same region of Sip1, it is likely that Merlin and Moesin forms a complex with Sip1 separately. My results further suggest that it is likely the active forms of both Merlin and Moesin interact with Sip1 and can compete for Sip1 binding. Merlin is able to bind to Sip1 in a closed conformation but whether or not Merlin can bind to Sip1 in a phosphorylated or open conformation has not yet been determined. Although the tumour suppressor active state of Merlin is thought to be the hypophosphorylated form, interaction with Sip1 may be necessary for proper Merlin function. It is possible that Merlin may need to interact with other proteins through Sip1 in order to control cell proliferation. This would suggest that even though there may not be mutations in Merlin, mutations in Sip1 that prevents Merlin binding could also lead to disease.

Although the potential Sip1 binding region is necessary for Merlin interaction with Sip1, the possibility remains that Merlin can interact with Sip1 in a phosphorylated state since the FERM domain of Merlin can bind to Sip1 (Figure 3-3). In agreement with a previous study using human Merlin and EBP50 (Nguyen et al., 2001), I show that the FERM domain of Merlin can interact with Sip1 (Figure 3-3). If Merlin phosphorylation leads to an open conformation similar to ERM phosphorylation, it may be possible that phosphorylated Merlin can interact with Sip1 as well. Merlin may contain more than one Sip1 binding site and different binding sites would be exposed depending on the conformation of Merlin. The different binding sites could allow Merlin binding to Sip1 in different conformations allowing for regulation of Merlin activity. Thus, a Sip1 regulatory complex could both phosphorylate and dephosphorylate Merlin. Initially, I hypothesized that it was possible that the binding between the FERM domain of Merlin and Sip1 was due to the FERM domain of Merlin being very similar to the FERM domain of Moesin. The FERM F3 subdomain of Moesin binds to Sip1 (Figure 3-2). However, since the FERM F3 subdomain of Merlin does not bind to Sip1 in GST affinity chromatography experiments (Figure 3-3), it is unlikely that the interaction between the FERM domain of Merlin and Sip1 is due to

similarity to the FERM domain of Moesin. This would support the idea that Merlin could contain more than one Sip1 binding domain.

Using GST affinity chromatography experiments I have determined that the interaction domains necessary for Merlin and Moesin binding to Sip1 (Figure 3-2, Figure 3-3). Moesin interacts with Sip1 via the FERM F3 subdomain (Figure 3-4). For Merlin, amino acids 306-405 are necessary for Sip1 binding (Figure 3-3). However, certain limitations are present in the GST affinity chromatography experiments and the binding assays used. Firstly, there is varying amounts of background binding. In general, there are low levels of background binding to the GST only negative control. However, in some deletion and amino acid substitutions, there is an increase in background binding. A possible explanation for this is that the deletions and substitutions result in a change in protein structure, and this change in structure could expose hydrophobic regions. These hydrophobic regions would then bind to any proteins available in order to avoid the aqueous environment. As well, high amounts of probe are used in the binding assays and proteins that would not normally interact at lower levels may result in low levels of binding when concentrations are high. These are *in vitro* experiments and useful for preliminary analysis, the results must be verified using *in vivo* systems.

5.2 The interaction between Merlin and Sip1 may be transient

Subcellular localization of Merlin is linked to its function and activity (LaJeunesse et al., 1998). In other studies, substituting a phosphorylation site in Merlin to a non-phosphorylatable residue results in more localization to cytoplasmic vesicles and substituting a phosphorylation site to a phosphomimic results in more localization at the plasma membrane (Hughes and Fehon, 2006). I have found that only the phosphomimic, S371D, showed a change in Merlin subcellular localization over time compared to wildtype Merlin. The S371D substitution results in Merlin being unable to traffic off the plasma membrane to cytoplasmic vesicles. However, GST affinity chromatography experiments show that both Merlin S371A and Merlin S371D protein has very little binding to GST-Sip1 (Figure 4-2). The non-phosphorylatable amino acid substitution S371A and both a non-phosphorylatable substitution and a phosphomimic of a nearby phosphorylatable residue T374 show no change in subcellular localization over time when compared to wildtype Merlin. These results raise an interesting question: how is Merlin localized more on the plasma membrane when the phosphomimic reduces its binding to Sip1, while the non-phosphorylatable substitution at S371 exhibits no change in subcellular localization over time. Since Merlin S371A results in a loss of binding to Sip1 *in vitro* and has no change in

subcellular localization, the simplest explanation is that alanine is not a good amino acid substitution for a non-phosphorylated Merlin at this site. Since the S371A mutation results in a loss of binding to Sip1, amino acid substitutions of S371 to either a cysteine or an asparagine may be a better choice. Both cysteine and asparagine are non-phosphorylatable and could be a better substitute for serine in maintaining proper protein structure. Conversely, since Merlin S371D results in both a loss of binding to Sip1 *in vitro* and affects subcellular localization similar to coexpression of Slik with wildtype Merlin, Merlin S371D may be a proper phosphomimic. Slik coexpression experiments will be discussed further in the next section. The Merlin T374A and T374D proteins were not tested for binding to Sip1, but it would be interesting to determine whether or not Sip1 binding is affected by these amino acid substitutions. Although both Merlin S371A and S371D lose binding to Sip1, their initial recruitment to the plasma membrane in the pulse chase assay is not impaired. Therefore it is likely that Sip1 is not involved in Merlin recruitment to the plasma membrane. Interaction with phosphatidylinositol 4,5-bisphosphate could be a potential mechanism for Merlin targeting to the plasma membrane. Similar to what happens to ERM proteins (Fehon et al., 2010; Fievet et al., 2004), phosphatidylinositol 4,5-bisphosphate binding to the FERM domain of Merlin in humans

targets Merlin to the plasma membrane (Mani et al., 2011). Thus, the initial recruitment of Merlin to the plasma membrane may be phosphatidylinositol 4,5-bisphosphate mediated and then protein interactions with regulatory complexes like Sip1 regulates the activity of Merlin through changes in phosphorylation (Figure 5-1) (Fehon et al., 2010; Fievet et al., 2004; Mani et al., 2011).

An interesting possibility is that the Sip1 regulatory complex interacts with Merlin transiently. Merlin may interact with the Sip1 complex only during activation or deactivation of Merlin. More specifically, Sip1 is important for acting as a scaffold for Merlin so that kinases and phosphatases can interact. Based on the requirement of Sip1 for the phosphorylation and activation of Moesin and the proper localization of Slik kinase, it supports the idea that Sip1 may be important for the recruitment of kinases and phosphatases that interact with Merlin such as Slik and Flapwing (Hughes and Fehon, 2006; Yang et al., Unpublished). After Merlin phosphorylation or dephosphorylation by the regulatory Sip1 complex depending on the growth conditions, Merlin dissociates from Sip1 and interacts with other proteins. Under growth permissive conditions, Merlin may be phosphorylated and act as a structural protein interacting with actin (Figure 5-1). While under growth repressive conditions, Merlin will not be phosphorylated which would result in interaction with other

Figure 5-1: Diagram of a model showing transient interaction with Sip1

This is a model showing initial recruitment of Merlin to the plasma membrane by phosphatidylinositol 4,5-bisphosphate. Merlin would then interact with Sip1 and other regulatory proteins like Slik and Flapwing (Flw). Phosphorylated Merlin is tumour suppressor inactive and possibly interacts with actin and other plasma membrane associated proteins. The interaction with Sip1 may be required to come in contact with proteins involved in Merlin tumour suppressor activity. It is possible that Merlin may be able to interact with Sip1 in a phosphorylated form. However, interaction between a phosphorylated form of Merlin and Sip1 may or may not require other proteins to stabilize. The proteins with question marks represent additional proteins that may be involved in Merlin tumour suppressor function or plasma membrane association.

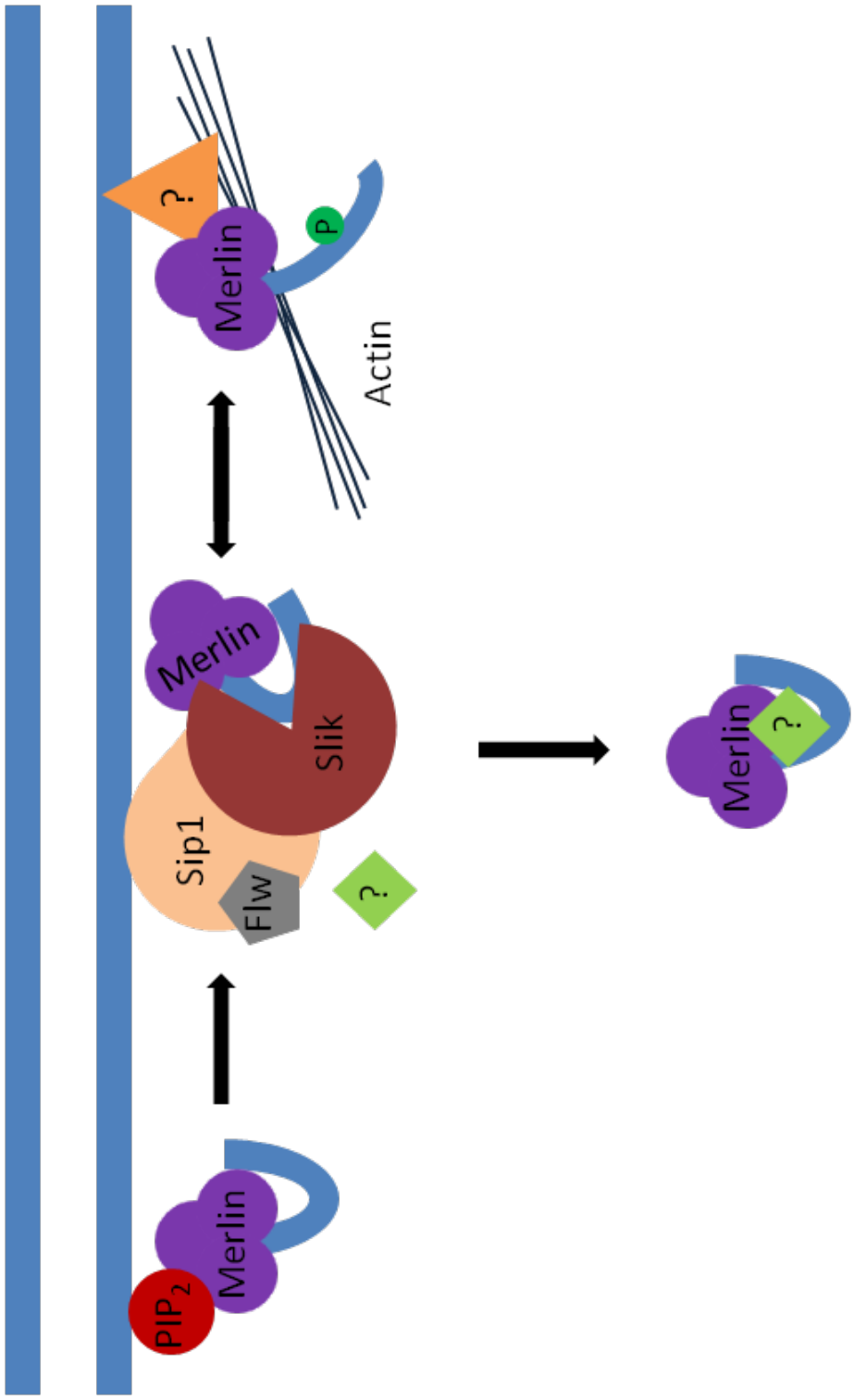

Figure 5-1

proteins potentially involved in growth control (Figure 5-1). It is known that Merlin interacts with other plasma membrane associated proteins (Scoles, 2008). Specifically, in humans, Merlin can form a complex with CD44 in both an open and closed conformation and it was suggested that such a complex could act as a molecular switch to control both proliferation and epithelial integrity; however there are no identified kinases or phosphatases in the CD44 complex (Morrison et al., 2001). The actin binding domain of Merlin is thought to be in the FERM domain or the coiled-coiled domain. Thus, the actin binding domain of Merlin is masked in its hypophosphorylated, closed conformation (Huang et al., 1998; Scoles et al., 1998; Sivakumar et al., 2009; Xu and Gutmann, 1998). This would allow Merlin to function as a structural protein when it is in a phosphorylated, open conformation which is inactive for tumour suppressor function (Sherman et al., 1997; Surace et al., 2004). It has been demonstrated that the loss of Merlin actin binding does not impair its tumour suppressor function (Lallemand et al., 2009). Merlin association with actin also promotes the phosphorylation of S518 which inactivates Merlin tumour suppressor function (Lallemand et al., 2009). Although Merlin actin binding and tumour suppressor function is independent of each other (Lallemand et al., 2009), the ability of Merlin to localize at the plasma membrane is necessary for its tumour suppressor function (Hughes and Fehon,

2006; LaJeunesse et al., 1998; Mani et al., 2011). Given the above observations, it supports the interaction between Merlin and Sip1 being transient such that Sip1 is required to facilitate the interaction of kinases and phosphatases with Merlin. This is also an attractive model because it would reconcile both the results that show Merlin localization at the plasma membrane being required for its tumour suppressor function as well as the active tumour suppressive form of Merlin being in a hypophosphorylated and closed conformation (Figure 5-1) (Kissil et al., 2002; LaJeunesse et al., 1998; Mani et al., 2011; Shaw et al., 1998; Sherman et al., 1997; Surace et al., 2004). If Merlin interaction with Sip1 is necessary for Merlin tumour suppressor function then localization to the plasma membrane would also be necessary for Merlin activation.

The *in vivo* pulse chase assays using S2 cells show that substitution of S371 to an aspartate results in a change in Merlin subcellular localization over time. The pulse chase assays used in this thesis are very limited in the information they provide. Although they are useful as a screen for amino acid substitutions that affect subcellular localization, pulse chase assays do not provide any information on the activity of the protein. Merlin subcellular localization and activity are linked but pulse chase assays are unable to determine if Merlin is active or inactive at the membrane (Hughes

and Fehon, 2006; LaJeunesse et al., 1998). To determine the activity of the Merlin constructs used in pulse chase assays, expression of these constructs in specific *Drosophila* tissues would be necessary. The overexpression of Merlin T616A in *Drosophila* wing tissue results in smaller wings and overexpression of Merlin T616D in *Drosophila* wing tissue results in larger wings. This suggests that Merlin T616A is more tumour suppressor active while Merlin T616D is less active. The overexpression of Merlin S371A and S371D could also be tested with this method. Additionally, a change in overall subcellular localization could also be due to the protein being degraded. In the case of Merlin S371D, the increased localization at the membrane could be due to the protein being degraded. Since Merlin is initially localized at the membrane, increased localization of Merlin S371D at the membrane could be due to Merlin S371D being degraded and only the initial localization of the protein is observed. The effect of degradation could be assayed by western blot of cell lysates at various time points and probing for the GFP tagged protein to observe changes in protein levels.

5.3 The interaction between Merlin and Sip1 may be regulated by Slik phosphorylation at S371

Coexpression of Slik with wildtype Merlin results in increased Merlin phosphorylation and an increase of Merlin localization on the

plasma membrane (Hughes and Fehon, 2006). My results of the coexpression of Slik with wildtype Merlin also show a similar increase in Merlin localization on the plasma membrane or an inability of Merlin to localize to cytoplasmic vesicles (Figure 4-8). In contrast, Slik coexpression with Merlin S371A or Merlin S371D results in very little change to subcellular localization when compared to Merlin S371A or Merlin S371D expression alone (Figure 4-9, Figure 4-10). However, Merlin S371A subcellular localization is very similar to wildtype Merlin. Proteins are synthesized in an unphosphorylated state and under growth permissive conditions, Slik phosphorylation is unnecessary since phosphorylation inactivates Merlin tumour suppressor activity. In addition, because Merlin S371A is also a Sip1 binding mutant, it is not a good representation of a non-phosphorylatable Merlin at S371 as discussed in section 5.2. On the other hand, Merlin S371D results in subcellular localization that is very similar to the coexpression of Slik with wildtype Merlin. Wildtype Merlin under growth permissive conditions normally traffics off the membrane and coexpression with Slik results in wildtype Merlin being retained at the membrane. Since Merlin S371D is also retained on the membrane and likely unable to traffic to cytoplasmic vesicles, the aspartate substitution is likely mimicking phosphorylation. These observations suggest that Slik may phosphorylate and regulate Merlin

at this site. However, it is not conclusive that Slik phosphorylates S371. Since the loss of Sip1 prevents Moesin phosphorylation and activation, another possible explanation for the lack of change in subcellular localization with Slik coexpression with Merlin S371A or Merlin S371D could be due to the reduced ability to bind to Sip1. As a consequence, Slik may not be able to interact with Merlin properly. Therefore Slik would be unable to phosphorylate Merlin at any phosphorylation site. Additionally, in humans, Merlin is regulated by multiple kinases and multistep phosphorylation (Kissil et al., 2002; Laulajainen et al., 2008; Laulajainen et al., 2011; Okada et al., 2009; Rong et al., 2004a; Shaw et al., 2001; Surace et al., 2004; Tang et al., 2007; Xiao et al., 2002). If the phosphorylation site that is initially phosphorylated is blocked, then the subsequent phosphorylation step will not occur (Laulajainen et al., 2011; Tang et al., 2007). Although these studies show multistep phosphorylation targeting Merlin for degradation, it does not eliminate the possibility that multistep phosphorylation could be used for regulation of Merlin tumour suppressor function. This would lead to another possible explanation as to why there is no change in Merlin S371A and Merlin S371D subcellular localization when coexpressed with Slik. If Merlin S371 is the initial phosphorylation site then blocking this site with amino acid substitutions would prevent Slik phosphorylation at other sites as well.

5.4 Protein regions important for Merlin activity have very little similarity when compared to Moesin

Often, protein regions that are conserved across species in a particular protein suggest that they are functionally important. Although Merlin is classified as part of the subfamily of ERM proteins, a number of the protein regions important for Merlin activity share very little similarity with Moesin (LaJeunesse et al., 1998; Laulajainen et al., 2008; Laulajainen et al., 2011). A region known as the blue box domain in Merlin lies in the FERM F2 subdomain and is completely conserved between human and *Drosophila* (LaJeunesse et al., 1998). The complete deletion or substitution of this domain, to seven alanines, results in a dominant negative form of Merlin (LaJeunesse et al., 1998). The expression of dominant negative form of Merlin results in increased proliferation even when endogenous Merlin is present (LaJeunesse et al., 1998). Comparison of the sequences of the FERM F2 subdomain of *Drosophila* Merlin to human Merlin shows that there is ~70% identity, whereas only ~54% identity exists when *Drosophila* Merlin is compared to *Drosophila* Moesin (Figure 5-2). In human Merlin, the phosphorylation site S10 which is important for actin organization and targeting Merlin for protein degradation is located just before the N-terminal FERM domain (Laulajainen et al., 2008; Laulajainen et al., 2011). This amino acid sequence is not present in

Drosophila Moesin or other ERMs homologs. Finally, the deletion of the C-terminal 35 amino acids of *Drosophila* Merlin results in a constitutively active tumour suppressive form (LaJeunesse et al., 1998). It has been stated that Merlin may be active in an open conformation since the C-terminal end of ERM proteins is necessary for their intramolecular interaction and loss of the C-terminal end of ERM proteins results in an open conformation (Bretscher et al., 2002; Gary and Bretscher, 1995; Matsui et al., 1998; Nakamura et al., 1995). Comparing the C-terminal 35 amino acids of *Drosophila* Merlin to human Merlin, there is ~54% identity while only ~36% identity exists between *Drosophila* Merlin and Moesin (Figure 5-2). Due to the low amount of conservation overall in the C-terminal tail, it is possible that the Merlin intramolecular interaction differs significantly from ERM intramolecular interactions. Similarly, the 100 amino acid potential Sip1 binding domain in *Drosophila* Merlin has ~28% identity when compared to *Drosophila* Moesin but has ~45% identity when compared to human Merlin (Figure 5-2). The substitution of two conserved arginines in the potential Sip1 binding domain is enough to abolish Sip1 binding (Figure 3-8). Therefore, the large difference between the C-terminal end of Merlin and Moesin may suggest that the intramolecular interaction in this region may also be different.

Figure 5-2: Diagram comparing percentage of identity between different protein domains in *Drosophila* Merlin, *Drosophila* Moesin, and human Merlin

The protein domains in *Drosophila* Merlin were compared to corresponding protein domains in *Drosophila* Moesin and human Merlin. The percentage identity of two protein domains is displayed between the proteins. The three FERM subdomains are labelled as F1, F2, and F3. The potential Sip1 binding domain is labelled CC for coiled-coiled region. The C-terminal 35 amino acids are represented by the box labelled C-term.

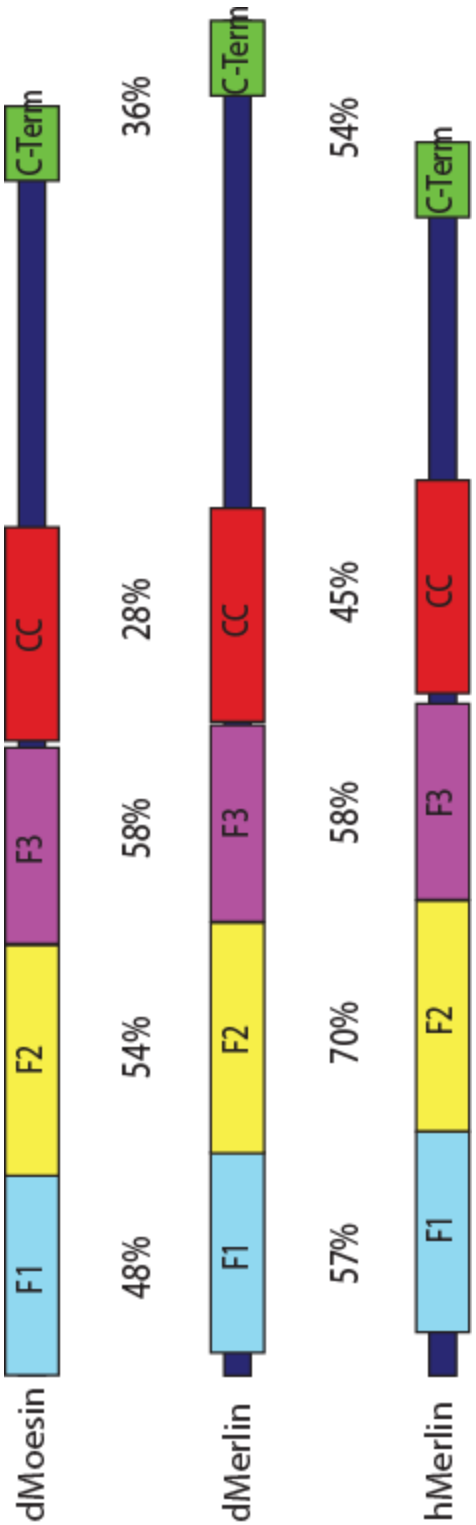
dMoesin
F1
F2
F3
CC
C-Term
48%
54%
58%
28%
36%
dMerlin
F1
F2
F3
CC
C-Term
57%
70%
58%
45%
54%
hMerlin
F1
F2
F3
CC
C-Term

Figure 5-2

The intramolecular interaction of the FERM domain of Ezrin and the C-terminal region of Ezrin known as the C-ERMAD is strong enough to compete for the binding to EBP50 in a competition assay (Nguyen et al., 2001). However, unlike the ERM proteins, Merlin interaction with EBP50 could not be abolished through competition using the region corresponding to the C-ERMAD (Nguyen et al., 2001). The inability of the C-ERMAD of Merlin to compete for binding with EBP50 suggests that Merlin intramolecular interactions may differ from ERMs.

Both comparisons with past and current research suggest that while the secondary structure of Merlin may be very similar to ERM proteins (McCartney and Fehon, 1996), the tertiary structure may be very different in the C-terminal tail because of the on low identity present. Previous crystallographic studies of the FERM domain of Merlin show that many residues that are divergent from ERMs are clustered on the surface (Kang et al., 2002; Shimizu et al., 2002). This may suggest a difference in potential protein interactions as compared to ERM proteins. The differences in the surface residues between Merlin and ERMs would allow different protein binding domains to exist. As well, the conformational changes resulting from potential protein interactions or phosphorylation would also be different between Merlin and ERMs because of the different residues present. These crystallographic studies may also help explain the difference in binding

of the FERM domain of Merlin and the FERM domain of Moesin to Sip1. Unfortunately, detailed analysis of Merlin protein domains required for interaction with other proteins is very much lacking.

5.5 Conclusions

My research is the first detailed analysis of the protein domains of *Drosophila* Merlin necessary for interaction with Sip1. Previous research shows that the FERM domain of Merlin is sufficient for binding to the Sip1 homolog EBP50 (Nguyen et al., 2001). I identified a novel Sip1 binding domain downstream of the FERM domain of Merlin which is necessary for binding to Sip1. Within this novel binding domain, the substitution of two conserved arginines at amino acid positions 325 and 335 results in a loss of binding to Sip1. In addition, experiments done by both Angela Effa and myself identify a novel potential phosphorylation site is present in this potential Sip1 binding domain. As well, phosphorylation of this site may be regulated by the kinase Slik. Having identified a potential binding domain necessary for Merlin and Sip1 interaction and a potential phosphorylation site that may regulate this interaction, future research on the role this interaction plays in Merlin cell proliferation control can be carried out.

5.6 Future directions

A common result of research seems to be that one ends up with more questions than answers. First and foremost, even though *in vitro* experiments have identified a novel Sip1 binding domain in Merlin, the

existence of this domain must be confirmed *in vivo*. To do this, transgenic flies can be created using constructs with UAS promoters and epitope tags along with mutations in the Merlin DNA sequence encoding the conserved arginines. Using the UAS/Gal4 system, overexpression in specific tissues like the wings can be carried out. The epitope tag will allow us to identify mutant Merlin expression. Past experiments using overexpression of Merlin constructs that express constitutively active and inactive Merlin in wings has an effect on wing size. This change in wing size can be correlated to the amount of cell proliferation. So simply overexpressing the mutant constructs in *Drosophila* wings may also affect wing size. However, it may be necessary to express this construct in specific tissues where wildtype Merlin is knocked down via RNAi. If interaction with Sip1 is necessary for Merlin activity, the inability to interact with Sip1 may result in non-functional Merlin and no change in a genetic background where wildtype protein is present and can mask the effect of a loss of Merlin function.

Currently, it is unknown how many phosphorylated isoforms of Merlin exists. To begin to address this, radioactive phosphate labelling using S2 cells with ^{32}P can be done. Immunoprecipitation of Merlin and 2D gel electrophoresis can separate different Merlin isoforms. From previous 2D gels of Merlin using Merlin antibody detection and

phosphatase treatment, there are likely 2-3 phosphorylation sites (Yang et al., Unpublished). However, phosphatase treatment only reduces the intensity of some of the detected Merlin isoforms using Merlin antibody and is inconclusive for determining the phosphorylated Merlin isoforms. Two different methods can be used to ascertain phosphorylated isoforms. Firstly, phosphoserine and phosphothreonine antibodies can be used to detect Merlin phosphorylation. In addition to determining the number of phosphorylated Merlin isoforms, this method may also identify a difference in the number of phosphorylated serines and threonines. Secondly, phosphate labelling of S2 cells can also be used to identify different phosphorylated Merlin isoforms. S2 cells can be grown in phosphate free media with radioactive ^{32}P-ATP. Using the same methods of immunoprecipitation and 2D gel electrophoresis, different phosphorylated isoforms of Merlin can be separated and visualized. Using constructs containing substitutions at potential phosphorylation sites to either non-phosphorylatable and phosphomimic residues to block a phosphorylation site, radioactive phosphate labelling may allow us to identify potential multistep phosphorylation if blocking a site results in the absence of more than one isoform. If the phosphorylated isoforms of Merlin can be identified, these phosphorylated isoforms of Merlin can be made and used in experiments to test binding to Sip1

and other proteins as well to determine whether or not phosphorylated Merlin can interact with Sip1.

Bibliography

Alfthan, K., Heiska, L., Gronholm, M., Renkema, G.H., and Carpen, O. (2004). Cyclic AMP-dependent protein kinase phosphorylates merlin at serine 518 independently of p21-activated kinase and promotes merlin-ezrin heterodimerization. J Biol Chem *279*, 18559-18566.

Amieva, M.R., and Furthmayr, H. (1995). Subcellular localization of moesin in dynamic filopodia, retraction fibers, and other structures involved in substrate exploration, attachment, and cell-cell contacts. Exp Cell Res *219*, 180-196.

Amieva, M.R., Wilgenbus, K.K., and Furthmayr, H. (1994). Radixin is a component of hepatocyte microvilli in situ. Exp Cell Res *210*, 140-144.

Bai, Y., Liu, Y.J., Wang, H., Xu, Y., Stamenkovic, I., and Yu, Q. (2007). Inhibition of the hyaluronan-CD44 interaction by merlin contributes to the tumor-suppressor activity of merlin. Oncogene *26*, 836-850.

Berryman, M., Franck, Z., and Bretscher, A. (1993). Ezrin is concentrated in the apical microvilli of a wide variety of epithelial cells whereas moesin is found primarily in endothelial cells. J Cell Sci *105 (Pt 4)*, 1025-1043.

Bretscher, A. (1983). Purification of an 80,000-dalton protein that is a component of the isolated microvillus cytoskeleton, and its localization in nonmuscle cells. J Cell Biol *97*, 425-432.

Bretscher, A., Chambers, D., Nguyen, R., and Reczek, D. (2000). ERM-Merlin and EBP50 protein families in plasma membrane organization and function. Annu Rev Cell Dev Biol *16*, 113-143.

Bretscher, A., Edwards, K., and Fehon, R.G. (2002). ERM proteins and merlin: integrators at the cell cortex. Nat Rev Mol Cell Biol *3*, 586-599.

Curto, M., Cole, B.K., Lallemand, D., Liu, C.H., and McClatchey, A.I. (2007). Contact-dependent inhibition of EGFR signaling by Nf2/Merlin. J Cell Biol *177*, 893-903.

Curto, M., and McClatchey, A.I. (2008). Nf2/Merlin: a coordinator of receptor signalling and intercellular contact. Br J Cancer *98*, 256-262.

Evans, D.G., Huson, S.M., Donnai, D., Neary, W., Blair, V., Newton, V., and Harris, R. (1992a). A clinical study of type 2 neurofibromatosis. Q J Med *84*, 603-618.

Evans, D.G., Huson, S.M., Donnai, D., Neary, W., Blair, V., Teare, D., Newton, V., Strachan, T., Ramsden, R., and Harris, R. (1992b). A genetic study of type 2 neurofibromatosis in the United Kingdom. I. Prevalence, mutation rate, fitness, and confirmation of maternal transmission effect on severity. J Med Genet *29*, 841-846.

Evans, D.G., Moran, A., King, A., Saeed, S., Gurusinghe, N., and Ramsden, R. (2005). Incidence of vestibular schwannoma and neurofibromatosis 2 in the North West of England over a 10-year period: higher incidence than previously thought. Otol Neurotol *26*, 93-97.

Fehon, R.G., McClatchey, A.I., and Bretscher, A. (2010). Organizing the cell cortex: the role of ERM proteins. Nat Rev Mol Cell Biol *11*, 276-287.

Fehon, R.G., Oren, T., LaJeunesse, D.R., Melby, T.E., and McCartney, B.M. (1997). Isolation of mutations in the Drosophila homologues of the human Neurofibromatosis 2 and yeast CDC42 genes using a simple and efficient reverse-genetic method. Genetics *146*, 245-252.

Fievet, B.T., Gautreau, A., Roy, C., Del Maestro, L., Mangeat, P., Louvard, D., and Arpin, M. (2004). Phosphoinositide binding and phosphorylation act sequentially in the activation mechanism of ezrin. J Cell Biol *164*, 653-659.

Finnerty, C.M., Chambers, D., Ingraffea, J., Faber, H.R., Karplus, P.A., and Bretscher, A. (2004). The EBP50-moesin interaction involves a binding site regulated by direct masking on the FERM domain. J Cell Sci *117*, 1547-1552.

Flaiz, C., Utermark, T., Parkinson, D.B., Poetsch, A., and Hanemann, C.O. (2008). Impaired intercellular adhesion and immature adherens junctions in merlin-deficient human primary schwannoma cells. Glia *56*, 506-515.

Fouassier, L., Duan, C.Y., Feranchak, A.P., Yun, C.H., Sutherland, E., Simon, F., Fitz, J.G., and Doctor, R.B. (2001). Ezrin-radixin-moesin-binding phosphoprotein 50 is expressed at the apical membrane of rat liver epithelia. Hepatology *33*, 166-176.

Franck, Z., Gary, R., and Bretscher, A. (1993). Moesin, like ezrin, colocalizes with actin in the cortical cytoskeleton in cultured cells, but its expression is more variable. J Cell Sci *105 (Pt 1)*, 219-231.

Funayama, N., Nagafuchi, A., Sato, N., and Tsukita, S. (1991). Radixin is a novel member of the band 4.1 family. J Cell Biol *115*, 1039-1048.

Gary, R., and Bretscher, A. (1995). Ezrin self-association involves binding of an N-terminal domain to a normally masked C-terminal domain that includes the F-actin binding site. Mol Biol Cell *6*, 1061-1075.

Gille, C., and Frommel, C. (2001). STRAP: editor for STRuctural Alignments of Proteins. Bioinformatics *17*, 377-378.

Gladden, A.B., Hebert, A.M., Schneeberger, E.E., and McClatchey, A.I. (2010). The NF2 tumor suppressor, Merlin, regulates epidermal development through the establishment of a junctional polarity complex. Dev Cell *19*, 727-739.

Golovnina, K., Blinov, A., Akhmametyeva, E.M., Omelyanchuk, L.V., and Chang, L.S. (2005). Evolution and origin of merlin, the product of the Neurofibromatosis type 2 (NF2) tumor-suppressor gene. BMC Evol Biol *5*, 69.

Gould, K.L., Bretscher, A., Esch, F.S., and Hunter, T. (1989). cDNA cloning and sequencing of the protein-tyrosine kinase substrate, ezrin, reveals homology to band 4.1. EMBO J *8*, 4133-4142.

Gould, K.L., Cooper, J.A., Bretscher, A., and Hunter, T. (1986). The protein-tyrosine kinase substrate, p81, is homologous to a chicken microvillar core protein. J Cell Biol *102*, 660-669.

Gronholm, M., Sainio, M., Zhao, F., Heiska, L., Vaheri, A., and Carpen, O. (1999). Homotypic and heterotypic interaction of the neurofibromatosis 2 tumor suppressor protein merlin and the ERM protein ezrin. J Cell Sci *112 (Pt 6)*, 895-904.

Gutmann, D.H., Giordano, M.J., Fishback, A.S., and Guha, A. (1997). Loss of merlin expression in sporadic meningiomas, ependymomas and schwannomas. Neurology *49*, 267-270.

Gutmann, D.H., Haipek, C.A., Burke, S.P., Sun, C.X., Scoles, D.R., and Pulst, S.M. (2001). The NF2 interactor, hepatocyte growth factor-regulated tyrosine kinase substrate (HRS), associates with merlin in the "open" conformation and suppresses cell growth and motility. Hum Mol Genet *10*, 825-834.

Gutmann, D.H., Wright, D.E., Geist, R.T., and Snider, W.D. (1995). Expression of the neurofibromatosis 2 (NF2) gene isoforms during rat embryonic development. Hum Mol Genet *4*, 471-478.

Haase, V.H., Trofatter, J.A., MacCollin, M., Tarttelin, E., Gusella, J.F., and Ramesh, V. (1994). The murine NF2 homologue encodes a highly conserved merlin protein with alternative forms. Hum Mol Genet *3*, 407-411.

Hanemann, C.O., and Evans, D.G. (2006). News on the genetics, epidemiology, medical care and translational research of Schwannomas. J Neurol *253*, 1533-1541.

Hara, T., Bianchi, A.B., Seizinger, B.R., and Kley, N. (1994). Molecular cloning and characterization of alternatively spliced transcripts of the mouse neurofibromatosis 2 gene. Cancer Res *54*, 330-335.

Hipfner, D.R., Keller, N., and Cohen, S.M. (2004). Slik Sterile-20 kinase regulates Moesin activity to promote epithelial integrity during tissue growth. Genes Dev *18*, 2243-2248.

Hirao, M., Sato, N., Kondo, T., Yonemura, S., Monden, M., Sasaki, T., Takai, Y., and Tsukita, S. (1996). Regulation mechanism of ERM (ezrin/radixin/moesin) protein/plasma membrane association: possible involvement of phosphatidylinositol turnover and Rho-dependent signaling pathway. J Cell Biol *135*, 37-51.

Huang, L., Ichimaru, E., Pestonjamasp, K., Cui, X., Nakamura, H., Lo, G.Y., Lin, F.I., Luna, E.J., and Furthmayr, H. (1998). Merlin differs from moesin in binding to F-actin and in its intra- and intermolecular interactions. Biochem Biophys Res Commun *248*, 548-553.

Huber, M.A., Kraut, N., and Beug, H. (2005). Molecular requirements for epithelial-mesenchymal transition during tumor progression. Curr Opin Cell Biol *17*, 548-558.

Hughes, S.C., and Fehon, R.G. (2006). Phosphorylation and activity of the tumor suppressor Merlin and the ERM protein Moesin are coordinately regulated by the Slik kinase. J Cell Biol *175*, 305-313.

Hughes, S.C., Formstecher, E., and Fehon, R.G. (2010). Sip1, the Drosophila orthologue of EBP50/NHERF1, functions with the sterile 20 family kinase Slik to regulate Moesin activity. J Cell Sci *123*, 1099-1107.

Huynh, D.P., Tran, T.M., Nechiporuk, T., and Pulst, S.M. (1996). Expression of neurofibromatosis 2 transcript and gene product during mouse fetal development. Cell Growth Differ *7*, 1551-1561.

James, M.F., Manchanda, N., Gonzalez-Agosti, C., Hartwig, J.H., and Ramesh, V. (2001). The neurofibromatosis 2 protein product merlin selectively binds F-actin but not G-actin, and stabilizes the filaments through a lateral association. Biochem J *356*, 377-386.

Kang, B.S., Cooper, D.R., Devedjiev, Y., Derewenda, U., and Derewenda, Z.S. (2002). The structure of the FERM domain of merlin, the neurofibromatosis type 2 gene product. Acta Crystallogr D Biol Crystallogr *58*, 381-391.

Kim, H., Kwak, N.J., Lee, J.Y., Choi, B.H., Lim, Y., Ko, Y.J., Kim, Y.H., Huh, P.W., Lee, K.H., Rha, H.K., *et al.* (2004). Merlin neutralizes the inhibitory effect of Mdm2 on p53. J Biol Chem *279*, 7812-7818.

Kissil, J.L., Johnson, K.C., Eckman, M.S., and Jacks, T. (2002). Merlin phosphorylation by p21-activated kinase 2 and effects of phosphorylation on merlin localization. J Biol Chem *277*, 10394-10399.

Kissil, J.L., Wilker, E.W., Johnson, K.C., Eckman, M.S., Yaffe, M.B., and Jacks, T. (2003). Merlin, the product of the Nf2 tumor suppressor gene, is an inhibitor of the p21-activated kinase, Pak1. Mol Cell *12*, 841-849.

Knudson, A.G. (1996). Hereditary cancer: two hits revisited. J Cancer Res Clin Oncol *122*, 135-140.

Knudson, A.G., Jr. (1971). Mutation and cancer: statistical study of retinoblastoma. Proc Natl Acad Sci U S A *68*, 820-823.

LaJeunesse, D.R., McCartney, B.M., and Fehon, R.G. (1998). Structural analysis of Drosophila merlin reveals functional domains important for growth control and subcellular localization. J Cell Biol *141*, 1589-1599.

Lallemand, D., Curto, M., Saotome, I., Giovannini, M., and McClatchey, A.I. (2003). NF2 deficiency promotes tumorigenesis and metastasis by destabilizing adherens junctions. Genes Dev *17*, 1090-1100.

Lallemand, D., Saint-Amaux, A.L., and Giovannini, M. (2009). Tumor-suppression functions of merlin are independent of its role as an

organizer of the actin cytoskeleton in Schwann cells. J Cell Sci *122*, 4141-4149.

Lankes, W.T., and Furthmayr, H. (1991). Moesin: a member of the protein 4.1-talin-ezrin family of proteins. Proc Natl Acad Sci U S A *88*, 8297-8301.

Laulajainen, M., Muranen, T., Carpen, O., and Gronholm, M. (2008). Protein kinase A-mediated phosphorylation of the NF2 tumor suppressor protein merlin at serine 10 affects the actin cytoskeleton. Oncogene *27*, 3233-3243.

Laulajainen, M., Muranen, T., Nyman, T.A., Carpen, O., and Gronholm, M. (2011). Multistep Phosphorylation by Oncogenic Kinases Enhances the Degradation of the NF2 Tumor Suppressor Merlin. Neoplasia *13*, 643-652.

Lazar, C.S., Cresson, C.M., Lauffenburger, D.A., and Gill, G.N. (2004). The Na+/H+ exchanger regulatory factor stabilizes epidermal growth factor receptors at the cell surface. Mol Biol Cell *15*, 5470-5480.

Li, Q., Nance, M.R., Kulikauskas, R., Nyberg, K., Fehon, R., Karplus, P.A., Bretscher, A., and Tesmer, J.J. (2007). Self-masking in an intact ERM-merlin protein: an active role for the central alpha-helical domain. J Mol Biol *365*, 1446-1459.

Lutchman, M., and Rouleau, G.A. (1995). The neurofibromatosis type 2 gene product, schwannomin, suppresses growth of NIH 3T3 cells. Cancer Res *55*, 2270-2274.

Mani, T., Hennigan, R.F., Foster, L.A., Conrady, D.G., Herr, A.B., and Ip, W. (2011). FERM domain phosphoinositide binding targets merlin to the membrane and is essential for its growth-suppressive function. Mol Cell Biol *31*, 1983-1996.

Matsui, T., Maeda, M., Doi, Y., Yonemura, S., Amano, M., Kaibuchi, K., and Tsukita, S. (1998). Rho-kinase phosphorylates COOH-terminal threonines of ezrin/radixin/moesin (ERM) proteins and regulates their head-to-tail association. J Cell Biol *140*, 647-657.

McCartney, B.M., and Fehon, R.G. (1996). Distinct cellular and subcellular patterns of expression imply distinct functions for the Drosophila homologues of moesin and the neurofibromatosis 2 tumor suppressor, merlin. J Cell Biol *133*, 843-852.

McClatchey, A.I., and Giovannini, M. (2005). Membrane organization and tumorigenesis--the NF2 tumor suppressor, Merlin. Genes Dev *19*, 2265-2277.

McClatchey, A.I., Saotome, I., Ramesh, V., Gusella, J.F., and Jacks, T. (1997). The Nf2 tumor suppressor gene product is essential for extraembryonic development immediately prior to gastrulation. Genes Dev *11*, 1253-1265.

Morales, F.C., Takahashi, Y., Kreimann, E.L., and Georgescu, M.M. (2004). Ezrin-radixin-moesin (ERM)-binding phosphoprotein 50 organizes ERM proteins at the apical membrane of polarized epithelia. Proc Natl Acad Sci U S A *101*, 17705-17710.

Morrison, H., Sherman, L.S., Legg, J., Banine, F., Isacke, C., Haipek, C.A., Gutmann, D.H., Ponta, H., and Herrlich, P. (2001). The NF2 tumor suppressor gene product, merlin, mediates contact inhibition of growth through interactions with CD44. Genes Dev *15*, 968-980.

Morrison, H., Sperka, T., Manent, J., Giovannini, M., Ponta, H., and Herrlich, P. (2007). Merlin/neurofibromatosis type 2 suppresses growth by inhibiting the activation of Ras and Rac. Cancer Res *67*, 520-527.

Murai, T., Miyazaki, Y., Nishinakamura, H., Sugahara, K.N., Miyauchi, T., Sako, Y., Yanagida, T., and Miyasaka, M. (2004). Engagement of CD44 promotes Rac activation and CD44 cleavage during tumor cell migration. J Biol Chem *279*, 4541-4550.

Murthy, A., Gonzalez-Agosti, C., Cordero, E., Pinney, D., Candia, C., Solomon, F., Gusella, J., and Ramesh, V. (1998). NHE-RF, a regulatory cofactor for Na(+)-H+ exchange, is a common interactor for merlin and ERM (MERM) proteins. J Biol Chem *273*, 1273-1276.

Nakamura, F., Amieva, M.R., and Furthmayr, H. (1995). Phosphorylation of threonine 558 in the carboxyl-terminal actin-binding domain of moesin by thrombin activation of human platelets. J Biol Chem *270*, 31377-31385.

Ng, T., Parsons, M., Hughes, W.E., Monypenny, J., Zicha, D., Gautreau, A., Arpin, M., Gschmeissner, S., Verveer, P.J., Bastiaens, P.I.*, et al.* (2001). Ezrin is a downstream effector of trafficking PKC-integrin complexes involved in the control of cell motility. EMBO J *20*, 2723-2741.

Nguyen, R., Reczek, D., and Bretscher, A. (2001). Hierarchy of merlin and ezrin N- and C-terminal domain interactions in homo- and

heterotypic associations and their relationship to binding of scaffolding proteins EBP50 and E3KARP. J Biol Chem *276*, 7621-7629.

Okada, M., Wang, Y., Jang, S.W., Tang, X., Neri, L.M., and Ye, K. (2009). Akt phosphorylation of merlin enhances its binding to phosphatidylinositols and inhibits the tumor-suppressive activities of merlin. Cancer Res *69*, 4043-4051.

Oshiro, N., Fukata, Y., and Kaibuchi, K. (1998). Phosphorylation of moesin by rho-associated kinase (Rho-kinase) plays a crucial role in the formation of microvilli-like structures. J Biol Chem *273*, 34663-34666.

Pakkanen, R., Hedman, K., Turunen, O., Wahlstrom, T., and Vaheri, A. (1987). Microvillus-specific Mr 75,000 plasma membrane protein of human choriocarcinoma cells. J Histochem Cytochem *35*, 809-816.

Pearson, M.A., Reczek, D., Bretscher, A., and Karplus, P.A. (2000). Structure of the ERM protein moesin reveals the FERM domain fold masked by an extended actin binding tail domain. Cell *101*, 259-270.

Pietromonaco, S.F., Simons, P.C., Altman, A., and Elias, L. (1998). Protein kinase C-theta phosphorylation of moesin in the actin-binding sequence. J Biol Chem *273*, 7594-7603.

Reczek, D., Berryman, M., and Bretscher, A. (1997). Identification of EBP50: A PDZ-containing phosphoprotein that associates with members of the ezrin-radixin-moesin family. J Cell Biol *139*, 169-179.

Reczek, D., and Bretscher, A. (1998). The carboxyl-terminal region of EBP50 binds to a site in the amino-terminal domain of ezrin that is masked in the dormant molecule. J Biol Chem *273*, 18452-18458.

Riemenschneider, M.J., Perry, A., and Reifenberger, G. (2006). Histological classification and molecular genetics of meningiomas. Lancet Neurol *5*, 1045-1054.

Rong, R., Surace, E.I., Haipek, C.A., Gutmann, D.H., and Ye, K. (2004a). Serine 518 phosphorylation modulates merlin intramolecular association and binding to critical effectors important for NF2 growth suppression. Oncogene *23*, 8447-8454.

Rong, R., Tang, X., Gutmann, D.H., and Ye, K. (2004b). Neurofibromatosis 2 (NF2) tumor suppressor merlin inhibits phosphatidylinositol 3-kinase through binding to PIKE-L. Proc Natl Acad Sci U S A *101*, 18200-18205.

Rouleau, G.A., Merel, P., Lutchman, M., Sanson, M., Zucman, J., Marineau, C., Hoang-Xuan, K., Demczuk, S., Desmaze, C., Plougastel, B.*, et al.* (1993). Alteration in a new gene encoding a putative membrane-organizing protein causes neuro-fibromatosis type 2. Nature *363*, 515-521.

Ruttledge, M.H., Sarrazin, J., Rangaratnam, S., Phelan, C.M., Twist, E., Merel, P., Delattre, O., Thomas, G., Nordenskjold, M., Collins, V.P.*, et al.* (1994). Evidence for the complete inactivation of the NF2 gene in the majority of sporadic meningiomas. Nat Genet *6*, 180-184.

Saotome, I., Curto, M., and McClatchey, A.I. (2004). Ezrin is essential for epithelial organization and villus morphogenesis in the developing intestine. Dev Cell *6*, 855-864.

Sato, N., Funayama, N., Nagafuchi, A., Yonemura, S., and Tsukita, S. (1992). A gene family consisting of ezrin, radixin and moesin. Its specific localization at actin filament/plasma membrane association sites. J Cell Sci *103 (Pt 1)*, 131-143.

Schulze, K.M., Hanemann, C.O., Muller, H.W., and Hanenberg, H. (2002). Transduction of wild-type merlin into human schwannoma cells decreases schwannoma cell growth and induces apoptosis. Hum Mol Genet *11*, 69-76.

Scoles, D.R. (2008). The merlin interacting proteins reveal multiple targets for NF2 therapy. Biochim Biophys Acta *1785*, 32-54.

Scoles, D.R., Huynh, D.P., Morcos, P.A., Coulsell, E.R., Robinson, N.G., Tamanoi, F., and Pulst, S.M. (1998). Neurofibromatosis 2 tumour suppressor schwannomin interacts with betaII-spectrin. Nat Genet *18*, 354-359.

Shaw, R.J., McClatchey, A.I., and Jacks, T. (1998). Regulation of the neurofibromatosis type 2 tumor suppressor protein, merlin, by adhesion and growth arrest stimuli. J Biol Chem *273*, 7757-7764.

Shaw, R.J., Paez, J.G., Curto, M., Yaktine, A., Pruitt, W.M., Saotome, I., O'Bryan, J.P., Gupta, V., Ratner, N., Der, C.J.*, et al.* (2001). The Nf2 tumor suppressor, merlin, functions in Rac-dependent signaling. Dev Cell *1*, 63-72.

Sherman, L., Xu, H.M., Geist, R.T., Saporito-Irwin, S., Howells, N., Ponta, H., Herrlich, P., and Gutmann, D.H. (1997). Interdomain binding mediates tumor growth suppression by the NF2 gene product. Oncogene *15*, 2505-2509.

Shimizu, T., Seto, A., Maita, N., Hamada, K., Tsukita, S., and Hakoshima, T. (2002). Structural basis for neurofibromatosis type 2. Crystal structure of the merlin FERM domain. J Biol Chem *277*, 10332-10336.

Simons, P.C., Pietromonaco, S.F., Reczek, D., Bretscher, A., and Elias, L. (1998). C-terminal threonine phosphorylation activates ERM proteins to link the cell's cortical lipid bilayer to the cytoskeleton. Biochem Biophys Res Commun *253*, 561-565.

Sivakumar, K.C., Thomas, B., and Karunagaran, D. (2009). Three dimensional structure of the closed conformation (active) of human merlin reveals masking of actin binding site in the FERM domain. Int J Bioinform Res Appl *5*, 516-524.

Speck, O., Hughes, S.C., Noren, N.K., Kulikauskas, R.M., and Fehon, R.G. (2003). Moesin functions antagonistically to the Rho pathway to maintain epithelial integrity. Nature *421*, 83-87.

Stemmer-Rachamimov, A.O., Ino, Y., Lim, Z.Y., Jacoby, L.B., MacCollin, M., Gusella, J.F., Ramesh, V., and Louis, D.N. (1998). Loss of the NF2 gene and merlin occur by the tumorlet stage of schwannoma development in neurofibromatosis 2. J Neuropathol Exp Neurol *57*, 1164-1167.

Stemmer-Rachamimov, A.O., Xu, L., Gonzalez-Agosti, C., Burwick, J.A., Pinney, D., Beauchamp, R., Jacoby, L.B., Gusella, J.F., Ramesh, V., and Louis, D.N. (1997). Universal absence of merlin, but not other ERM family members, in schwannomas. Am J Pathol *151*, 1649-1654.

Sun, C.X., Haipek, C., Scoles, D.R., Pulst, S.M., Giovannini, M., Komada, M., and Gutmann, D.H. (2002). Functional analysis of the relationship between the neurofibromatosis 2 tumor suppressor and its binding partner, hepatocyte growth factor-regulated tyrosine kinase substrate. Hum Mol Genet *11*, 3167-3178.

Surace, E.I., Haipek, C.A., and Gutmann, D.H. (2004). Effect of merlin phosphorylation on neurofibromatosis 2 (NF2) gene function. Oncogene *23*, 580-587.

Takeuchi, K., Sato, N., Kasahara, H., Funayama, N., Nagafuchi, A., Yonemura, S., and Tsukita, S. (1994). Perturbation of cell adhesion and microvilli formation by antisense oligonucleotides to ERM family members. J Cell Biol *125*, 1371-1384.

Tang, X., Jang, S.W., Wang, X., Liu, Z., Bahr, S.M., Sun, S.Y., Brat, D., Gutmann, D.H., and Ye, K. (2007). Akt phosphorylation regulates the tumour-suppressor merlin through ubiquitination and degradation. Nat Cell Biol *9*, 1199-1207.

Thiery, J.P., and Sleeman, J.P. (2006). Complex networks orchestrate epithelial-mesenchymal transitions. Nat Rev Mol Cell Biol *7*, 131-142.

Tikoo, A., Varga, M., Ramesh, V., Gusella, J., and Maruta, H. (1994). An anti-Ras function of neurofibromatosis type 2 gene product (NF2/Merlin). J Biol Chem *269*, 23387-23390.

Tran Quang, C., Gautreau, A., Arpin, M., and Treisman, R. (2000). Ezrin function is required for ROCK-mediated fibroblast transformation by the Net and Dbl oncogenes. EMBO J *19*, 4565-4576.

Trofatter, J.A., MacCollin, M.M., Rutter, J.L., Murrell, J.R., Duyao, M.P., Parry, D.M., Eldridge, R., Kley, N., Menon, A.G., Pulaski, K.*, et al.* (1993). A novel moesin-, ezrin-, radixin-like gene is a candidate for the neurofibromatosis 2 tumor suppressor. Cell *75*, 826.

Tsukita, S., and Hieda, Y. (1989). A new 82-kD barbed end-capping protein (radixin) localized in the cell-to-cell adherens junction: purification and characterization. J Cell Biol *108*, 2369-2382.

Tsukita, S., Oishi, K., Sato, N., Sagara, J., and Kawai, A. (1994). ERM family members as molecular linkers between the cell surface glycoprotein CD44 and actin-based cytoskeletons. J Cell Biol *126*, 391-401.

Wheeler, D., Sneddon, W.B., Wang, B., Friedman, P.A., and Romero, G. (2007). NHERF-1 and the cytoskeleton regulate the traffic and membrane dynamics of G protein-coupled receptors. J Biol Chem *282*, 25076-25087.

Wiley, L.A., Dattilo, L., Kang, K.B., Giovannini, M., and Beebe, D.C. (2010). The tumor suppressor, Merlin, is required for cell cycle exit, terminal differentiation, and cell polarity in the developing murine lens. Invest Ophthalmol Vis Sci.

Woods, R., Friedman, J.M., Evans, D.G., Baser, M.E., and Joe, H. (2003). Exploring the "two-hit hypothesis" in NF2: tests of two-hit and three-hit models of vestibular schwannoma development. Genet Epidemiol *24*, 265-272.

Xiao, G.H., Beeser, A., Chernoff, J., and Testa, J.R. (2002). p21-activated kinase links Rac/Cdc42 signaling to merlin. J Biol Chem *277*, 883-886.

Xiao, G.H., Gallagher, R., Shetler, J., Skele, K., Altomare, D.A., Pestell, R.G., Jhanwar, S., and Testa, J.R. (2005). The NF2 tumor suppressor gene product, merlin, inhibits cell proliferation and cell cycle progression by repressing cyclin D1 expression. Mol Cell Biol *25*, 2384-2394.

Xu, H.M., and Gutmann, D.H. (1998). Merlin differentially associates with the microtubule and actin cytoskeleton. J Neurosci Res *51*, 403-415.

Yang, Y., Primrose, D.A., Leung, A.C., Fitzsimmons, R.B., McDermand, M.C., Missellbrook, A., Haskins, J., Smylie, A.S., and Hughes, S.C. (Unpublished). The PP1 phosphatase Flapwing regulates the activity of Merlin and Moesin in Drosophila.

Yonemura, S., Matsui, T., and Tsukita, S. (2002). Rho-dependent and -independent activation mechanisms of ezrin/radixin/moesin proteins: an essential role for polyphosphoinositides in vivo. J Cell Sci *115*, 2569-2580.

Appendix A: List of DNA Primers

Primer Name on Label	5' Sequence 3'	Notes
Merlin FERM Forward	CACCATGAGCCCCTTCGGCTCCAAG	
Merlin FERM Reverse	GCGGCGGCGCATATATAGATC	
Merlin CC Forward	CACCAAACCCGACACCATGGAAATC	
Merlin CC Reverse	TCAGAGCTCCTCGAAGAAGGC	
Moesin FERM Forward	CACCATGTCTCCAAAAGCGCTAAATGTGCG	
Moesin FERM Reverse	GCGGCGACGCATGTACAGCTC	
Moesin CC Forward	CACCAAGCCGGACACCATCGATGT	
Moesin CC Reverse	TTACATGTTCTCAAACTGATCGACGCG	
CG8023 N-Terminal Forward	CACCATGGTGTACACCGGTTACGTA	
CG8023 N-Terminal Reverse	GACCATGTAGTCATTGAATATCTTCAGATC	
CG8023 C-Terminal Forward	CACCTTCAAGAAAAATATTCGTCCC	
CG8023 C-Terminal Reverse	CTACAATGTGTAGATGGCATT	
CG8023 eIF4E Forward	CACCAAGCATCCATTGGAGCATACC	
CG8023 Unique Reverse	CATGGCCAGGTCGTAGTCGAT	
Sip1 N-Terminal Forward	CACCATGTCCACGCCCACTTCCCCG	
Sip1 N-Terminal Reverse	GCTACTGATATTGGCACTTGCTCCGGG	
Sip1 C-Terminal Forward	CACCATCAGTATGGTGAGCACCAAG	
Sip1 C-Terminal Reverse	TCAGAGCTTCTGAATGATGTCGAACTT	

Merlin FERM F3	GACATGTACGGAGTAAACTACTTTCCT	Sequencing
Moesin FERM F3	GAGATGTACGGCGTTAACTACTTT	Sequencing
Merlin S371A	CGATGCACTTCGGCGTGCCGAAGAGACCA	SDM
Merlin S371A antisense	TGGTCTCTTCGGCACGCCGAAGTGCATCG	SDM
Merlin S371D	CAACGATGCACTTCGGCGTGACGAAGAGACCAAGGAG	SDM
Merlin S371D antisense	CTCCTTGGTCTCTTCGTCACGCCGAAGTGCATCGTTG	SDM
Merlin S476A	CAGCGGCCGCAAGGCCTCCACGGATAG	SDM
Merlin S476A antisense	CTATCCGTGGAGGCCTTGCGGCCGCTG	SDM
Merlin S476D	ACAGCGGCCGCAAGGACTCCACGGATAGCC	SDM
Merlin S476D antisense	GGCTATCCGTGGAGTCCTTGCGGCCGCTGT	SDM
Merlin S477A	GGCCGCAAGTCCGCCACGGATAGCC	SDM
Merlin S477A antisense	GGCTATCCGTGGCGGACTTGCGGCC	SDM
Merlin S477D	GCGGCCGCAAGTCCGACACGGATAGCCTGC	SDM
Merlin S477D antisense	GCAGGCTATCCGTGTCGGACTTGCGGCCGC	SDM
Merlin S476A S477A	AGCGGCCGCAAGGCCGCCACGGATAGCC	SDM
Merlin S476A S477A antisense	GCCTATCCGTGGCGGCCTTGCGGCCGCT	SDM
Merlin S476D S477D	CTCAACAGCGGCCGCAAGGACGACACGGATAGCCTGCTGAC	SDM
Merlin S476D S477D antisense	GTCAGCAGGCTATCCGTGTCGTCCTTGCGGCCGCTGTTGAG	SDM
Merlin S510A	CCCTGATCACAAGCAGCGCAACCAATGATTTGGAG	SDM
Merlin S510A antisense	CTCCAAATCATTGGTTGCGCTGCTTGTGATCAGGG	SDM
Merlin S510D	CCTCCCTGATCACAAGCAGCGATACCAATGATTTGGAGACCGC	SDM
Merlin S510D antisense	GCGGTCTCCAAATCATTGGTATCGCTGCTTGTGATCAGGGAGG	SDM

Merlin S624A	CTCAAGTCCGGCGCGACCAAGGCGC	SDM
Merlin S624A antisense	GCGCCTTGGTCGCGCCGGACTTGAG	SDM
Merlin S624D	AGAAACTCAAGTCCGGCGATACCAAGGCGCGTGTCGC	SDM
Merlin S624D antisense	GCGACACGCGCCTTGGTATCGCCGGACTTGAGTTTCT	SDM
Merlin F1 Reverse	GATCAGCTCCTCGCTGACGTTCTC	
Merlin F2 Forward	CACCCTGATCCAGGAGATCACGCAG	
Merlin F2 Reverse	TACTCCGTACATGTCCAGGTC	
Merlin F3 Forward	CACCGGAGTAAACTACTTTCCTATTACG	
Merlin F3 Reverse	GGGTTTGCGGCGGCGCATATA	
Merlin 330 Forward	CACCAAAAAGTTCATCAGGGAAAAG	
Merlin 355 Reverse	CTCCATGCTCTTCTCCAGCTCGTA	
Merlin 356 Forward	CACCCACCTGCAAAACGAAATGCGC	
Merlin 356 Forward	CACCTGCAAAACGAAATGCGC	No CACC
Merlin 380 Reverse	TTCGAAGTACAGCTCCTTGGT	
Merlin Mid Half Reverse	CCGGTCCATTTCCGTCTTGAAGTG	Position 405
Merlin Mid Half Forward	CACCCTGCGCGAGCGACAAATGAAA	Position 406
Merlin CC Middle Reverse	GCTATCCGTGGAGGACTTGCG	Position 480
Merlin CC Tail Forward	CACCCTGCTGACCGCCTCCAGTGTG	Position 481
Moesin F1 Reverse	GATCAGCTCCTCGGCCACATC	
Moesin F2 Forward	CACCCTGATCCAGGACATTACACTG	
Moesin F2 Reverse	AACGCCGTACATCTCCAGGTC	
Moesin F3 Forward	CACCGGCGTTAACTACTTTGAGATC	

Moesin F3 Reverse	CGGCTTGCGGCGACGCATGTA	
Sip PDZ Reverse	GGCCTTGCCATCCACATCGAT	
Delta EB50 Reverse	TGGTGTAGTGGGTGTGGTCATGCC	
Sip1 EBP50 Forward	CACCCCCCCACCGACCAGTGGCTAT	
Merlin S370 Reverse	ACGCCGAAGTGCATCGTTGGCCAT	Site 370
Merlin S375 Forward	AAGGAGCTGTACTTCGAAAAGAGT	Site 375
Merlin 406 Forward	CTGCGCGAGCGACAAATGAAA	No CACC
Merlin AEEA Forward	GCACTTCGGCGTGCCGAAGAGGCCAAGGAGCTGTACTTCG	SDM
Merlin AEEA Reverse	CGAAGTACAGCTCCTTGGCCTCTTCGGCACGCCGAAGTGC	SDM
Merlin AQQA Forward	GCACTTCGGCGTGCCCAACAGGCCAAGGAGCTGTACTTCG	SDM
Merlin AQQA Reverse	CGAAGTACAGCTCCTTGGCCTGTTGGGCACGCCGAAGTGC	SDM
Merlin 329 Reverse	GCGTTCGATCTGGCGGCGTTG	
Merlin 381 Forward	AAGAGTCGTGTCAACGAGGAG	
Merlin 600 Reverse	GTCCAGGTTGCTCTGGTTCTC	
Merlin 321 F	GAGGAGAAGCAACGCCGCCAG	
Merlin 331 F	AAAAAGTTCATCAGGGAAAAG	
Merlin 341 F	GAAAAGGCGGAGCACGAGCGC	
Merlin 351 F	GAGAAGAGCATGGAGCACCTG	
Merlin 361 F	ATGCGCATGGCCAACGATGCA	
Merlin 371 F	TCCGAAGAGACCAAGGAGCTG	
Merlin 315 R	CATCTGCTGGATTTCCATGGT	
Merlin 325 R	GCGTTGCTTCTCCTCCTTGGC	
Merlin 335 R	CCTGATGAACTTTTTGCGTTC	
Merlin 345 R	GTGCTCCGCCTTTTCGCGCAG	
Merlin 365 R	GTTGGCCATGCGCATTTCGTT	SDM
R325A	AGCCAAGGAGGAGAAGCAAGCCCGCCAGATC	SDM
R325A Antisense	GATCTGGCGGGCTTGCTTCTCCTCCTTGGCT	SDM

R335L	GATCGAACGCAAAAAGTTCATCCTAGAAAAGAAGCTGCGCGAAAAGG	SDM
R335L Antisense	CCTTTTCGCGCAGCTTCTTTTCTAGGATGAACTTTTTGCGTTCGATC	SDM
ACTf	GAGCATTGCGGCTGATAAGG	Sequencing
HSPf	TATAAATAGAGGCGCTTCGT	Sequencing
SVr	GGCATTCCACCACTGCTCCC	Sequencing

Appendix B: List of DNA Constructs

Name of Insert	Encodes	Vector	Type
Merlin	1-635	p/ENTRD	Entry
MerF	1-305	p/ENTRD	Entry
MerC	306-635	p/ENTRD	Entry
MerlinF1	1-104	p/ENTRD	Entry
MerlinF2	103-213	p/ENTRD	Entry
MerlinF3	212-307	p/ENTRD	Entry
Merlin CC	306-405	p/ENTRD	Entry
Merlin CC Mid	406-480	p/ENTRD	Entry
Merlin CC Tail	481-635	p/ENTRD	Entry
Merlin 306-355	306-355	p/ENTRD	Entry
Merlin 330-380	330-380	p/ENTRD	Entry
Merlin 356-405	356-405	p/ENTRD	Entry
Merlin Δ306-405		p/ENTRD	Entry
Merlin Δ306-355		p/ENTRD	Entry
Merlin Δ330-380		p/ENTRD	Entry
Merlin Δ356-405		p/ENTRD	Entry
Merlin Δ306-320		p/ENTRD	Entry
Merlin Δ316-330		p/ENTRD	Entry
Merlin Δ326-340		p/ENTRD	Entry
Merlin Δ336-350		p/ENTRD	Entry
Merlin Δ346-360		p/ENTRD	Entry
Merlin Δ356-370		p/ENTRD	Entry
Merlin Δ366-380		p/ENTRD	Entry
Merlin 1-405	1-405	p/ENTRD	Entry
Merlin 1-480	1-480	p/ENTRD	Entry
Merlin 1-600	1-600	p/ENTRD	Entry
Merlin S371A	1-635	p/ENTRD	Entry
Merlin S371D	1-635	p/ENTRD	Entry
Merlin T374A	1-635	p/ENTRD	Entry
Merlin T374D	1-635	p/ENTRD	Entry
Merlin AQQA	1-635	p/ENTRD	Entry
Moesin	1-578	p/ENTRD	Entry
MoeF	1-296	p/ENTRD	Entry
MoeC	297-578	p/ENTRD	Entry
MoesinF1	1-95	p/ENTRD	Entry
MoesinF2	94-204	p/ENTRD	Entry
MoesinF3	203-298	p/ENTRD	Entry

Sip1	1-296	p/ENTRD	Entry
Sip1 ΔEB50	1-246	p/ENTRD	Entry
Sip1 EB50	247-296	p/ENTRD	Entry
Merlin	1-635	pDest14	Expression
MerF	1-305	pDest14	Expression
MerC	306-635	pDest14	Expression
MerlinF1	1-104	pDest14	Expression
MerlinF2	103-213	pDest14	Expression
MerlinF3	212-307	pDest14	Expression
Merlin CC	306-405	pDest14	Expression
Merlin CC Mid	406-480	pDest14	Expression
Merlin CC Tail	481-635	pDest14	Expression
Merlin 306-355	306-355	pDest14	Expression
Merlin 330-380	330-380	pDest14	Expression
Merlin 356-405	356-405	pDest14	Expression
Merlin Δ306-405		pDest14	Expression
Merlin Δ306-355		pDest14	Expression
Merlin Δ330-380		pDest14	Expression
Merlin Δ356-405		pDest14	Expression
Merlin Δ306-320		pDest14	Expression
Merlin Δ316-330		pDest14	Expression
Merlin Δ326-340		pDest14	Expression
Merlin Δ336-350		pDest14	Expression
Merlin Δ346-360		pDest14	Expression
Merlin Δ356-370		pDest14	Expression
Merlin Δ366-380		pDest14	Expression
Merlin 1-405	1-405	pDest14	Expression
Merlin 1-480	1-480	pDest14	Expression
Merlin 1-600	1-600	pDest14	Expression
Merlin S371A	1-635	pDest14	Expression
Merlin S371D	1-635	pDest14	Expression
Merlin AQQA	1-635	pDest14	Expression
Moesin	1-578	pDest14	Expression
MoeF	1-296	pDest14	Expression
MoeC	297-578	pDest14	Expression
MoesinF1	1-95	pDest14	Expression
MoesinF2	94-204	pDest14	Expression
MoesinF3	203-298	pDest14	Expression
GST-Sip1	1-296	pDest15	Expression

GST-Sip1 ΔEB50	1-246	pDest15	Expression
GST-Sip1 EB50	247-296	pDest15	Expression
GST-Merlin	1-635	pDest15	Expression
GST-MerF	1-305	pDest15	Expression
GST-MerC	306-635	pDest15	Expression
GST-Moesin	1-578	pDest15	Expression
Merlin S371A	1-635	pHGW 1073	Expression
Merlin S371D	1-635	pHGW 1073	Expression
Merlin T374A	1-635	pHGW 1073	Expression
Merlin T374D	1-635	pHGW 1073	Expression
Merlin AQQA	1-635	pHGW 1073	Expression

Appendix C: Additional potential Merlin protein interactions

GST affinity chromatography experiments using ^{35}S radiolabelled Merlin, CG8023 and Wings Up A proteins. GST-8023 1-244 is full length, 1-65 is the unique region, and 66-244 is the eIF4E region. GST-MerF is the FERM domain of Merlin (1-305) and GST-MerC is the C-terminal tail of Merlin (306-635). Merlin protein shows binding to all three GST-8023 protein constructs. CG8023 protein shows some binding to GST-MerF and possibly GST-MerC. Wings Up A protein shows binding to both GST-MerF and GST-MerC.